THE UNIVERSITY OF ALBERTA

THE ISOLATION AND CHARACTERIZATION OF THE COMPONENTS OF BOVINE CARDIAC TROPONIN AND AN INVESTIGATION OF THEIR INTERACTION PROPERTIES

by

© LESLIE DAVID BURTNICK

A THESIS

SUBMITTED TO THE FACULTY OF GRADUATE STUDIES AND RESEARCH

IN PARTIAL FULFILMENT OF THE REQUIREMENTS FOR THE DEGREE

OF DOCTOR OF PHILOSOPHY

DEPARTMENT OF BIOCHEMISTRY

EDMONTON, ALBERTA

SPRING, 1977

ABSTRACT

Troponin was isolated from bovine cardiac muscle employing the LiCl extraction procedure of Tsukui and Ebashi (33). By a combination of ion exchange and gel filtration chromatographies in the presence of urea, cardiac troponin could be separated into three homogeneous components. These included: troponin I (TN-I), an ATPase inhibitory protein; troponin C (TN-C), a calcium binding protein; and troponin T (TN-T), a protein which interacts strongly with tropomyosin.

Biological activity studies using a synthetic cardiac actomyosin ATPase assay system, in the presence of tropomyosin, demonstrated that TN-I could inhibit the Mg^{2+} activated actomyosin ATPase by 60%. Addition of TN-C reversed the inhibitory effect of TN-I. Incorporation of TN-T into the assay system, with TN-I and TN-C, converted the regulatory process into a Ca^{2+} dependent one. In the absence of Ca^{2+}, the ATPase activity was inhibited. In the presence of Ca^{2+}, the inhibition was reversed completely.

The cardiac troponin subunits were characterized with respect to a number of chemical and physical properties. Amino acid analysis disclosed that TN-C was rich in acidic residues, while TN-I and TN-T were basic proteins. Sedimentation equilibrium data suggested molecular weights for TN-C, TN-I and TN-T, respectively, of 17,700, 22,900 ± 500 and 36,300 ± 2,000. Circular dichroism (CD) spectra indicated that a significant percentage of the amino acid residues of each of the subunits were involved in α helical structures.

CD data revealed that upon binding Ca^{2+}, TN-C underwent a major conformational change. Although analytical gel filtration studies

determined that TN-C could bind 3 moles of Ca^{2+} per mole, titration of the observed change in ellipticity in CD spectra implied the binding of a single Ca^{2+} to a particular site on TN-C generated the complete conformational change observed by this method.

CD measurements also demonstrated that interprotein interactions occurred in solutions containing mixtures of TN-C and TN-T, TN-C and TN-I, and tropomyosin and TN-T. In those complexes involving TN-C, TN-IC, TN-CT and reconstituted troponin (TN-ICT), Ca^{2+} was able to elicit a conformational change analogous to that observed in isolated TN-C in solution. In TN-ICT, the presence of TN-I and TN-T appeared to enhance the magnitude of the conformational change.

Polyacrylamide gel electrophoresis and cosedimentation experiments provided further evidence for complex formation between TN-C and TN-I, TN-C and TN-T, and TN-T and tropomyosin.

ACKNOWLEDGEMENTS

I wish to express my sincere thanks to the many people in the Department of Biochemistry who have helped me during the course of my studies. In particular, I wish to thank my supervisor, Dr. Cyril Kay, and Dr. Bill McCubbin for their guidance and encouragement in the design, execution and interpretation of the experiments described in this thesis. I am also grateful to Toni Keri, Vic Ledsham and Kim Oikawa for their expert technical assistance.

The preparation of this thesis was greatly facilitated by the excellent typing of Jaclyn Dorsey and the superb graphics of Vic Ledsham.

Finally, I wish to express my gratitude to the National Research Council of Canada, which provided me with personal financial support in the form of a 1967 Science Scholarship.

TABLE OF CONTENTS

Page

ABSTRACT iv

ACKNOWLEDGEMENTS vi

LIST OF TABLES xi

LIST OF FIGURES xii

ABBREVIATIONS AND SYMBOLS xv

CHAPTER I: INTRODUCTION 1

A. Vertebrate Striated Muscle 1

B. Regulation of Striated Muscle Contraction in Vertebrates . 5

C. Cardiac Muscle Troponin 9

1. TN-C 11

2. TN-I 13

3. TN-T 15

D. Aims of This Project 15

CHAPTER II: EXPERIMENTAL METHODS 17

A. pH Measurement 17

B. Gel Electrophoresis Methods 17

1. Polyacrylamide Gel Electrophoresis 17

2. SDS Polyacrylamide Gel Electrophoresis 17

C. Amino Acid Analysis 18

D. Optical Methods 18

1. Absorption Spectrophotometry 18

2. Circular Dichroism Spectra 19

E. Ultracentrifugal Methods 20

1. Protein Extinction Coefficients 20

Page

2. Sedimentation Velocity Experiments 20

3. Sedimentation Equilibrium Experiments 22

F. Biological Activity Studies 23

G. Cosedimentation Analysis 24

H. Calcium Binding Studies 25

1. Free Ca^{2+} Ion Concentration 25

2. CD Ca^{2+} Titrations 29

3. Gel Filtration 31

CHAPTER III: TROPONIN PREPARATIVE METHODOLOGY 34

A. Cardiac Troponin 34

1. Muscle Powder Method 35

2. LiCl Extraction Procedure 36

B. Separation of the Cardiac Troponin Components 37

1. DEAE-Sephadex Column Chromatography 37

2. Purification of TN-C 39

3. Purification of TN-I 39

4. Purification of TN-T 42

C. Summary 47

CHAPTER IV: CARDIAC TROPONIN SUBUNITS 51

A. TN-C 51

1. Amino Acid Analysis 51

2. Extinction Coefficient 53

3. Sedimentation Coefficient 53

4. Molecular Weight 56

5. UV Absorption Properties 56

Page

6. CD Properties 60

a. Aromatic Absorption Region (250-310 nm) 60

b. Peptide Absorption Region (190-250 nm) 60

7. Stabilizing Effect of Ca^{2+} 66

8. Ca^{2+} Binding 68

a. CD Titration Studies 68

b. Gel Filtration Studies 73

c. Summary 77

B. TN-I 78

1. Amino Acid Analysis 78

2. Solubility 78

3. Extinction Coefficient 80

4. Molecular Weight 80

5. UV Absorption Properties 85

6. CD Properties 85

C. TN-T 88

1. Amino Acid Analysis 88

2. Solubility 88

3. Extinction Coefficient 90

4. Molecular Weight 90

5. UV Absorption Properties 94

6. CD Properties 94

CHAPTER V: INTERACTION STUDIES 98

A. Biological Activity 99

B. Polyacrylamide Gel Studies 103

Page

1. TN-IC 103

2. TN-CT 105

C. Cosedimentation Analysis 107

D. CD Studies 110

CHAPTER VI: GENERAL DISCUSSION 117

BIBLIOGRAPHY 121

APPENDIX: STRUCTURAL HOMOLOGIES AMONG MUSCLE PROTEINS 127

LIST OF TABLES

Table		Page
I	Amino acid composition of bovine cardiac TN-C	52
II	Amino acid composition of bovine cardiac TN-I	79
III	Amino acid composition of bovine cardiac TN-T	89
IV	Reconstitution of the regulatory system of bovine cardiac muscle	102
V	Cosedimentation analysis of solutions containing tropomyosin and TN-T	108
VI	Emission dissymmetry factors for Tb(III) emission in muscle proteins	130

LIST OF FIGURES

Figure		Page
1.	Schematic representation of myofibrillar structure	2
2.	Model for sarcomere contraction	4
3.	Model for the fine structure of the thin filament of muscle	7
4.	Model for the regulation of muscle contraction	8
5.	Amino acid sequences of bovine cardiac and rabbit skeletal TN-C	12
6.	Amino acid sequences of rabbit cardiac and rabbit skeletal TN-I	14
7.	Chromatography of crude troponin on DEAE-Sephadex A-25	38
8.	Purification of TN-C on Biogel A 0.5 m	40
9.	SDS polyacrylamide gels of cardiac TN-C	41
10.	Chromatography of TN-I enriched material on CM-Sephadex C-25	43
11.	Purification of TN-I on Biogel P-200	44
12.	SDS polyacrylamide gels of cardiac TN-I	45
13.	Chromatography of TN-T enriched material on CM-Sephadex C-25	46
14.	Desalting of TN-T solutions on Biogel P-2	48
15.	SDS polyacrylamide gels of cardiac TN-T	49
16.	SDS polyacrylamide gels of LiCl extracted cardiac troponin and purified TN-T, TN-I and TN-C	50
17.	Determination of the extinction coefficient of TN-C	54
18.	Determination of the intrinsic sedimentation coefficient of TN-C	55
19.	Determination of the molecular weights of the cardiac troponin subunits by SDS polyacrylamide gel electrophoresis	57
20.	Sedimentation equilibrium log Y versus r^2 plot for TN-C	58

Figure		Page
21.	UV absorption spectrum of TN-C	59
22.	UV difference absorption spectrum of TN-C in the presence and absence of calcium	61
23.	Aromatic CD spectra of TN-C in the presence and absence of calcium	62
24.	Far UV CD spectra of TN-C in the presence and absence of calcium	64
25.	CD thermal denaturation studies of TN-C in the presence and absence of calcium or strontium	67
26.	CD calcium titration of the conformational change in TN-C (minus Mg^{2+})	70
27.	CD calcium titration of the conformational change in TN-C (plus Mg^{2+})	71
28.	Elution of TN-C and calcium from a Sephadex G-25 column	74
29.	Determination of the moles of calcium bound per mole of TN-C at various concentrations of free calcium ion	76
30.	Determination of the extinction coefficient of TN-I	81
31.	Comparison of the mobilities of skeletal and cardiac TN-I on SDS polyacrylamide gels	82
32.	Sedimentation equilibrium log A *versus* r^2 plot for TN-I in a non-denaturing buffer	83
33.	Sedimentation equilibrium log A *versus* r^2 plot for TN-I in the presence of 8 M urea	84
34.	UV absorption spectrum of TN-I	86
35.	Far UV CD spectrum of TN-I	87
36.	Determination of the extinction coefficient of TN-T	91
37.	Sedimentation equilibrium log Y *versus* r^2 plot for TN-T in a non-denaturing buffer	92
38.	Sedimentation equilibrium log A *versus* r^2 plot for TN-T in the presence of 8 M urea	93
39.	UV absorption spectrum of TN-T	95

Figure		Page
40.	Far UV CD spectra of TN-T in the presence and absence of magnesium	96
41.	Inhibition of the Mg^{2+} activated ATPase of synthetic cardiac actomyosin by TN-I	100
42.	Reversal of the TN-I induced inhibitory effect on synthetic cardiac actomyosin by TN-C	101
43.	Polyacrylamide gel electrophoresis of TN-IC	104
44.	Polyacrylamide gel electrophoresis of TN-CT	106
45.	SDS polyacrylamide gel analysis of the precipitates from cosedimentation studies	109
46.	Calculated and observed CD spectra of TN-T - tropomyosin	112
47.	Calculated and observed CD spectra of TN-CT in the presence and absence of calcium	113
48.	Calculated and observed CD spectra of TN-IC in the presence and absence of calcium	114
49.	Calculated and observed CD spectra of reconstituted cardiac troponin in the presence and absence of calcium	115

ABBREVIATIONS AND SYMBOLS

The units for mass, length, volume and time have been abbreviated according to standard procedure. Terms appearing in a mathematical relation are defined in the text referring to that equation.

ATP	adenosine triphosphate
CD	circular dichroism
CM-	carboxymethyl
CPE	circularly polarized emission
DEAE-	diethylaminoethyl
DTT	dithiothreitol
$E^{1\%}_{1cm,\lambda}$	absorbance of a 1% protein solution in a 1 cm pathlength cell at the wavelength, λ
EGTA	ethyleneglycol bis(β-aminoethylether)-N,N'-tetraacetate
f	fraction titrated
g	emission dissymmetry factor
i	the number of moles of ligand which bind to a mole of the macromolecule of interest
K_{app}	the apparent association constant for the interaction of two molecular species
mA	milliamperes
pX	negative logarithm of the number, X
r	radial distance from the axis of rotation
S	Svedberg unit of sedimentation velocity (10^{-13} sec)
$s_{20,w}$	sedimentation coefficient corrected to water at 20°C
$s^{o}_{20,w}$	intrinsic sedimentation coefficient
SAM	synthetic actomyosin
SDS	sodium dodecyl sulfate

TCA	trichloroacetic acid
TE	total emission intensity
TN-C	the calcium binding protein of the troponin complex
TN-I	the ATPase inhibitory protein of the troponin complex
TN-T	the tropomyosin binding component of the troponin complex
tris	tris-(hydroxymethyl)aminomethane
UV	ultraviolet
$\bar{v}$	partial specific volume
v/v	concentration expressed as fraction by volume of the final solution
Y	a measure of protein concentration in fringe displacement units
$[X]_f$	the molar concentration of substance, X, which is present in solution in an uncomplexed state
λ	wavelength
$[\theta]_\lambda$	mean residue ellipticity at the wavelength λ
θ_{obs}	observed ellipticity value
$\frac{\theta_{T,obs}}{\theta_{T,min}}$	the ratio of $[\theta]_{221}$ at a temperature, T, to its value at the minimal temperature at which the experiment was performed
$\sim$	approximately
$\simeq$	approximately equal to
$>$	greater than
$\geq$	greater than or equal to
$<$	less than
$\leq$	less than or equal to
$\lvert X \rvert$	the absolute value of the number, X

CHAPTER I

INTRODUCTION

A. VERTEBRATE STRIATED MUSCLE

Several excellent reviews have been published which concern the molecular nature of contraction in vertebrate skeletal muscle (1, 2, 3). Cardiac, like skeletal muscle, is a cross-striated muscle. The great overall similarities, as well as distinct differences, between these two muscle types also have been reviewed extensively (4, 5, 6). Therefore, a detailed description of muscle structure at this point will be forgone in favour of a brief, general review. This discussion will be drawn from the above articles and will centre upon the schematic depiction of a striated muscle in Figure 1. This diagram could apply equally well to cardiac or skeletal muscle.

A muscle fibre is composed of a longitudinally arranged, in register, array of myofilaments which exhibit a periodic band pattern when observed under the light microscope. These characteristic cross-striations are the result of alternating optically dense and less-dense transverse regions along the myofibril. Under polarized light, the optically dense or A bands are strongly birefringent (anisotropic), indicating that the molecular components in the region are asymmetric and are oriented in a specific direction. The optically light or I bands are relatively nonbirefringent (isotropic).

Each A band is bisected by a dark line, the M line. Immediately adjacent to each side of the M line is a relatively less dense region. This narrow region of relatively low optical density in the middle of the dense A band is called the H zone.

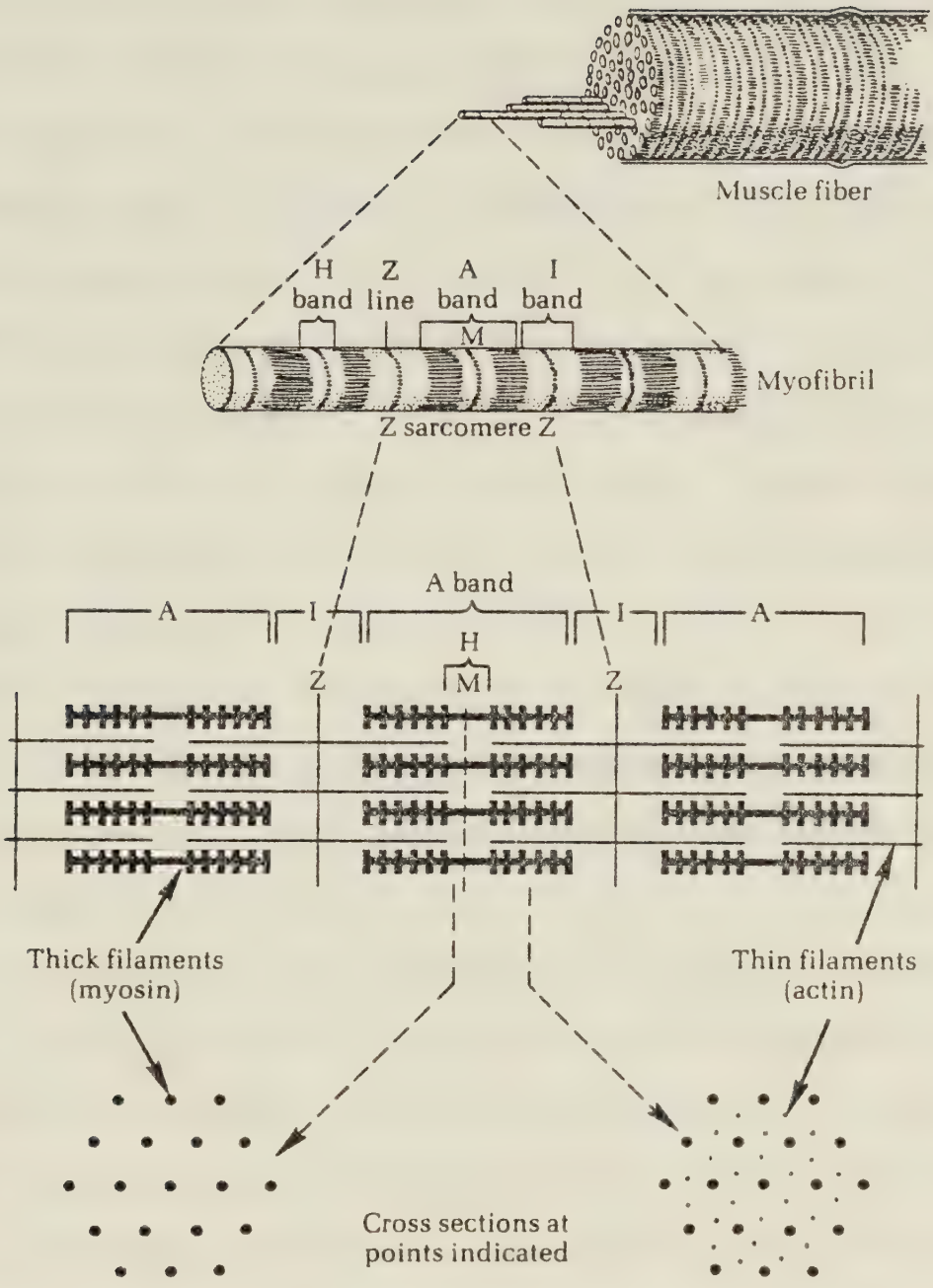

Figure 1. Schematic representation of myofibrillar structure. [From Lehninger (116).]

Bisecting the I bands is another set of dark lines, the Z lines. The space between two adjacent Z lines represents the functional unit of muscle contraction, the sarcomere. Sarcomere length is a function of total muscle length and ranges maximally from about 1.5 to 2.5 μ.

The band pattern of the sarcomere, and its alteration with the physiological state of the muscle, reflects both the disposition of the contractile macromolecules in the myofibril and their mode of action. The myofibrils consist of two kinds of myofilaments. In electron micrographs, thick filaments, about 150 Å in diameter and 1.6 μ long, are observed to extend the length of the A bands. Thinner filaments, about 60 Å in diameter, run from the Z line at the sarcomere edge, completely through the I band, and into the A band up to the edge of the H zone. There is an overlapping of the thick and thin filaments only within the A band. In this overlap region, electron micrographs show the existence of interfilamentous cross-bridges between the two filament types.

In cross-section, the myofilaments are arranged in a hexagonal lattice. The thick and thin filaments are easily discernible and their interdigitation is apparent in the overlap region of the A band.

Upon contraction, the sarcomere shortens. However, two dimensions within the sarcomere do not change, the length of the A band and the distance from the Z line to the edge of the H zone. This is depicted schematically in Figure 2.

Figure 2 is, in fact, a crude representation of the sliding filament theory of muscle contraction. This model is characterized by three important features: (1) The proteins of the sarcomere are arranged in two separate kinds of filaments which can cross-connect; (2) Each type

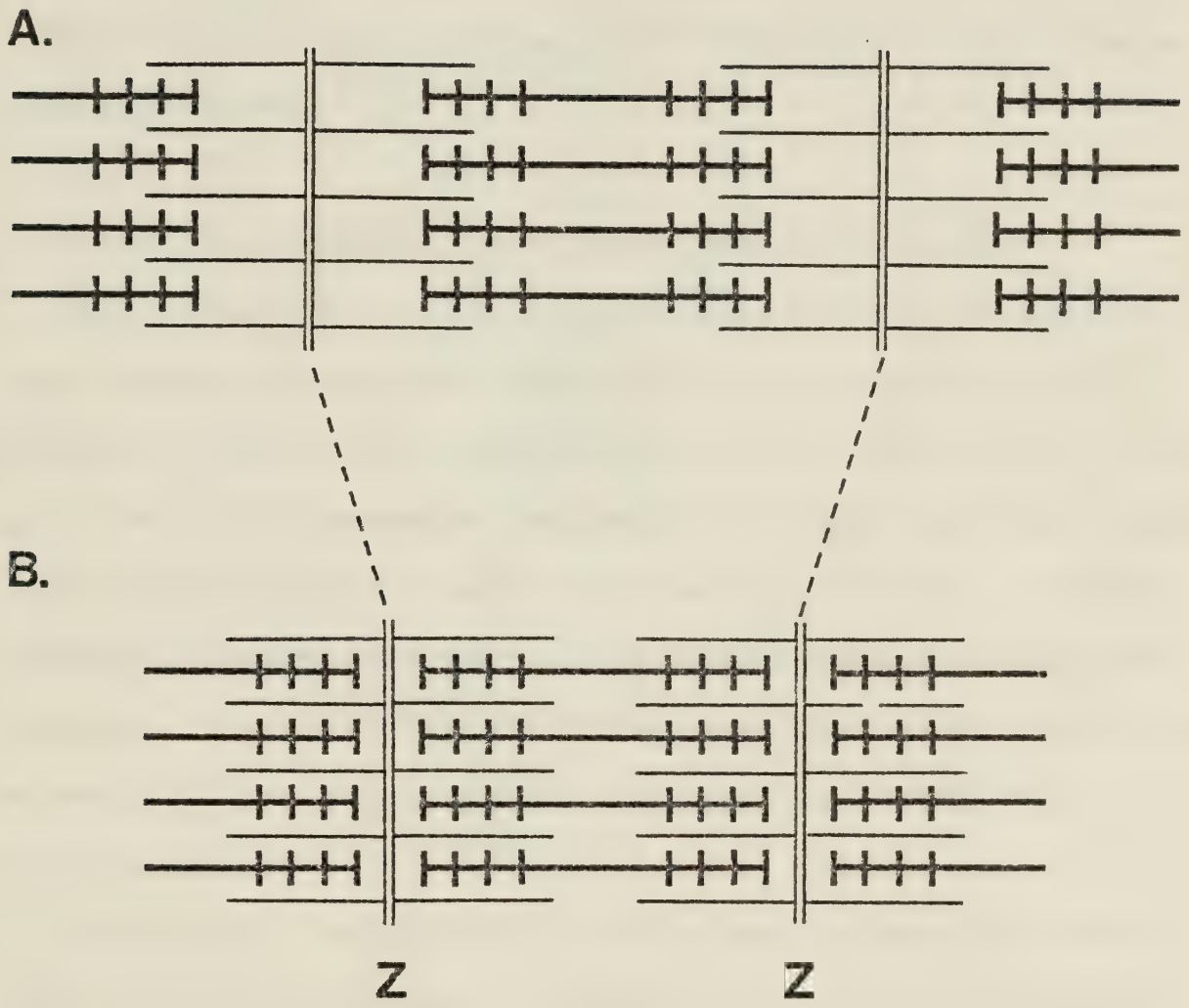

Figure 2. Model for sarcomere contraction. The diagram displays one complete sarcomere and parts of the neighbouring ones. The differences in the striated pattern observed in resting muscle (A) and contracted muscle (B) can be explained by a sliding filament hypothesis.

of filament is discontinuous along the length of the myofibril; (3) Muscle shortening is due to a relative motion of one type of filament along the other, with no appreciable change in the lengths of the filaments themselves. This relative sliding motion is the result of the constant formation and disruption of the cross-bridges between the two myofilament classes.

B. REGULATION OF STRIATED MUSCLE CONTRACTION IN VERTEBRATES

The most important functional proteins in muscle are myosin and actin, the main constituents, respectively, of the thick and thin filaments. Aside from the proteins of the M and Z lines, and a number of, as yet, little understood components of the thick and thin filaments, two other proteins play a major role in muscle contraction. These are tropomyosin and troponin, which are located as a complex on the thin filaments. Together, they confer calcium sensitivity to the interaction between myosin and actin (7) and so represent the "on-off" switch for muscle contraction.

The regulatory mechanism of vertebrate skeletal muscle has been under intensive investigation for about a decade and is thought to be reasonably well understood. Several reviews have dealt exclusively with this aspect of muscle action (8 - 11).

Skeletal muscle troponin is a complex of three proteins (12 - 17): troponin I (TN-I), which inhibits the Mg^{2+}-activated ATPase of actomyosin; troponin C (TN-C), a calcium-binding protein which is responsible for reversing the TN-I-induced inhibitory effect; and troponin T (TN-T), which interacts strongly with tropomyosin. Each subunit has been characterized in detail and the amino acid sequence of each is known

(18 - 20).

The abundance of recent studies on troponin and tropomyosin has resulted in the development of a useful model to explain the regulatory process (21 - 23). Prior to a brief discussion of the model, consider a schematic representation of the structure of the thin filament (Figure 3, after Ebashi et al. (24)). F-Actin is represented as two strands of pearls wound around each other. Tropomyosin molecules are depicted as rods which lie end-to-end in the grooves of the actin strands, each spanning the length of 7 actin monomers. Associated with each tropomyosin, at a specific site, is one unit of troponin.

In cross-section, the thin filament of resting muscle ($pCa_f \simeq 8$) can be represented as in Figure 4A (23). Troponin binds to the actin-tropomyosin filament at two sites; TN-T is attached to tropomyosin and TN-I to a site comprised of both actin and tropomyosin. In this configuration, troponin-tropomyosin links to f-actin sterically block the site on each actin monomer for interaction with myosin.

On release of Ca^{2+} ions into the sarcoplasm bathing the myofilaments ($pCa_f \simeq 5$), the calcium binding sites on TN-C are saturated. Upon binding Ca^{2+}, TN-C undergoes a dramatic conformational change (25, 26) which is transmitted through the remaining components of the system. The TN-I-tropomyosin-actin interaction is disrupted and the tropomyosin molecules shift deeper into the grooves between the f-actin strands, as depicted in Figure 4B (23). The movement of tropomyosin exposes the previously blocked interaction sites, allowing myosin molecules to contact actin. The net result is the hydrolysis of ATP and concomitant muscle contraction.

Recent support has come for this model from 3-dimensional image

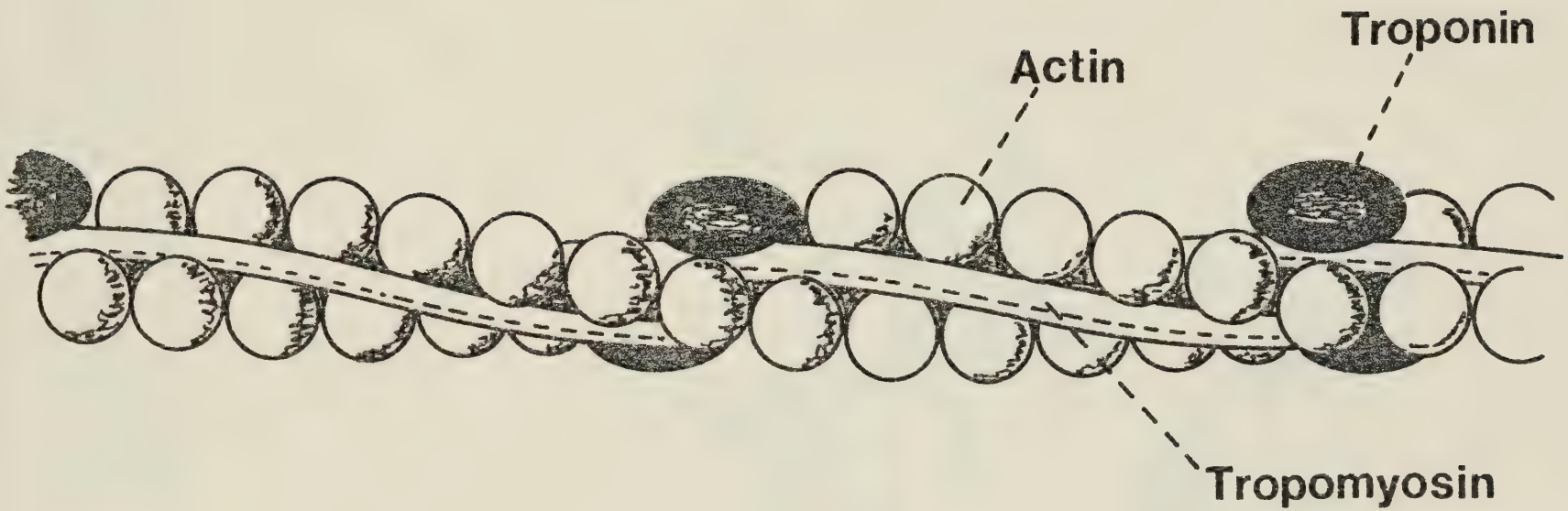

Figure 3. Model for the fine structure of the thin filament of muscle. [From Ebashi *et al.* (24).]

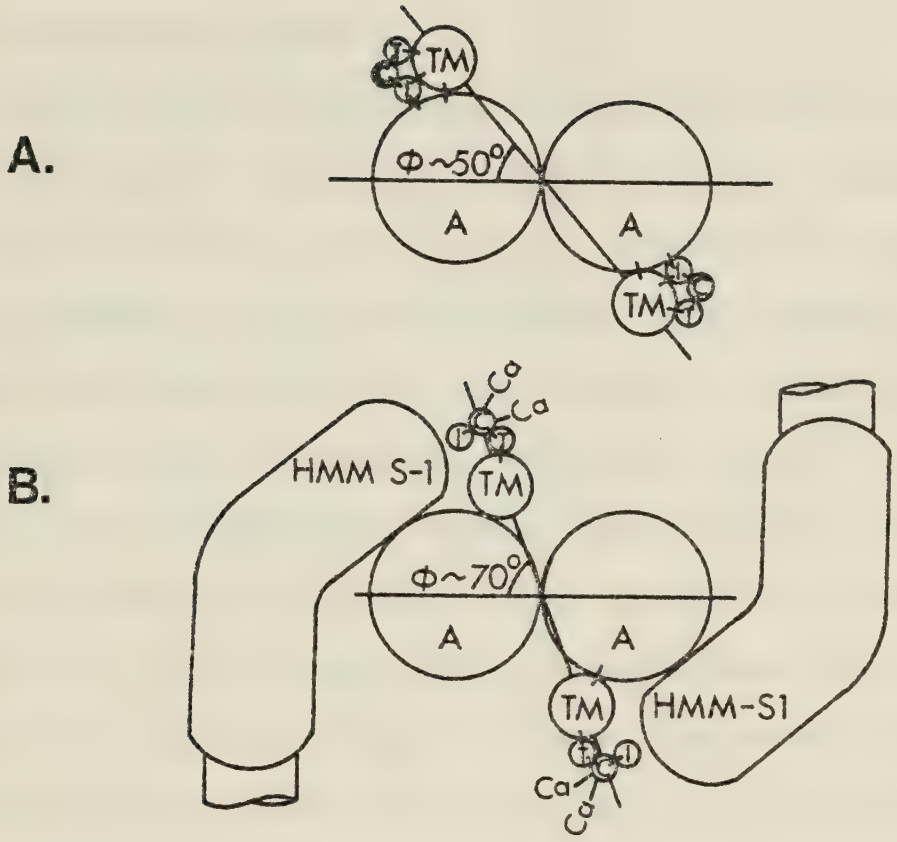

Figure 4. Model for the regulation of muscle contraction. The proteins represented are: actin, A; tropomyosin, TM, troponin I, I; troponin C, C; troponin T, T; the heavy meromyosin subfragment one portion of myosin, HMM S-1. Short connecting lines represent molecular interactions. (A) Molecular positions in relaxed muscle (pCa ≈ 8). (B) Molecular positions in contracting muscle (pCa ≈ 5). [From Potter and Gergely (23).]

reconstruction from electron micrographs (27), which also suggest that tropomyosin molecules shift from one position to another between the "on" and "off" states of muscle activity.

C. CARDIAC MUSCLE TROPONIN

Ebashi *et al.* (28) isolated a fraction from bovine cardiac muscle which performed the same function as the analogous fraction, called troponin, from rabbit skeletal muscle. It rendered desensitized actomyosin sensitive to regulation by calcium ions. Troponin from either tissue could perform its regulatory function on actomyosin from either muscle type. Therefore, cardiac muscle was proposed to have a calcium sensitization system similar to that found in skeletal muscle.

The interpretation of the results of preliminary studies on cardiac troponin (29 - 32) was hampered by the large number of contaminants present in protein preparations. However, the reports did suggest that cardiac troponin possessed the same number and type of components as its skeletal analogue, although some of the subunits possessed different mobilities on SDS gels.

At this time, a project was initiated in our laboratory to isolate troponin from beef hearts and to separate and characterize its constituent subunits. Using skeletal troponin preparative methodology, problems similar to those mentioned already were encountered.

Tsukui and Ebashi (33), fortunately, produced a preparative scheme that allowed the isolation of reasonably homogeneous troponin from cardiac tissue. This procedure, derived from that of Ebashi *et al.* (12) for the preparation of skeletal troponin, involved a LiCl extraction of the regulatory complex from a muscle mince, a pH 5.1 isoelectric

precipitation of tropomyosin, and an ammonium sulfate fractionation to obtain troponin. Tsukui and Ebashi were also able to separate cardiac troponin into three fractions which approached homogeneity by ion exchange chromatography in urea and ammonium sulfate precipitation in the presence of SDS. Using a desensitized skeletal actomyosin super-precipitation assay system, they confirmed that troponins I, C and T from cardiac muscle could substitute qualitatively, although not quantitatively, for their skeletal counterparts. This suggested, again, that cardiac and skeletal muscle were regulated in a similar manner, but that distinct differences might exist at the level of the individual molecules involved.

Upon successfully adapting the LiCl extraction methodology to our own needs, our goal became to devise a separation scheme to isolate each of the cardiac troponin components in a pure form and to characterize each subunit with the physico-chemical tools available to us. Subsequently, this aim was extended to study the nature of the interactions which occurred among the proteins of the cardiac muscle regulatory complex and either to confirm that cardiac muscle was sensitized to calcium ions in essentially the same fashion as skeletal muscle or to propose an alternative model.

Since 1974, several reports and abstracts detailing the progress of this project have appeared (34 - 42). These comprise a major part of the published work specifically related to cardiac troponin. As the data presented in these articles provide the raw material for this thesis, discussion of this material will be postponed until subsequent chapters.

However, other laboratories have also contributed to the understanding

of cardiac troponin since 1973. It is appropriate to discuss some of these results at this point.

1. TN-C

Head and Perry (43), using an isotope dilution technique, demonstrated that the ratio of actin to TN-C in rabbit white (psoas) and red (soleus) skeletal, and cardiac muscles was about 7:1, confirming the existence of similar stoichiometries of the proteins in different muscle types.

Several laboratories reported that TN-C from different muscle sources possessed similar mobilities on SDS gels (29, 32, 33) and on polyacrylamide gels in the presence of urea (43). However, Hirabayashi and Perry (44) established that antiserum to TN-C from chicken skeletal muscle did not react with TN-C from chicken heart muscle. They also reported that the amino acid composition of chicken skeletal TN-C was more similar to TN-C from the skeletal muscles of other species than to chicken cardiac TN-C. Cardiac and skeletal TN-C also differ in their capacity to bind Ca^{2+} ions (45, 46), cardiac TN-C binding fewer Ca^{2+} than the skeletal homologue.

The predictions that the two types of TN-C were different were substantiated when the amino acid sequence of bovine cardiac troponin C was determined (47). In comparison to the rabbit skeletal TN-C sequence (18, 48) (Figure 5), bovine cardiac troponin C contained 55 replacements and 2 additional residues. Further analysis revealed only 3 regions in the cardiac TN-C sequence which bore significant homology with the calcium-binding regions of parvalbumin (49). These 3 stretches of homology corresponded to 3 of the 4 proposed Ca^{2+} binding sites in skeletal TN-C (18), predicted on the same basis. This may explain the

```
                                                                  15
Ac-Met-Asp-Asp-Ile-Tyr-Lys-Ala-Ala-Val-Glu-Gln-Leu-Thr-Glu-Glu-
    Ac- " -Thr-Gln-Gln-Ala-Glu- " -Arg-Ser-Tyr- " -Ser- "   " -

                                                                  30
Gln-Lys-Asn-Glu-Phe-Lys-Ala-Ala-Phe-Asp-Ile-Phe-Val-Leu-Gly-
Met-Ile-Ala- "   "   "   "   "   "   " -Met- " [Asp-----Ala-

                                                                  45
Ala-Glu-Asp-Gly-Cys-Ile-Ser-Thr-Lys-Glu-Leu-Gly-Lys-Val-Met-
Asp-Gly-Gly- " -Asp- "   " -Val- "   " ] "   " -Thr- "   "

                                                                  60
Arg-Met-Leu-Gly-Gln-Asn-Pro-Thr-Pro-Glu-Glu-Leu-Gln-Glu-Met-
 "   "   "   "   " -Thr- "   " -Lys- "   "   " -Asp-Ala-Ile-

                                                                  75
Ile-Asp-Glu-Val[Asp-Glu-Asp-Gly-Ser-Gly-Thr-Val-Asp-Phe-Asp-
 " -Glu- "   " [ "   "   "   "   "   "   " -Ile- "   " -Glu-

                                                                  90
Glu]Phe-Leu-Val-Met-Met-Val-Arg-Cys-Met-Lys-Asp-Asp-Ser-Lys-
 " ] "   "   "   "   "   "   " -Gln- "   " -Glu- " -Ala- "

                                                                 105
Gly-Lys-Ser-Glu-Glu-Glu-Leu-Ser-Asp-Leu-Phe-Arg-Met-Phe[Asp-
 "   "   "   "   "   "   " -Ala-Glu-Cys- "   " -Ile- " [ "

                                                                 120
Lys-Asn-Ala-Asp-Gly-Tyr-Ile-Asp-Leu-Glu-Glu]Leu-Lys-Ile-Met-
Arg- "   "   "   "   "   "   " -Ala- "   " ] " -Ala-Glu-Ile-

                                                                 135
Leu-Gln-Ala-Thr-Gly-Glu-Thr-Ile-Thr-Glu-Asp-Asp-Ile-Glu-Glu-
Phe-Arg- " -Ser- "   " -His-Val- " -Asp-Glu-Glu- "   " -Ser-

                                                                 150
Leu-Met-Lys-Asp-Gly[Asp-Lys-Asn-Asn-Asp-Gly-Arg-Ile-Asp-Tyr-
 "   "   "   "   " [ "   "   "   "   "   "   "   "   " -Phe-

Asp-Glu]Phe-Leu-Glu-Phe-Met-Lys-Gly-Val-Glu-OH
 "   " ] "   " -Lys-Met- " -Glu- "   " -Gln-OH
```

Figure 5. Amino acid sequences of bovine cardiac (upper line) (47) and rabbit skeletal TN-C (lower line) (48). Square brackets enclose the proposed calcium binding sites of each molecule.

lowered Ca^{2+} binding capacity of cardiac, relative to skeletal, TN-C.

2. TN-I

Polyacrylamide gel electrophoresis of muscle extracts in the presence of 6 M urea and 2 mM EGTA ("minus Ca^{2+}" state) demonstrated that TN-C from rabbit psoas, soleus and cardiac muscles possessed similar mobilities (43). But in the presence of Ca^{2+}, the bands believed to represent TN-IC complexes in soleus (red) and cardiac muscle electrophoresed more slowly than that of psoas (white) muscle, suggesting that TN-I in soleus and cardiac muscles differed from that of psoas muscle.

In a later report (50), TN-I was purified from rabbit psoas, soleus and cardiac muscles by an affinity chromatographic technique using Sepharose-4B - linked TN-C. On SDS gels, the two types of skeletal muscle TN-I migrated with apparent molecular weights of 23,000 while cardiac TN-I migrated at 29,000. On polyacrylamide gels in 6 M urea, cardiac TN-I electrophoreses at a rate 15% slower than either type of skeletal TN-I. Electrophoresis of mixtures of each TN-I and skeletal TN-C on urea-polyacrylamide gels showed each TN-IC complex possessed a different mobility, indicating that TN-I from each muscle source was unique.

This prediction has been substantiated, at least for rabbit psoas and cardiac TN-I, by sequence studies (51, 52) (Figure 6). Although considerable homology exists between the two sequences, cardiac TN-I has an additional 26 residues at its N terminus. In this extra string of residues, the serine at position 20 is readily phosphorylated in a reaction catalysed by cyclic AMP - dependent protein kinase (52, 53). This phosphorylation of serine-20 accounts, in a large part, for

```
                                                                    25
X-Ala-Asp-Glu-Ser-Arg-Asp-Ala-Ala-Gly-Glu-Ala-Lys-Pro-Ala-Pro-Ala-Val-Arg-Arg-Ser-Asp-Arg-Ala-Tyr-Ala-

                                                                    50
Thr-Glu-Pro-His-Ala-Lys-Ser-Lys-Lys-Lys-Ile-Ser-Ala-Ser-Arg-Lys-Leu-Gln-Leu-Lys-Thr-Leu-Met-Leu-Gln-
 Ac-Gly-Asp-Glu-Glu-  "  -Arg-Asn-Arg-Ala-  "  -Thr-  "  ------  "  -Arg-Gln-His-  "    "  -Ser-Val-  "    "    "

                                                                    75
Ile-Ala-Lys-Gln-Glu-Leu-Glu-Arg-Glu-Ala-Glu-Glu-Arg-Arg-Gly-Glu-Lys-Gly-Arg-Ala-Leu-Ser-Thr-Arg-Cys-
  "    "  -Ala-Thr-  "    "    "  -Lys-  "  -Glu-Gly-Arg-  "  -Glu-Ala-  "    "  -Gln-Asn-Tyr-  "  -Ala-Glu-His-  "

                                                                   100
Gln-Pro-Leu-Glu-Leu-Ala-Gly-Leu-Gly-Phe-Ala-Glu-Leu-Gln-Asp-Leu-Cys-Arg-Gln-Leu-His-Ala-Arg-Val-Asp-
Pro-  "    "  -Ser-  "  -Pro-  "  ------Ser-Met-  "    "  -Val-  "  -Glu-  "    "  -Lys-  "    "    "    "  -Lys-Ile-  "

                                                                   125
Lys-Val-Asp-Glu-Glu-Arg-Tyr-Asp-Val-Glu-Ala-Lys-Val-Thr-Lys-Asn-Ile-Thr-Glu-Ile-Ala-Asp-Leu-Thr-Gln-
Ala-Ala-Glu-  "    "  -Lys-  "    "  -Met-  "  -Ile-  "    "  -Gln-  "  -Ser-Ser-Lys-  "  -Leu-Glu-  "  -Met-Asn-  "

                                                                   150
Lys-Ile-Phe-Asp-Leu-Arg-Gly-Lys-Phe-Lys-Arg-Pro-Thr-Leu-Arg-Leu-Arg-Val-Arg-Ile-Ser-Ala-Asp-Ala-Met-
  "  -Leu-  "    "    "    "    "    "    "    "    "    "  -Pro-  "    "  -Arg-  "    "    "  -Met-  "    "    "    "    "

                                                                   175
Met-Gln-Ala-Leu-Leu-Gly-Thr-Arg-Ala-Lys-Glu-Thr-Leu-Asp-Leu-Arg-Ala-His-Leu-Lys-Gln-Val-Lys-Lys-Glu-
Leu-Lys-  "    "    "    "  -Ser-Lys-His-  "  -Val-Cys-Met-  "    "    "    "  -Asn-  "    "    "    "    "    "    "

                                                                   200
Asp-Thr-Glu-Lys-Glu-Asn-Arg-Glu-Val-Gly-Asp-Trp-Arg-Lys-Asn-Ile-Asp-Leu-Leu-Ser-Gly-Met-Glu-Gly-Arg-
  "    "    "    "    "  ------  "  -Asp-  "    "    "    "    "    "    "    "  -Glu-Glu-Lys-  "    "    "    "    "    "


Lys-Lys-Lys-Phe-Glu-Gly-OH
  "    "  -Met  "    "  -Ser-Glu-Ser-OH
```

Figure 6. Amino acid sequences of rabbit cardiac (upper line) (52) and rabbit skeletal TN-I (lower line) (51). X denotes an unknown blocking group.

the differences between the phosphorylation properties of cardiac and skeletal TN-I (54). These differences are apparently physiologically relevant. England (55) demonstrated that stimulation of perfused rat hearts with 10^{-6} M adrenaline resulted in a simultaneous increase in both the degree of phosphorylation of TN-I and the force of contraction. Similar results for rabbit hearts were confirmed by Solaro et al. (53)

The mechanism by which phosphorylation of cardiac TN-I may promote the interaction between actin and myosin is not yet understood. Ray and England (56), studying whole myofibrils and native tropomyosin (troponin plus tropomyosin) from beef hearts, observed that phosphorylation of TN-I did not alter the V_{max} of the actomyosin ATPase and, in fact, increased the amount of calcium required to activate the ATPase activity. They were led to the conclusion that the effects of catacholamines in perfused hearts must be two-fold in order to stimulate contraction: a phosphorylation of TN-I and an increase in the sarcoplasmic Ca^{2+} concentration during systole. Investigations are in progress to shed further light onto this complex situation.

3. TN-T

Little has been reported on cardiac TN-T. Brekke and Greaser (46) reported that cardiac TN-T caused changes in tropomyosin paracrystal patterns similar to those described for skeletal TN-T (57). However, they also observed differences in the amino acid composition of cardiac and skeletal TN-T.

D. AIMS OF THIS PROJECT

Subsequent chapters of this thesis will reveal that work on this project proceeded with 3 major goals in mind. First, it was necessary

to develop a reliable preparative methodology to isolate troponin from cardiac tissue and to separate each of its constituent subunits. Second, each component had to be characterized with respect to its chemical, physical and biological properties. Third, it was important to understand how the isolated members of the troponin complex could interact with each other.

Attainment of these goals, we hoped, would enable us to conclude whether the cardiac muscle regulatory muscle mechanism differed significantly from that in skeletal muscle and to detail the extent of any differences.

CHAPTER II

EXPERIMENTAL METHODS

A. pH MEASUREMENT

Routine pH measurements were performed using a Radiometer pH meter equipped with a variable temperature compensator and combination glass electrode. Standard pH buffers (Fisher Scientific Co.) were used to calibrate the instrument.

B. GEL ELECTROPHORETIC METHODS

1. Polyacrylamide Gel Electrophoresis

Electrophoresis through 8% polyacrylamide gels was performed essentially as described by Schaub and Perry (58). The tank buffer, 25 mM tris - 160 mM glycine at pH 8.5, was prepared so as to contain 2 mM EGTA or 0.5 mM $CaCl_2$, depending on the desired run conditions. In certain experiments, 6 M urea was incorporated into the gels.

2. SDS Polyacrylamide Gel Electrophoresis

Methodology similar to that of Shapiro *et al.* (59) was used. Samples were prepared in 2% SDS containing 1 mM DTT by heating them in a boiling water bath for 5 - 10 min. Electrophoresis was performed on 10% polyacrylamide gels for 3 1/2 h at 7 mA/gel. Gels were stained with Coomassie Brilliant Blue and destained in several changes of 7% acetic acid, 7.5 % methanol (v/v). Destained gels were scanned in a Gilford 240 spectrophotometer equipped with a gel scanning module. Relative quantities of each component present were estimated by tracing each peak, cutting out the traced area and weighing.

Molecular weight estimations were made according to Weber and

Osborn (60), by comparing the migration distances of the "unknown" proteins with those of proteins of known molecular weight.

C. AMINO ACID ANALYSIS

Amino acid analyses were performed essentially as described by Moore and Stein (61). The amino acid compositions of protein hydrolysates were determined using a Beckman 121 or Durrum D-500 automated amino acid analyser.

Duplicate samples were hydrolysed in constant boiling 6 N HCl for 24, 48 and 72 h. The values reported are averaged over the three hydrolysis times. Threonine and serine contents were estimated by extrapolating to zero time. 72 h hydrolysate values were used to determine valine and isoleucine contents. Phenol (1%) was added to the 6 N HCl used for hydrolysis to preserve the integrity of tyrosine residues. Total cysteine plus cystine content was determined as cysteic acid after performic acid oxidation of the protein sample according to Moore (62). Using this method, methionine levels were checked as methionine sulfone. Tryptophan content was established spectrophotometrically with the protein dissolved in 0.1 N NaOH as outlined by Goodwin and Morton (63) and Bencze and Schmid (64). The absence of tryptophan in cardiac TN-C was confirmed fluorimetrically by the absence of a tryptophan emission band near 340 nm upon excitation of the protein solution near 276 nm.

D. OPTICAL METHODS

1. Absorption Spectrophotometry

Routine absorbance measurements, such as monitoring effluent

from a chromatographic column, were performed using a Gilford 240 spectrophotometer. UV absorbance and difference spectra were recorded employing a Cary 118C recording spectrophotometer.

Baselines for absorbance spectra were established using dialysate. Those for difference spectra were determined with protein solutions of identical compositions in both the sample and reference beampaths. Difference spectra were obtained by adding an aliquot of a solution containing the desired perturbant to the protein solution in the sample cell and an equal volume of the same solution, minus the perturbant, to the protein solution in the reference beam, and, subsequently, scanning the wavelength region of interest.

2. Circular Dichroism Spectra

Circular Dichroism (CD) measurements were performed using a Cary 6001 CD attachment to a Cary 60 recording spectropolarimeter, as described by Oikawa *et al.* (65). The instrument was calibrated with an aqueous solution of recrystallized d-10-camphor sulfonic acid. Constant nitrogen flushing was employed.

In the wavelength region from 200 - 250 nm, approximately 0.1% protein solutions were scanned in 0.5 mm cells. In the 250 - 320 nm region, approximately 0.3% protein solutions were scanned in 1 cm cells.

The mean residue ellipticity, $[\theta]_\lambda$, at a particular wavelength, λ, was calculated from the equation:

$$[\theta]_\lambda = \frac{\theta_{obs}\ MRW}{100\ lc} \qquad [1]$$

where:

MRW is the mean residue weight (taken as 115 in these studies),

θ_{obs} is the observed ellipticity value at the wavelength of interest,

l is cell pathlength in dm, and

c is the protein concentration in g/cm^3.

The units of $[\theta]_\lambda$ are degree·cm^2/dmole.

The apparent α helix contents of proteins were estimated using parameters and equations given by Chen et al. (66).

E. ULTRACENTRIFUGAL METHODS

Ultracentrifugal studies were performed at 20°C in a Beckman Spinco Model E analytical ultracentrifuge equipped with a photoelectric scanner, multiplex accessory, and high intensity light source. Rayleigh interference and Schlieren optical systems were also used. The basic methodology employed in these studies was derived from an ultracentrifuge methods manual compiled by Chervenka (67).

1. Protein Extinction Coefficients

The concentrations of a set of protein solutions were determined by the method of Babul and Stellwagen (68), using ultracentrifugal synthetic boundary runs with Rayleigh interference optics. Babul and Stellwagen determined, for proteins, an average refractive increment of 4.1 fringes/mg/ml. Therefore, a measurement of the number of fringes crossed on each photographic plate, using a Nikon model 6C microcomparater, provided a direct estimate of protein concentration. By correlating the protein concentration of each sample with its absorbance value at 278 nm, the extinction coefficient for a 1% solution of the protein in a 1 cm pathlength cell at 278 nm ($E^{1\%}_{1cm,278}$) was determined.

2. Sedimentation Velocity Experiments

Sedimentation studies were performed in 12 mm 4° synthetic boundary cells at 60,000 rpm. Schlieren optics were used and photographs

taken at specific time intervals. A Nikon model 6C microcomparater was employed to measure the distance from the maximum ordinate of the sedimenting peak to the reference hole.

The sedimentation coefficient, s (in sec), is related to the distance from the centre of rotation to the maximum ordinate, r (in cm), at time, t (in sec), and the angular velocity ω (in rad/sec), by:

$$s = (\frac{1}{\omega^2})(\frac{d \ln r}{dt}) \qquad [2]$$

Values for s were obtained by taking the natural logarithm of the measured r values, plotting them against t, and multiplying the resultant slope by $1/\omega^2$. To express the sedimentation coefficient in terms of water at 20°C, $s_{20,w}$, the following equation was used (69):

$$s_{20,w} = (s)(\frac{\eta_T}{\eta_{20}})_w (\frac{\eta}{\eta_0})_T (\frac{1 - \bar{v}\rho_{20,w}}{1 - \bar{v}\rho_T}) \qquad [3]$$

where:

$(\frac{\eta_T}{\eta_{20}})_w$ is the ratio of the viscosity of water at the experimental temperature, T, to that at 20°C,

$(\frac{\eta}{\eta_0})_T$ is the viscosity of the solvent relative to that of water at the temperature, T,

$\rho_{20,w}$ is the density of water at 20°C,

ρ_T is the density of the solvent at the temperature, T,

$\bar{v}$ is the partial specific volume of the solute.

In this study, $\bar{v}$ for a protein was estimated from its amino acid composition (70). Density and viscosity values were taken from tables in the Handbook of Chemistry and Physics.

Intrinsic sedimentation coefficients, $s^o_{20,w}$, were determined by plotting $s_{20,w}$ against the initial protein concentration of the sample

and extrapolating the results to zero concentration.

3. Sedimentation Equilibrium Experiments

Conventional sedimentation equilibrium runs (71) were performed in 12 mm double sector cells with charcoal-filled Epon centrepieces and sapphire windows. Data were recorded either on photographic plates using Rayleigh interference optics or on the chart paper of a photoelectric scanner accessory, using UV absorption optics. Runs were assumed to be at equilibrium when no further changes in fringe position or pen tracing occurred.

The apparent weight average molecular weight, M_w, of a homogeneous protein, determined by such an experiment, is given by:

$$M_w = \left(\frac{2RT}{(1 - \bar{v}\rho)\omega^2}\right)\left(\frac{d \ln c}{dr^2}\right) \qquad [4]$$

where:

R is the universal gas constant,

T is the experimental temperature in °K,

$\bar{v}$ is the partial specific volume of the protein,

ρ is the solvent density,

ω is the angular velocity, and

c is the protein concentration at a distance, r, from the axis of rotation.

Where Rayleigh interference optics were employed, protein concentrations at the meniscus, c_m, were calculated according to:

$$c_m = c_o - \frac{r_b^2(c_b - c_m) - \int_{c_m}^{c_b} r^2 dc}{r_b^2 - r_m^2} \qquad [5]$$

where:

c_o is the initial protein concentration,

r_m is the distance from the meniscus to the axis of rotation,

r_b is the distance from the cell bottom to the axis of rotation,

c_b is the protein concentration at the cell bottom, and

c is the protein concentration at any distance, r, from the axis of rotation.

A direct measure of protein concentration in terms of fringes, Y, at any value of r, was determined by adding the fringe displacement at the point r to the concentration at the meniscus (expressed in fringes).

If the photoelectric scanner was employed, the absorption value, A, at any point along the cell provided a direct measure of protein concentration.

A plot of the natural logarithm of the protein concentration (expressed in fringes, Y, or absorbance units, A) *versus* r^2 yielded a straight line, the slope of which, $d \ln c/dr^2$, was used to determine the weight average molecular weight (using equation [4]) at any position along the cell.

To facilitate these calculations, computer programs, written by Dr. W.T. Wolodko (72) in the programming language APL, were employed.

F. BIOLOGICAL ACTIVITY STUDIES

A synthetic cardiac actomyosin system was used to investigate the biological role of each of the cardiac troponin components.

Myosin was isolated according to Tonomura *et al.* (73). Nucleotide contaminants were removed from the myosin by batch treatment with DEAE-Cellulose. Actin was purified according to Spudich and Watt (74). Tropomyosin was purified by hydroxyapatite column chromatography, as described by Eisenberg and Kielley (75), of the tropomyosin-rich

ammonium sulfate fraction obtained during the preparation of cardiac troponin (see Chapter III). Alternatively, tropomyosin was prepared by repeated isoelectric precipitation of the same starting material at pH 4.6.

The assay system consisted of 750 µg of synthetic cardiac actomyosin (SAM), prepared by mixing myosin and actin in a 4:1 ratio by weight (76), and 50 µg of tropomyosin in 10 mM tris-HCl, pH 7.6, 2.5 mM $MgCl_2$, 1 mM EGTA and 2.5 mM ATP at 20°C. The total volume of the reaction mixture was 3.0 ml.

The reaction was initiated by the addition of the SAM to the remaining constituents and followed by monitoring the liberation of inorganic phosphate ions released on hydrolysis of ATP using the method of Fiske and SubbaRow (77).

G. COSEDIMENTATION ANALYSIS

To test whether any of the components of cardiac troponin could interact with tropomyosin, a method similar in principle to that used by Drabikowski and his colleagues (78, 79) was employed. Cardiac tropomyosin was dissolved in 8 M urea, 50 mM tris-HCl, pH 7.5, to a concentration of 2 - 3 mg/ml. The solution was partitioned into four 1.0 ml aliquots. In separate studies, one member of the troponin complex was added to three of these aliquots, such that mole ratios of tropomyosin to the troponin component of 0.5:1, 1:1 and 2:1 were obtained. The four samples plus one containing the troponin subunit under investigation were then dialysed 24 - 48 h at 4°C against 0.5 M KCl, 50 mM tris-HCl, pH 7.5. Each solution was then centrifuged for 20 min at 35,000 g in a Beckman Model L preparative ultracentrifuge and each tube was analysed

for sediment. Where a precipitate was visible, it was washed with 10% TCA to remove traces of KCl which would interfere with subsequent SDS gel analysis of the sediment.

Under the solvent conditions employed, tropomyosin was fully soluble. Therefore, where a sediment occurred, and SDS gel analysis showed both tropomyosin and the troponin component to be present, the results provided evidence for an interaction occurring between the two regulatory subunits.

H. CALCIUM BINDING STUDIES

1. Free Ca^{2+} Ion Concentration

At concentrations near or below 10^{-5} M, it is difficult to prepare, accurately, metal ion solutions unless a metal ion buffer is employed. In studies of Ca^{2+} binding to TN-C, the protein was dissolved in a buffer solution of known pH and ionic strength which contained a known level of the calcium chelator, EGTA. Using principles outlined by Perrin and Dempsey (80), any desired level of free Ca^{2+} ions in solution could be attained by the addition of an appropriate amount of $CaCl_2$.

Metal complexes are formed in a solution containing a metal ion, M, and a chelating agent, L:

$$M + nL \rightleftharpoons ML_n$$

with an appropriate equilibrium or stability constant, K_M:

$$K_M = \frac{[ML_n]}{[M][L]^n} \qquad [6]$$

The chelating agent, L, generally can undergo protonation to form species which possess differing complexing abilities, with respect to M:

$$H^+ + L \rightleftharpoons HL, \text{ etc.}$$

Therefore, protons will compete with the metal ions for L. The apparent stability constant, K'_M, of a metal complex at any specified pH depends not only on the stability constant, K_M, of the complex, but on the stepwise dissociation constants (K_{a1}, K_{a2}, ...) for the chelating agent.

Also, the metal ion may undergo a hydrolysis reaction:

$$M + H_2O \rightleftharpoons MOH, M(OH)_2, \text{ etc.}$$

The appropriate equilibrium constants for these reactions must be known to describe properly the equilibrium situation.

The apparent stability constant, K'_M, is defined in terms of the equilibrium between a metal complex and its components, except that free chelator concentration is replaced by the total concentration of all species of the chelating agent not actually complexed to the metal ion, and free metal ion concentration includes hydrolysed metal ions and metal ions bound to other complexing species:

$$K'_M = \frac{K_M}{(\alpha_M)(\alpha_L)^n} \qquad [7]$$

where:

$$\alpha_M = ([M] + [MOH] + [M(OH)_2] + \ldots)/[M] \qquad [8]$$

$$\alpha_L = ([L] + [HL] + [H_2L] + \ldots)/[L] \qquad [9]$$

To evaluate α_L for a chelating agent such as EGTA (represented as H_4L in its fully protonated state), consideration must be given to the following stepwise equilibria:

$$H_4L \rightleftharpoons H_3L + H^+ \qquad K_{a1} = \frac{[H^+][H_3L]}{[H_4L]} \qquad [10]$$

$$H_3L \rightleftharpoons H_2L + H^+ \qquad K_{a2} = \frac{[H^+][H_2L]}{[H_3L]} \qquad [11]$$

$$H_2L \rightleftharpoons HL + H^+ \qquad K_{a3} = \frac{[H^+][HL]}{[H_2L]} \qquad [12]$$

$$HL \rightleftharpoons L + H^+ \qquad K_{a4} = \frac{[H^+][L]}{[HL]} \qquad [13]$$

(For convenience, the charges on the different chelator species have been neglected.) A rearrangement and combination of equations [10] - [13] gives:

$$[H_4L] = \frac{[H^+]^4[L]}{K_{a1}\,K_{a2}\,K_{a3}\,K_{a4}} \qquad [14]$$

$$[H_3L] = \frac{[H^+]^3[L]}{K_{a2}\,K_{a3}\,K_{a4}} \qquad [15]$$

$$[H_2L] = \frac{[H^+]^2[L]}{K_{a3}\,K_{a4}} \qquad [16]$$

$$[HL] = \frac{[H^+][L]}{K_{a4}} \qquad [17]$$

Therefore, α_L becomes:

$$\alpha_L = 1 + \frac{[H^+]}{K_{a4}} + \frac{[H^+]^2}{K_{a3}\,K_{a4}} + \frac{[H^+]^3}{K_{a2}\,K_{a3}\,K_{a4}} + \frac{[H^+]^4}{K_{a1}\,K_{a2}\,K_{a3}\,K_{a4}} \qquad [18]$$

An evaluation of α_L for an EGTA containing solution buffered to a specific pH can be made using the following stepwise equilibrium constants for EGTA (81): $pK_{a1} = 2.0$, $pK_{a2} = 2.65$, $pK_{a3} = 8.85$, and $pK_{a4} = 9.46$.

For the metal ions used in our experiments, Ca^{2+}, Sr^{2+} and Mg^{2+}, the pK_1 values for hydrolysis are, respectively (80): 12.6, 13.2 and 11.4. Therefore, under the experimental conditions employed ($7.5<pH<8.0$),

α_M reduces to unity. This allows K'_M to be approximated by:

$$K'_M = \frac{K_M}{\alpha_L} \qquad [19]$$

From Schwarzenbach *et al.* (81), $pK_{Ca} = 10.97$, $pK_{Sr} = 8.50$ and $pK_{Mg} = 5.21$. Under given experimental conditions, placing these values into equations [18] and [19] allows the calculation of apparent stability constants for the metal ion of interest.

Once the K'_M values are known, the free metal ion concentration, [M], can be obtained by substituting the expression for K_M (equation [6]) into equation [19]:

$$K'_M = \frac{[ML_n]}{[M][L]^n \alpha_L} \qquad [20]$$

Note that, in the experimental pH range, only a 1:1 complex between EGTA and metal ion will occur, resulting in n = 1. Also [ML] may be represented as the total metal concentration, $[M]_T$, minus that portion which is free:

$$[ML] = [M]_T - [M] \qquad [21]$$

From the definition of α_L (equation [9]), $[L]\alpha_L$ represents the total concentration of chelator in all its protonation states, $[L]_T$, minus that portion which is in the form of the metal complex:

$$[L]\alpha_L = [L]_T - [ML] \qquad [22]$$

$$= [L]_T - [M]_T + [M] \qquad [23]$$

Therefore:

$$K'_M = \frac{[M]_T - [M]}{[M]\,([L]_T - [M]_T + [M])} \qquad [24]$$

Equation [24] is a quadratic equation, more clearly seen on rearrangement:

$$K'_M[M]^2 + (K'_M[L]_T - K'_M[M]_T + 1)[M] - [M]_T = 0 \qquad [25]$$

The two solutions to this quadratic are given by:

$$[M] = \frac{-b \pm \sqrt{4ac}}{2a} \qquad [26]$$

where:

$$a = K'_M \qquad [27]$$

$$b = K'_M[L]_T - K'_M[M]_T + 1 \qquad [28]$$

$$c = -[M]_T \qquad [29]$$

The positive real number solution to [M] is the only physically possible one.

Often, to describe calcium concentration in a buffer in this thesis, the phrases "minus Ca^{2+}" and "plus Ca^{2+}" will be used to denote solutions containing 1 mM EGTA and no added $CaCl_2$, and solutions containing a free Ca^{2+} concentration of 2×10^{-4} M, respectively. Exceptions will be noted.

2. CD Ca^{2+} Titrations

TN-C was dissolved in 0.15 M KCl, 50 mM tris-HCl, pH 7.5, 1 mM EGTA and dialysed 24 h at 4°C against the same solvent prior to recording its CD spectrum in the peptide absorption range. After the addition of an aliquot of $CaCl_2$, the spectrum was recorded again. This process was repeated until no further change in the spectrum could be detected. Similar sets of spectra were collected with TN-C equilibrated against the same solvent, but containing 2 mM $MgCl_2$.

From these data, the number of Ca^{2+} ions bound per TN-C molecule, i, and an apparent binding constant, K_{app}, could be estimated as described by Willick and Kay (82) for the evaluation of the same parameters for Mg^{2+} binding to tRNA. Such calculations assume that the structural transition observed by CD involves only 2 states. Either TN-C has Ca^{2+} bound and has undergone the complete conformational change or no Ca^{2+} is bound and the conformational change has not occurred. This may be represented as:

$$\text{TN-C} + i\text{Ca}^{2+} \rightleftharpoons \text{TN-C} - \text{Ca}^{2+}_{i}$$

with:

$$K_{app} = \frac{[\text{TN-C} - \text{Ca}^{2+}_{i}]}{[\text{TN-C}][\text{Ca}^{2+}]^{i}} \qquad [30]$$

The fraction of TN-C molecules in the Ca^{2+}-bound state, f, can then be determined as the ratio of the change in ellipticity value at a particular free Ca^{2+} concentration at a particular wavelength, $\delta\theta$, to the maximum change which can be elicited in the ellipticity value at that wavelength, $\Delta\theta$:

$$f = \frac{\delta\theta}{\Delta\theta} = \frac{[\text{TN-C} - \text{Ca}^{2+}_{i}]}{[\text{TN-C}] + [\text{TN-C} - \text{Ca}^{2+}_{i}]} \qquad [31]$$

Substitution from equation [30] gives:

$$f = \frac{K_{app}[\text{Ca}^{2+}]^{i}}{1 + K_{app}[\text{Ca}^{2+}]^{i}} \qquad [32]$$

Rearrangement of equation [32] and taking logarithms gives:

$$\log\left(\frac{1}{f} - 1\right) = \log\frac{1}{K_{app}} - i\log[\text{Ca}^{2+}] \qquad [33]$$

By plotting the titration data in the form of log (1/f - 1) versus pCa, a straight line is obtained with log $1/K_{app}$ given by the intersection point of the line with the ordinate axis, and i given by the slope of the line.

In these titration studies, $\delta\theta$ and $\Delta\theta$ were determined at 221 nm, the position of one of the minima in the TN-C CD spectrum.

3. Gel Filtration

Hummel and Dreyer (83) first used gel filtration as a rapid and accurate method to study protein binding phenomena. Using this technique, with the modifications of Voordouw and Roche (84), the number of Ca^{2+} ions bound per molecule of TN-C, and an apparent association constant, were determined.

In principle, the gel filtration column is equilibrated against a buffer containing a certain level of the ligand of interest (Ca^{2+} in this study). The protein is equilibrated against the same buffer, but containing a higher ligand concentration, and applied to the column. On elution with the same solution used to equilibrate the column, the protein moves down the column in the exterior mobile phase. Excess ligand is removed from the protein band until the binding equilibrium is satisfied by the concentration of unbound ligand ahead of the band. Finally, the protein and its complexed ligand elute from the column at the void volume, followed later by a peak containing excess ligand. The ratio of ligand to protein concentrations in the void volume peak reflects the number of ligand molecules bound per molecule of the protein. By manipulation of the ligand concentration in the solution against which the column is initially equilibrated, the effect of ligand concentration on ligand binding may be investigated, and an apparent binding constant

determined.

To determine the maximal number of Ca^{2+} ions which would bind to each cardiac TN-C molecule, a 1.0 x 30 cm column of Sephadex G-25 Fine was equilibrated against 0.15 M KCl, 50 mM tris-HCl, pH 7.5 and 1 x 10^{-4} M $CaCl_2$. Three to four mg of lyophilized TN-C were dissolved in 0.6 ml of the same buffer, but containing 5 x 10^{-4} M $CaCl_2$, and dialysed overnight at 4°C. The TN-C solution then was allowed to equilibrate to 22°C and was applied to the column. A constant elution rate of 20 ml/h was maintained by an LKB peristaltic pump and 2.5 min fractions were collected. Each fraction was analysed for protein content by measuring its absorbance at 278 nm, and for calcium content using a Unicam SP90A Series 2 atomic absorption spectrophotometer, with instrumental settings adjusted as described in Unicam Atomic Absorption Method Ca-2 (85).

To determine the dependence of Ca^{2+} binding on Ca^{2+} concentration, the column equilibration buffer was altered to contain 5 x 10^{-5} M EGTA and a specific concentration of $CaCl_2$ which would produce submaximal Ca^{2+} binding to TN-C. In these experiments, the TN-C was applied to the column after it had been dialysed against 0.15 M KCl, 50 mM tris-HCl, pH 7.5, 5 x 10^{-5} M EGTA and 1 x 10^{-4} M $CaCl_2$. Again, integration of the amount of Ca^{2+} eluting in the void volume peak and division of this sum by the total amount of protein in the peak provided the number of Ca^{2+} ions bound to each TN-C molecule under the experimental conditions.

For each experiment, a new standard curve for the determination of calcium was prepared. The column equilibration buffer was used in each case as the zero readout or baseline value to which additions of $CaCl_2$ yielded standard solutions covering the range of calcium concentration from zero to 1 x 10^{-4} M, in increments of 1 x 10^{-5} M, above the

baseline level.

As in the case of the CD titration studies, an analogous set of Ca^{2+} binding experiments was performed in the presence of 2 mM $MgCl_2$ to observe how Mg^{2+} ion affected the Ca^{2+} binding parameters of cardiac TN-C.

To avoid contamination of solutions with Ca^{2+} from laboratory glassware, Nalgene beakers, test tubes, volumetric flasks, solution bottles and pipets were employed throughout the study.

CHAPTER III

TROPONIN PREPARATIVE METHODOLOGY

The development of the methodology to obtain homogeneous protein preparations on which to perform biochemical investigations was, as is usual in such an endeavour, a major part of the whole project. This chapter is devoted to the presentation of a detailed account of the preparative schemes used to isolate the components of bovine cardiac troponin. It is intended to serve as a bridge between the chapter presenting the experimental procedures employed in this study and those chapters reporting the results of the experiments.

The preparative methods related in this chapter represent the final refinements of procedures already presented in publications stemming from this investigation (35, 37, 38).

A. CARDIAC TROPONIN

During the initial stages of this project, troponin was prepared from fresh or fresh-frozen beef hearts essentially as described by Murray and Kay (14) for the isolation of rabbit skeletal muscle troponin. Later it became evident that such preparations were suitable only for the further purification of cardiac TN-C. This became evident on the basis of the following two phenomena. First, SDS gels demonstrated a large number of contaminating proteins in these troponin preparations and, second, the procedure was a protracted one, requiring 4 days to progress from muscle tissue to dialysing troponin. During this time, endogenous proteases destroyed most of the TN-T and much of the TN-I originally present. These problems were overcome by switching to methodology

devised by Tsukui and Ebashi (33). This method was rapid (1 day) and selective, carrying few contaminants over with the troponin.

As the first reports of work on cardiac TN-C from this laboratory (34, 35) employed the Murray and Kay, or muscle powder, method, a description of this scheme is included in this chapter. Also described is the Tsukui and Ebashi, or LiCl extraction procedure, to which minor modifications were made.

1. Muscle Powder Method

The entire procedure was conducted at 4°C. One kg of cardiac tissue was minced in a Waring blender for 30 sec in 3 volumes of 0.3 M KCl, 0.15 M potassium phosphate buffer at pH 6.5, and 0.2 mM ATP. After extracting for 15 minutes, the mince was centrifuged at 2000 g for 10 minutes. The supernatant, containing dissolved myosin, was discarded. The sediment was suspended in 3 volumes of distilled water, mixed for 20 min and centrifuged again. The sediment was subjected to a similar wash in 0.01 M $NaHCO_3$ followed by another in distilled water. These washings removed soluble protein contaminants, such as haemoglobin, from the mince. The resultant muscle residue was washed twice with 3 volumes of 95% ethanol, followed by 2 washes with acetone. About 110 g of dried muscle powder was obtained from the original kilogram of muscle tissue.

The powder from a kilogram of heart was extracted at room temperature for 18 h in 7 volumes of 1 M KCl, 25 mM tris-HCl, pH 7.6, and 1 mM DTT. After centrifugation, the supernatant was cooled to 4°C. The sediment was re-extracted in the same manner for 3 h more. After centrifugation the second supernatant was mixed with the first and the pH of the combined supernatants adjusted to 4.6. The supernatant pH was readjusted to neutrality after the precipitated tropomyosin was

removed by centrifugation at 5000 g for 30 min. The protein solution was dialysed at 4°C overnight against 4 volumes of 0.5 mM DTT and then subjected to ammonium sulfate fractionation. The precipitate collected between 40 and 70% ammonium sulfate saturation was collected by centrifugation at 5000 g for 45 min. The sediment was taken up in 100 - 200 ml of 5 mM tris-HCl, pH 7.6, 0.5 mM DTT and dialysed against 2 x 7 ℓ of the solvent solution. Solid KCl was added to the dialysed protein solution to a concentration of 1 M and a second isoelectric precipitation at pH 4.6 was performed to remove tropomyosin. The resulting supernatant (crude troponin) was dialysed against distilled water and lyophilized. Approximately 1 g of crude troponin was obtained from 1 kg of muscle by this procedure.

2. LiCl Extraction Procedure

The full procedure was carried out at 4°C. One kg of cardiac muscle was minced and extracted, as in the muscle powder method, in 3 volumes of 0.3 M KCl, 0.15 M potassium phosphate buffer, pH 6.5, and 0.2 mM ATP. After centrifugation, the sediment was subjected to numerous washes; once with 3 volumes of distilled water, 5 times with 0.1 M KCl containing 1 mM $NaHCO_3$, and twice more with 1 mM $NaHCO_3$. The muscle residue was adjusted to 0.4 M in LiCl by adding to it 0.25 volume of 2 M LiCl. This suspension was centrifuged immediately for 10 min at 7000 g and the sediment resuspended in 0.4 M LiCl to 2 times the original volume of the mince. The pH was lowered to 5.1 and the mince was stirred continuously on a magnetic stirring apparatus for 3 h. After centrifugation, the supernatant was collected and its pH adjusted to 7.5. Two ammonium sulfate fractions were saved from the protein solution. The fraction between 35 and 45% saturation yielded crude troponin and

that between 45 and 60% gave a crude tropomyosin. Each was redissolved in about 50 ml of 1 mM $NaHCO_3$ and dialysed at 4° against the same solvent. The crude troponin fraction, after dialysis, generally appeared opalescent. Therefore, it was clarified by centrifugation prior to lyophilization. This procedure generated about 600 mg of crude troponin and 800 mg of crude tropomyosin per kilogram of initial heart muscle.

B. SEPARATION OF THE CARDIAC TROPONIN COMPONENTS

1. DEAE-Sephadex Column Chromatography

The next stage in the isolation of the individual cardiac troponin subunits involved a preliminary separation on DEAE-Sephadex A-25 in the presence of 6 M urea. About 600 mg of crude troponin were dissolved in about 30 ml of 6 M urea, 50 mM tris-HCl, pH 7.5, 2 mM EGTA, 0.5 mM DTT and dialysed against 2 x 500 ml of the same buffer. The protein solution was applied to a 2.5 x 30 cm column of DEAE-Sephadex A-25 which had been equilibrated against the starting solvent. A linear one-litre gradient from 0 to 0.5 M KCl was used to elute the protein from the column. The elution profile of such a column is shown in Figure 7. Four sets of fractions (I, II, III, IV) were collected.

Crude troponin prepared by the muscle powder or LiCl extraction procedures gave similar profiles on DEAE-Sephadex. However, analysis by SDS gel electrophoresis revealed that the compositions of peaks I and II for one type of troponin differed significantly from those for the second type. Starting with muscle powder troponin, the two peaks each contained several classes of protein molecules, most of which were unidentifiable. However, starting with LiCl extracted troponin, peak I material, eluting prior to the application of the KCl gradient, proved

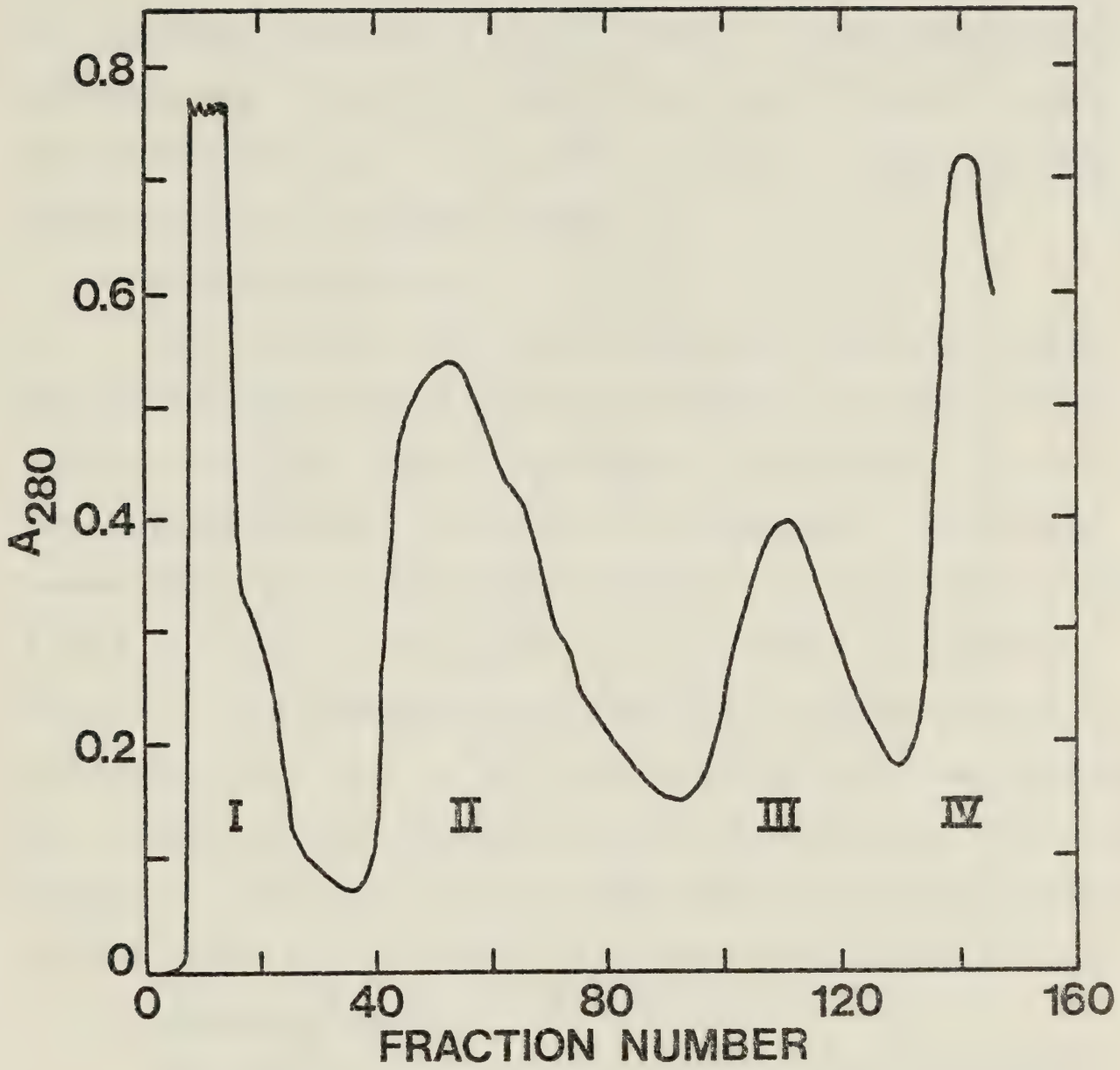

Figure 7. Chromatography of crude troponin on DEAE-Sephadex A-25. Protein was applied to the column in 6 M urea, 50 mM tris-HCl, pH 7.5, 2 mM EGTA, 0.5 mM DTT and eluted with a linear one-litre KCl gradient from 0 to 0.5 M. The flow rate was 55 ml/h and 10 min fractions were collected.

to be rich in TN-I. Peak II material, eluting at low KCl concentrations, was rich in TN-T.

For both kinds of troponin, peak III protein contained mainly TN-C, with some contamination by TN-T. Region IV of the profile was determined to be nucleotide in nature, due to its high ratio of absorbance at 260 nm relative to that at 280 nm and its very high extinction coefficient in this wavelength region.

2. Purification of TN-C

Peak III fractions were pooled and dialysed extensively against water made slightly alkaline (pH 8) by the addition of ammonia. After lyophilization, about 100 mg of this material was recovered. It consisted primarily of TN-C, with some TN-T contamination. TN-T could be removed effectively by gel filtration through a 2 x 100 cm bed of Biogel A 0.5 m in 8 M urea, 50 mM tris-HCl, pH 7.5, 2 mM EGTA, 0.5 mM DTT (Figure 8). This chromatography was performed at room temperature. A clean separation of TN-T and TN-C generally was obtained. The TN-C peak was collected, dialysed extensively against slightly alkaline water, and lyophilized. About 60 mg of TN-C, judged homogeneous by SDS gel electrophoresis (Figure 9), was obtained per kilogram of original heart muscle.

3. Purification of TN-I

Peak I from chromatography of LiCl-extracted troponin on DEAE-Sephadex, after dialysis against 10^{-4} M HCl and lyophilization, proved to be rich in TN-I. Two further chromatographic steps were necessary to purify the TN-I.

The entire yield of the peak I region, 250 - 300 mg of lyophilized powder, was dissolved in about 20 ml of 8 M urea, 70 mM Na formate buffer at pH 4.0, 0.1 M NaCl, 2 mM EGTA, 0.5 mM DTT and dialysed

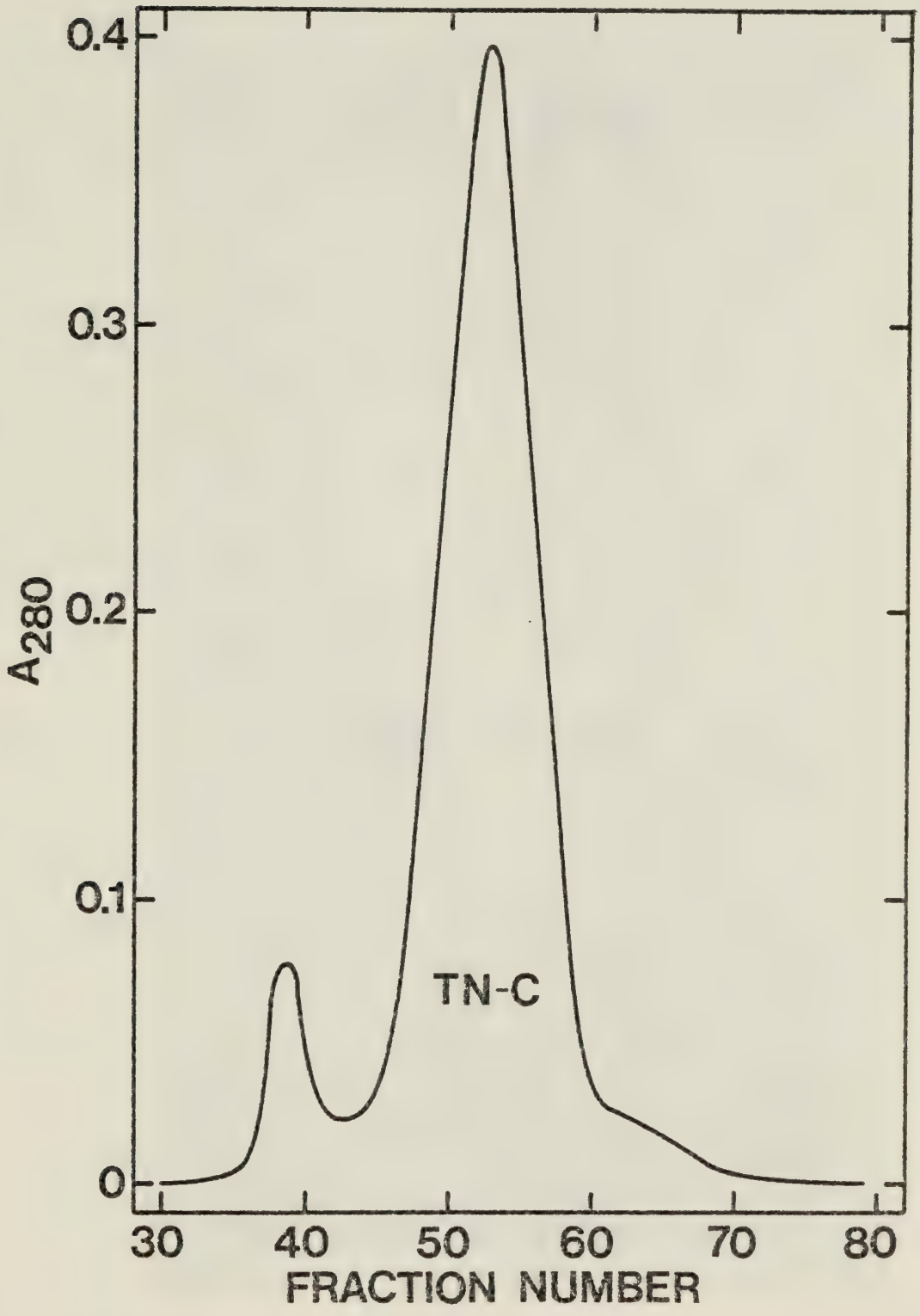

Figure 8. Purification of TN-C on Biogel A 0.5 m. The protein was applied to a 2.5 x 100 cm column in 3 ml of 8 M urea, 50 mM tris-HCl, pH 7.5, 2 mM EGTA, 0.5 mM DTT. The flow rate was 20 ml/h and 12 min fractions were collected.

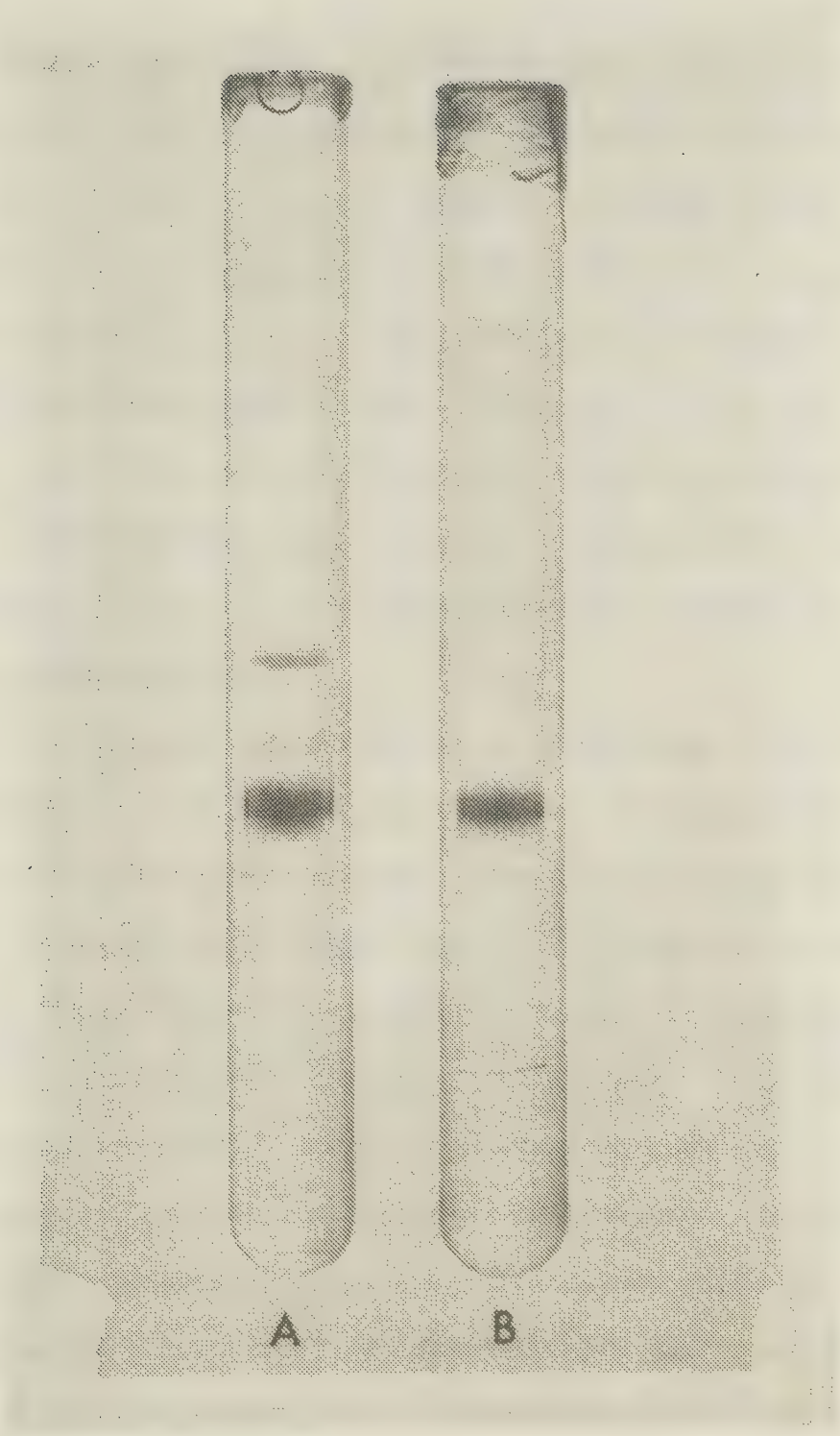

Figure 9. SDS polyacrylamide gels of TN-C. Gel A represents peak III material from a DEAE-Sephadex column. Gel B shows purified bovine cardiac TN-C from a Biogel A 0.5 m column. 50 µg of protein were applied to each gel.

against 2 x 500 ml of the same solvent. The dialysed protein solution was applied to a 2.5 x 30 cm column of CM-Sephadex C-25 in the same buffer and eluted with a linear one-litre gradient from 0.1 to 0.5 M NaCl (Figure 10). SDS gel electrophoresis revealed that the peak eluting subsequent to the start of the salt gradient contained mainly TN-I. A high molecular weight contaminant (∿60,000 on SDS gels) was also present. This contaminant could be removed by gel filtration through a 2 x 100 cm bed of Biogel P-200 equilibrated against 8 M urea, 0.2 M NaCl, 1% acetic acid (Figure 11). The TN-I fractions were pooled and dialysed against 10^{-4} M HCl and lyophilized, yielding about 90 mg of powder. SDS gel analysis showed the protein to be homogeneous TN-I (Figure 12).

4. Purification of TN-T

The isolation of cardiac TN-T in a homogeneous form was complicated by the extreme lability of the molecule. Dialysis against non-denaturing buffers for extended periods led to the appearance of increasing amounts of low molecular weight polypeptide fragments on SDS gels. The principal cause of TN-T break-down was thought to be digestion by proteases endogenous to heart tissue and which were carried over in troponin preparations (86). In 6 or 8 M urea, TN-T appeared to be stable. Therefore, peak II material from DEAE-Sephadex chromatography of LiCl extracted troponin was not dialysed against water and lyophilized, but rather against 8 M urea, 70 mM sodium formate buffer at pH 4.0, 0.1 M NaCl, 2 mM EGTA, 0.5 mM DTT. The dialysed TN-T - rich protein was applied to a 2.5 x 30 cm column of CM-Sephadex C-25, equilibrated against the same buffer. The protein retained by the column matrix was eluted with a linear one-litre 0.1 to 0.5 M NaCl gradient (Figure 13). The TN-T fractions were pooled, made 5% in formic acid and applied

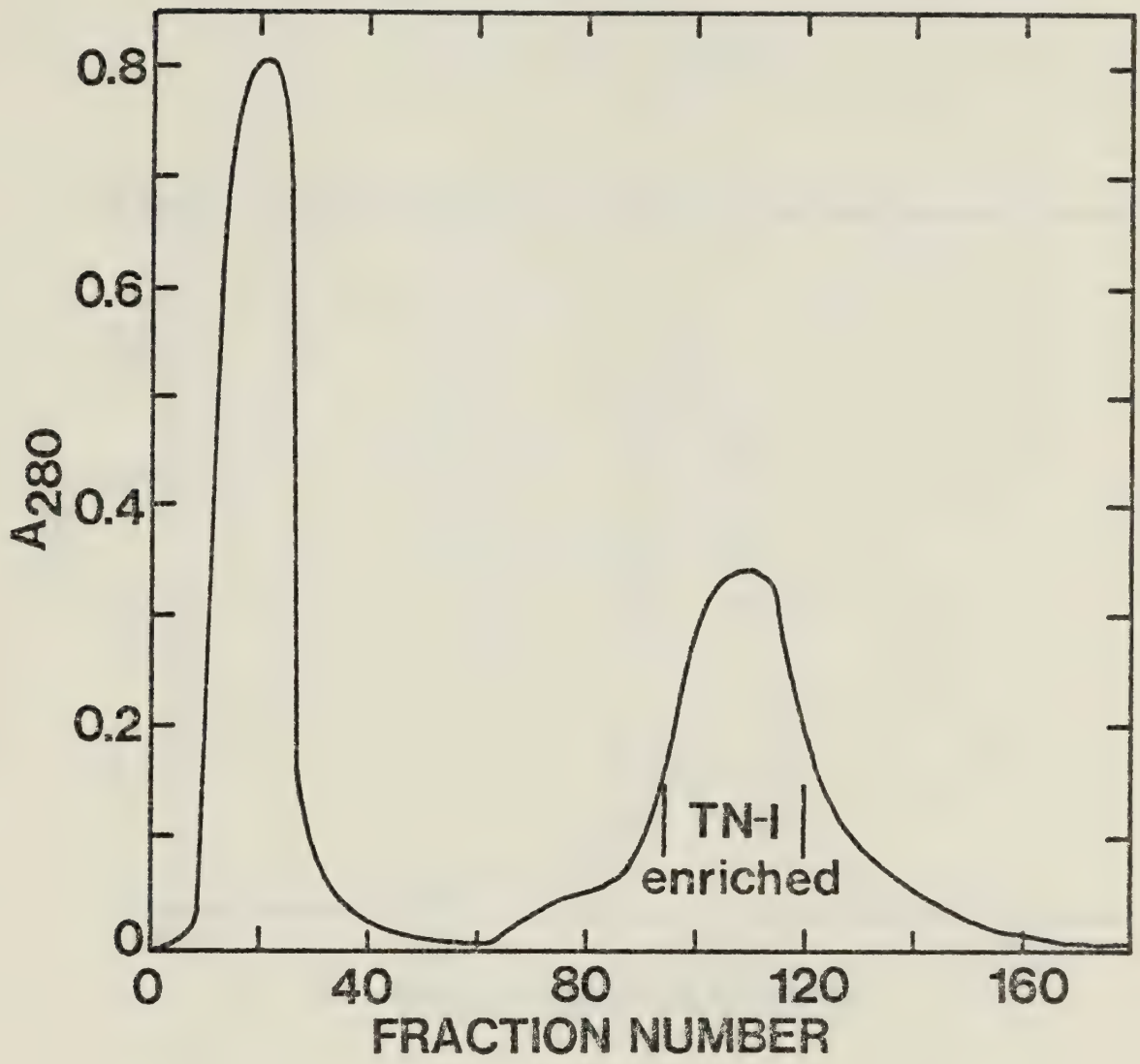

Figure 10. Chromatography of TN-I enriched material on CM-Sephadex C-25. Protein was applied to the column in 8 M urea, 70 mM sodium formate buffer, pH 4.0, 0.1 M NaCl, 2 mM EGTA, 0.5 mM DTT and eluted with a linear 0.1 - 0.5 M NaCl gradient. The flow rate was 55 ml/h and 10 min fractions were collected.

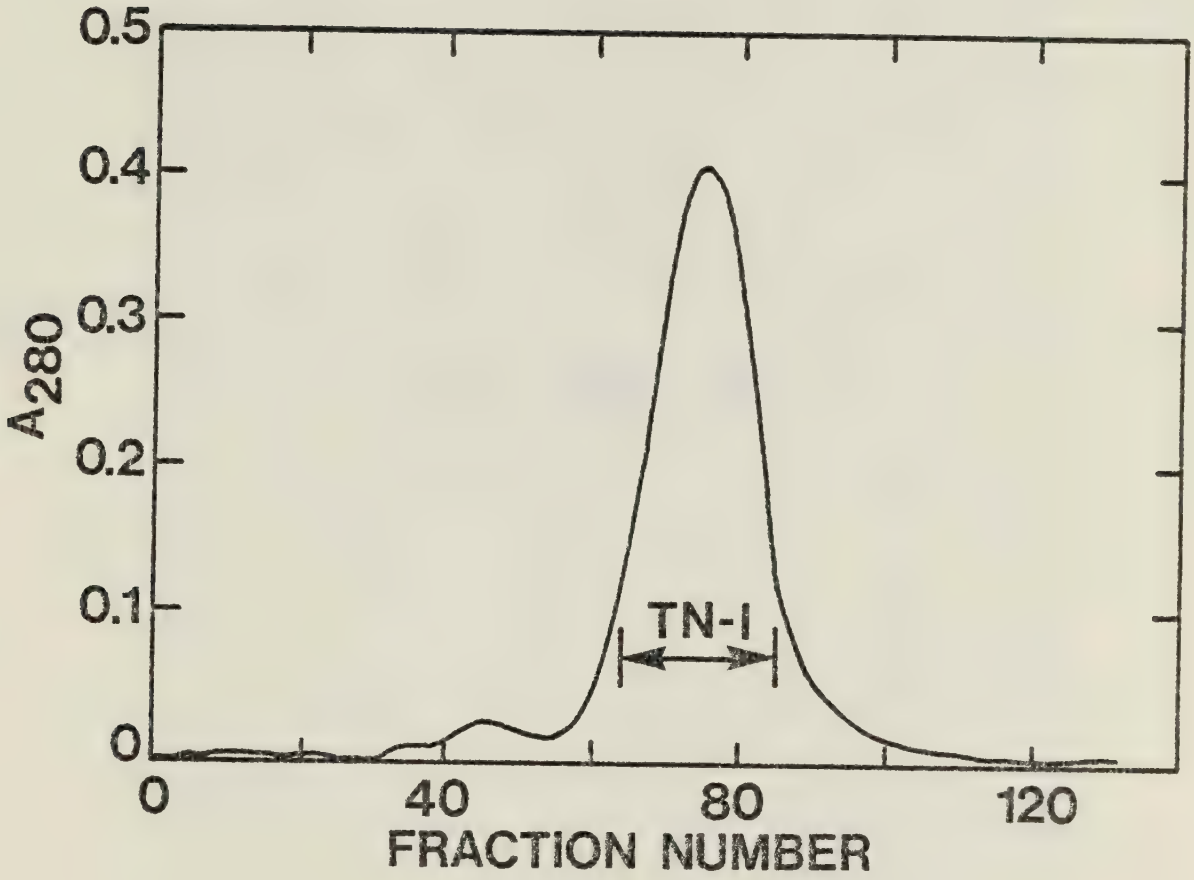

Figure 11. Purification of TN-I on Biogel P-200. The protein was applied to a 2.5 x 100 cm column in 3 ml of 8 M urea, 1% acetic acid and 0.2 M NaCl. The flow rate was 7 ml/h and 80 ml of eluant were collected prior to initiation of collection of 18 min fractions.

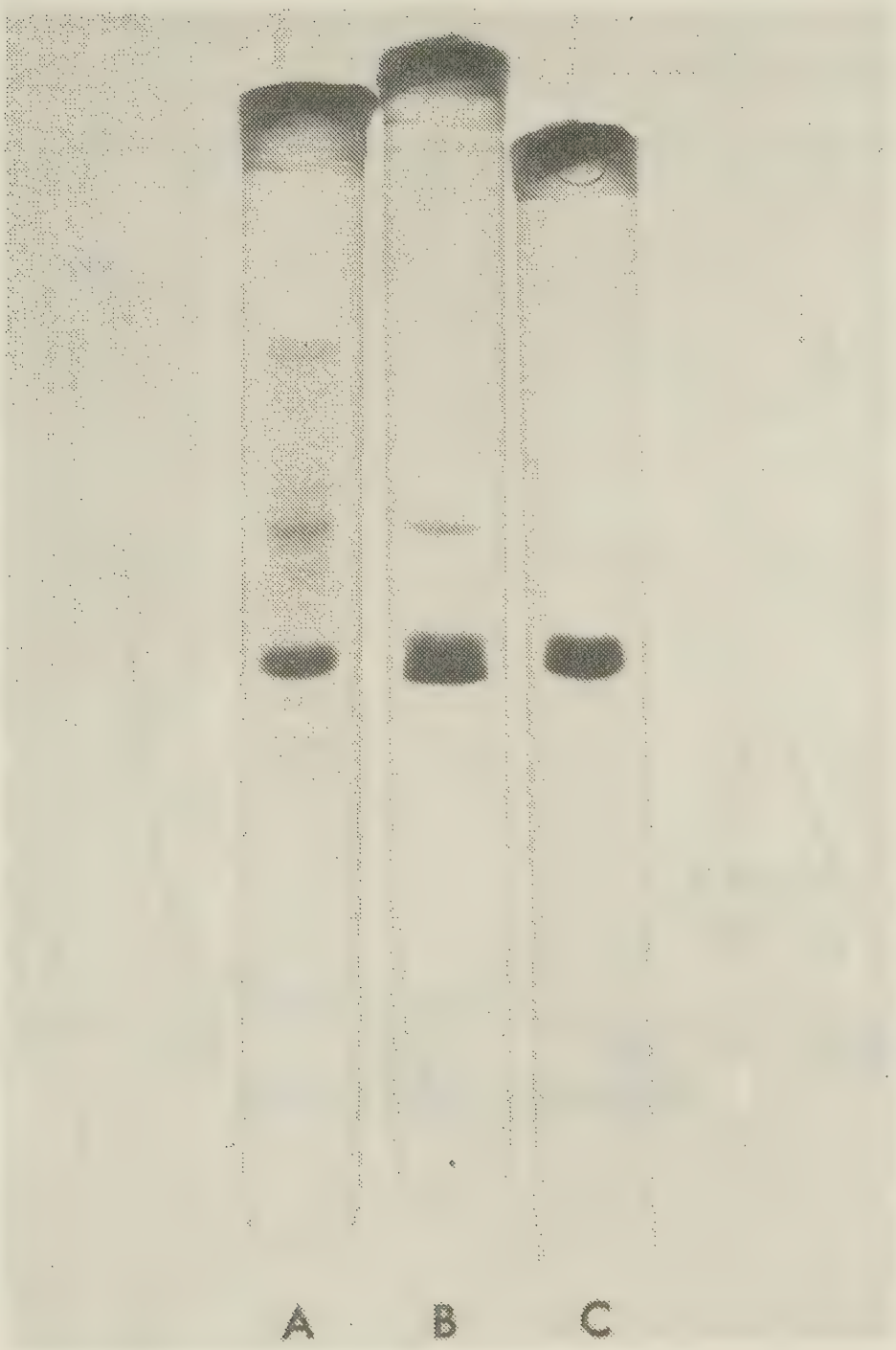

Figure 12. SDS polyacrylamide gels of cardiac TN-I. Gel A shows peak I material from a DEAE-Sephadex column. Gel B presents TN-I enriched material after CM-Sephadex chromatography. Gel C reveals TN-I from a Biogel P-200 column to be homogeneous. 50 µg of protein were applied to each gel.

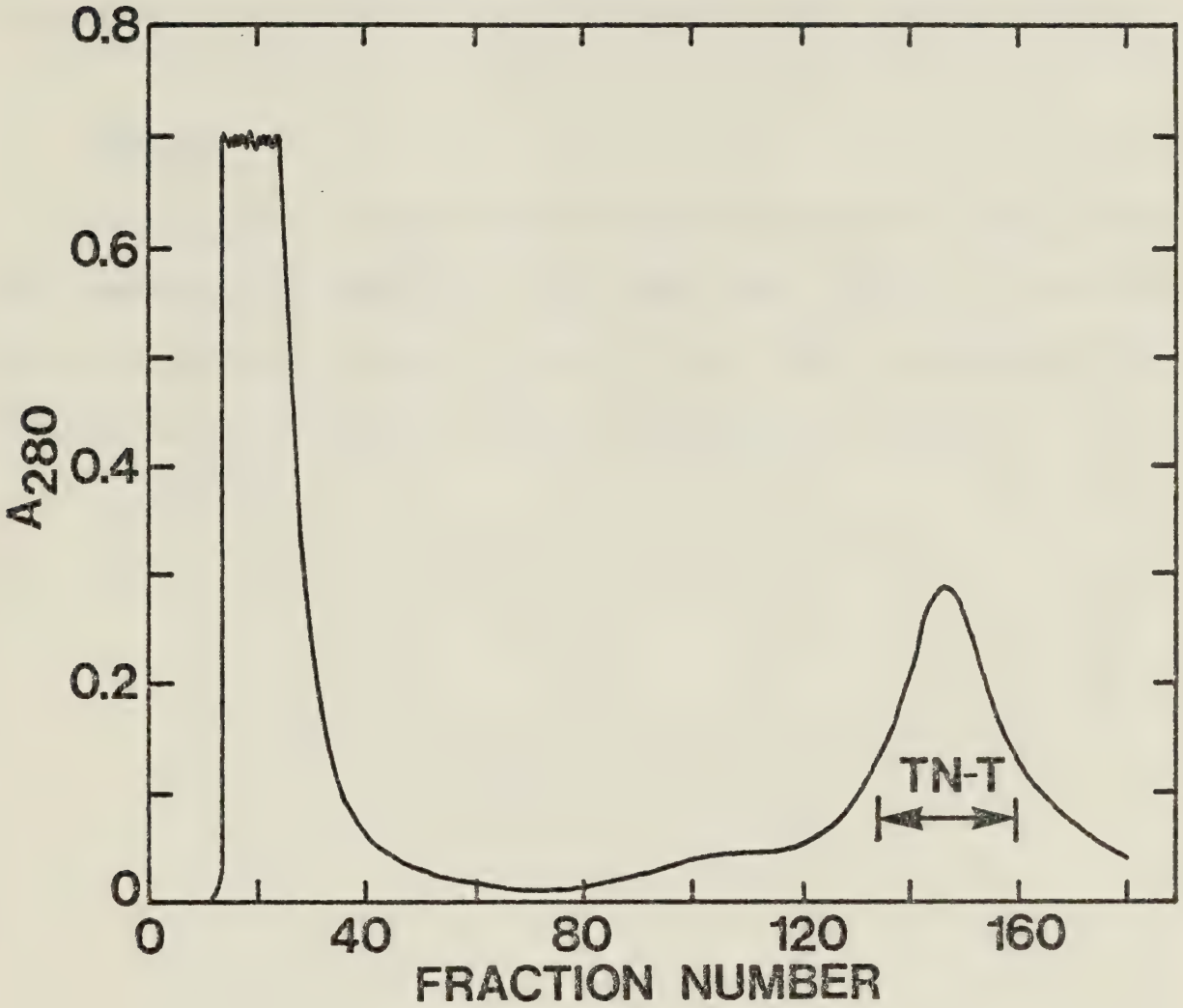

Figure 13. Chromatography of TN-T enriched material on CM-Sephadex C-25. Protein was applied in 8 M urea, 70 mM sodium formate buffer, pH 8.0, 0.1 M NaCl, 2 mM EGTA, 0.5 mM DTT and eluted with a linear 0.1 - 0.5 M NaCl gradient. The flow rate was 55 ml/h and 10 min fractions were collected.

directly to a 5 x 100 cm Biogel P-2 desalting column. The protein was eluted with 5% formic acid (Figure 14). Within 6 h, the protein came off the column and was lyophilized immediately. The final yield of homogeneous TN-T (Figure 15) per kilogram of heart was about 60 mg.

C. SUMMARY

The results of the purification schemes described in this chapter are summarized in Figure 16. Gel A shows crude troponin, prepared by the LiCl extraction method. Gels B, C and D show, respectively, TN-T, TN-I and TN-C, as isolated from the crude troponin in gel A.

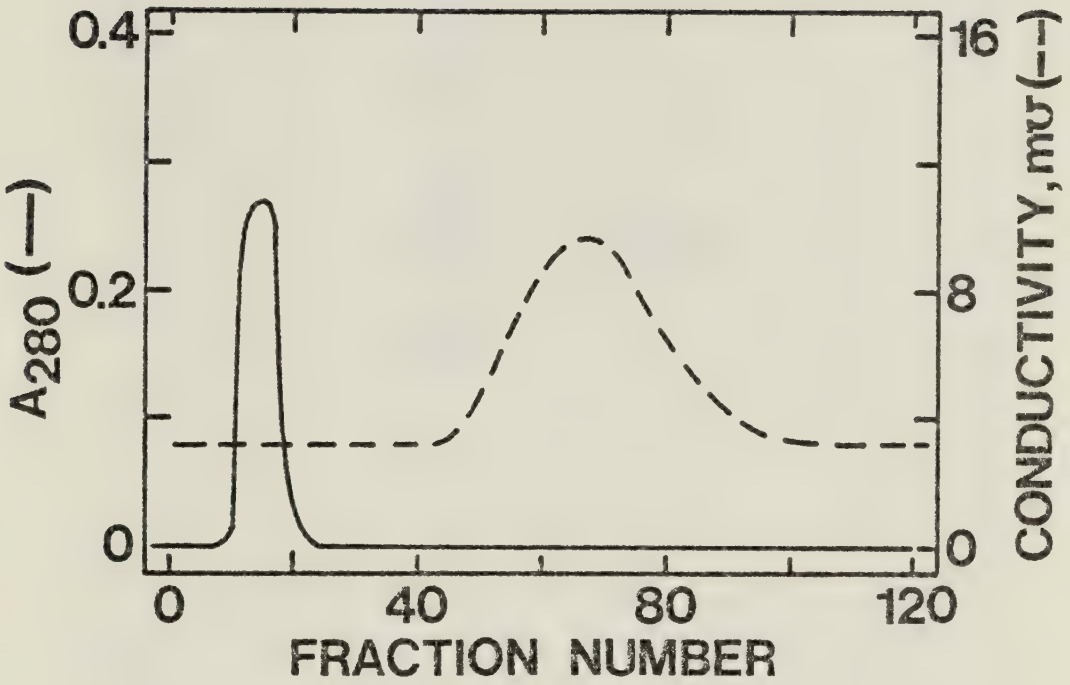

Figure 14. Desalting of TN-T solutions on Biogel P-2. The pooled TN-T fractions from a CM-Sephadex column were made 5% in formic acid and applied to a 5 x 100 cm column of Biogel P-2. The protein was eluted with 5% formic acid at a flow rate of ∿100 ml/h. 400 ml of eluant were collected prior to initiation of collection of 10 min fractions. The solid line represents protein elution measured by absorption at 280 nm. The dashed line represents salt elution measured with a Radiometer type CDM 2 e Conductivity Meter.

Figure 15. SDS polyacrylamide gels of cardiac TN-T. Gel A presents peak II material from a DEAE-Sephadex column. Gel B shows TN-T purified by CM-Sephadex chromatography. 60 µg of protein were applied to each gel.

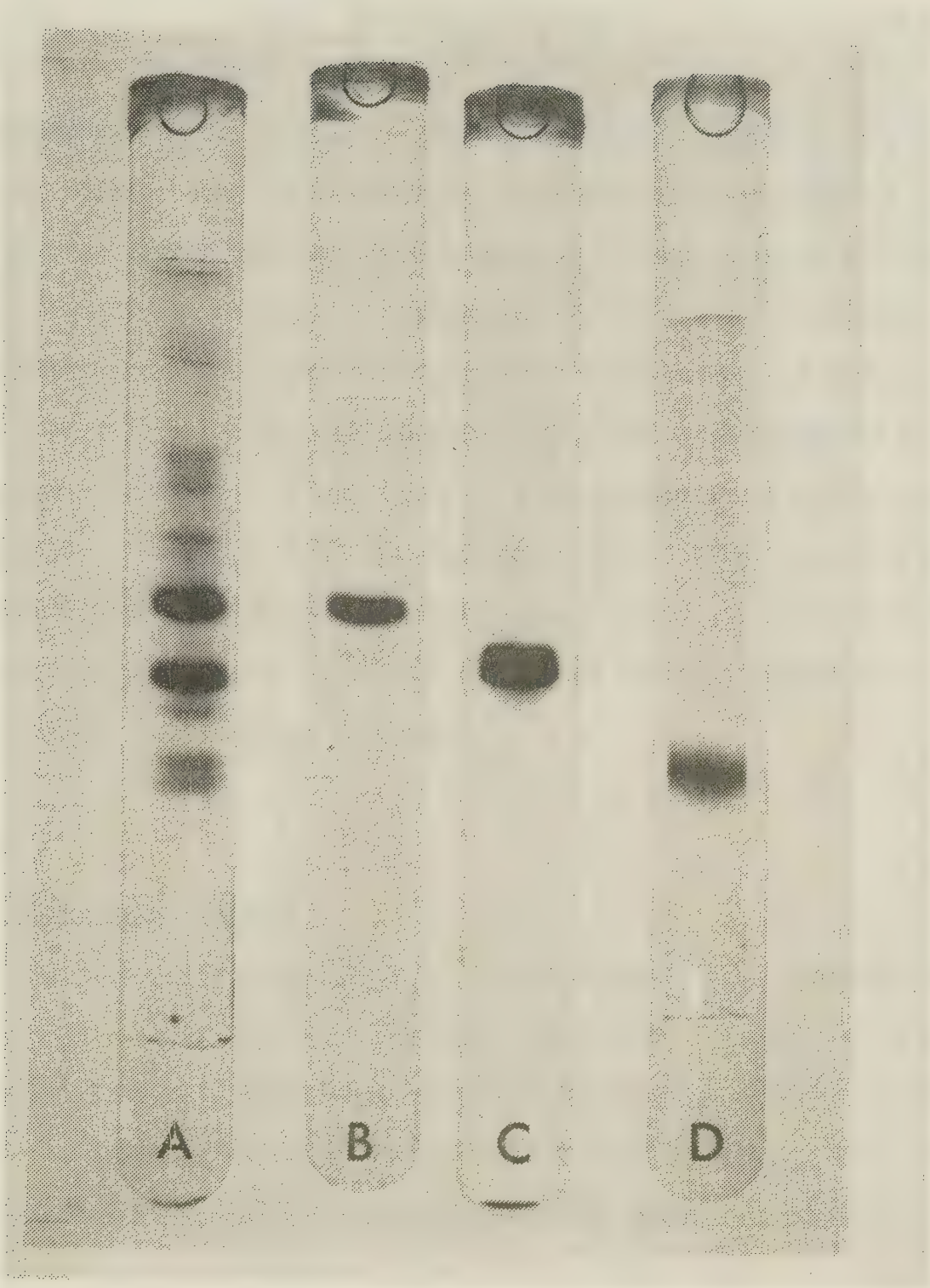

Figure 16. SDS polyacrylamide gels of LiCl extracted cardiac troponin (gel A) and purified TN-T (gel B), TN-I (gel C) and TN-C (gel D). 50 µg of protein were applied to each gel.

CHAPTER IV

CARDIAC TROPONIN SUBUNITS

This chapter is devoted to the presentation and discussion of the results of physico-chemical studies on the isolated constituents of bovine cardiac troponin. Most of the material presented in this chapter is drawn from 3 publications on the subject (35, 37, 38). Recently, other investigators have reported the amino acid sequences of bovine cardiac TN-C (47) and rabbit cardiac TN-I (52), and have presented a general characterization of the individual bovine cardiac troponin components (46). A comparison of the data presented in these papers with our own provided a new basis for interpreting some of our results, for performing new experiments to obtain additional information and for a reevaluation of some earlier findings.

A. TN-C

1. Amino Acid Analysis

The amino acid composition of bovine cardiac TN-C, prepared in our laboratory, is presented in Table I. The values are reported as residues per molecule, assuming a molecular weight of 18,500 (47). Also presented in Table I are the amino acid contents of rabbit skeletal (48) and bovine cardiac (47) TN-C, as determined from amino acid sequence studies.

Cardiac TN-C is rich in acidic residues, lacks histidine and tryptophan, and possesses a relatively high phenylalanine to tyrosine ratio. Such characteristics manifest themselves in the isolation properties of the protein, its electrophoretic mobility and its UV absorption

TABLE I

Amino acid composition of bovine cardiac TN-C

Amino Acid	Residues per molecule of protein		
	Rabbit Skeletal TN-C*	Bovine Cardiac TN-C**	Bovine Cardiac TN-C***
Lys	9	13.0	13
His	1	0.0	0
Arg	7	3.9	4
Asx	22	27.4	27
Thr	6	7.3	7
Ser	7	5.0	5
Glx	31	29.9	29
Pro	1	2.1	2
Gly	13	12.2	12
Ala	13	7.3	7
Val	7	8.2	8
Met	10	11.8	11
Ile	10	9.1	9
Leu	9	13.7	13
Tyr	2	2.7	3
Phe	10	8.2	9
Trp	0	0.0	0
1/2 Cys	1	2.0	2

*Collins (48).

**Assuming a molecular weight of 18,500.

***van Eerd and Takahashi (47).

spectrum.

Bovine cardiac and rabbit skeletal TN-C are not identical molecules. For example, cardiac TN-C contains two cysteine and three tyrosine residues compared with one cysteine and two tyrosines in skeletal TN-C. Van Eerd and Takahashi (47) argue, based upon a comparison of the two sequences and an estimated gene mutation rate, that differences between the two molecules represent tissue- as opposed to species-dependent variations. This statement is supported by the recent publication of the chicken skeletal muscle TN-C amino acid sequence by Wilkinson (87). He discovered an 11% difference (17 substitutions) between the sequences of chicken and rabbit skeletal TN-C. There exists a 31% variance between chicken skeletal and bovine cardiac TN-C, whereas that between rabbit skeletal and bovine cardiac TN-C is 35%. Therefore, the skeletal TN-C molecules of a bird (chicken) and a mammal (rabbit) are more alike than two types of mammalian TN-C (rabbit skeletal and bovine cardiac). The class of TN-C molecule of a particular tissue may represent the end-product of a unique set of evolutionary stresses, implying that subtle, but significant, functional differences may exist among the various types of TN-C.

2. Extinction Coefficient

Cardiac TN-C was determined to have an extinction coefficient at 278 nm, for a 1% solution, in a 1 cm pathlength cell ($E^{1\%}_{1cm,278}$) of 3.4 (Figure 17).

3. Sedimentation Coefficient

Sedimentation velocity experiments in 0.15 M KCl, 50 mM tris-HCl, pH 8.0, 1 mM EGTA indicated an intrinsic sedimentation coefficient ($s^{o}_{20,w}$) for cardiac TN-C of 1.93 S (Figure 18). Substitution of 1 mM

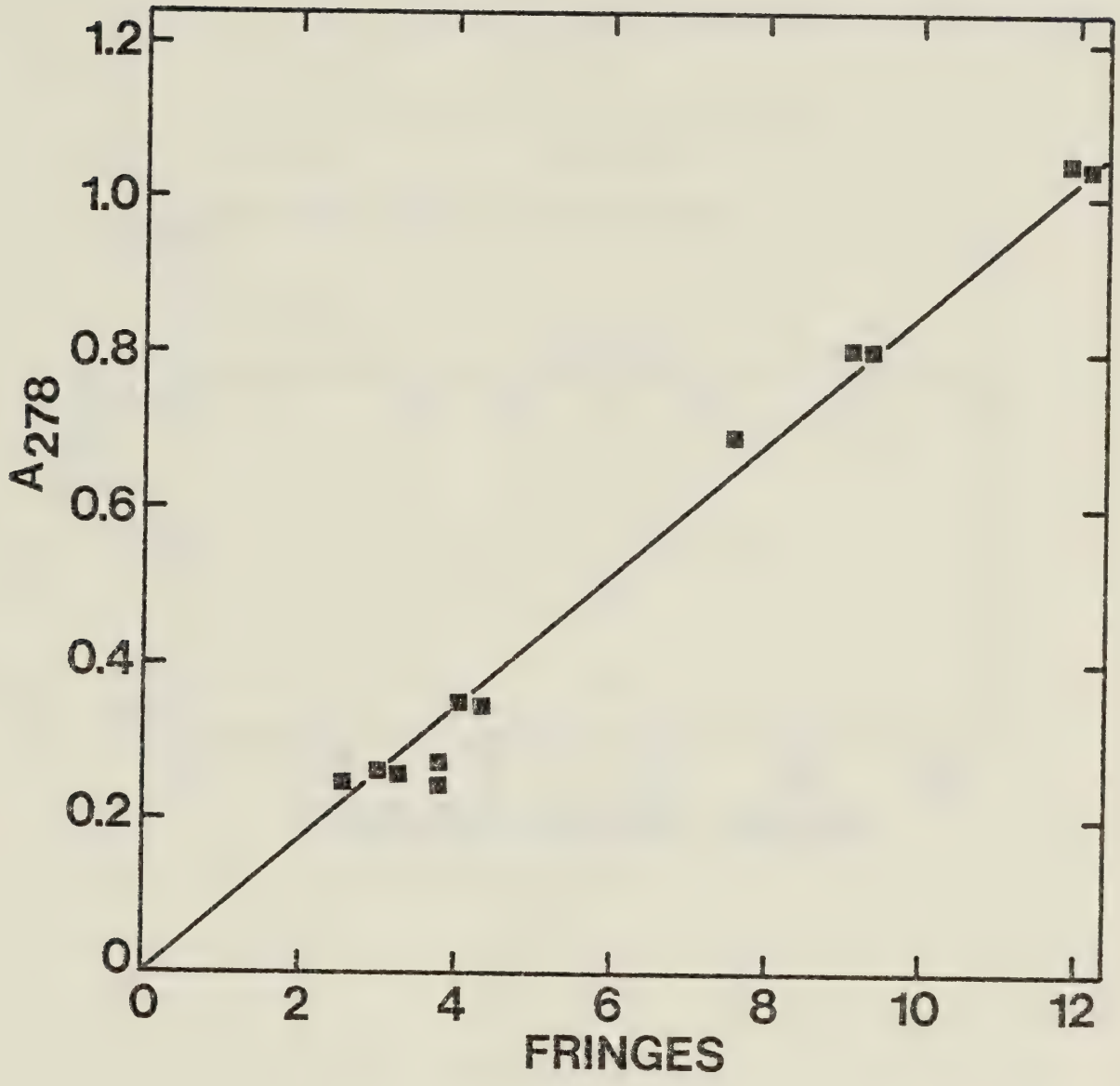

Figure 17. Determination of the extinction coefficient of TN-C. The protein was dissolved in 0.15 M KCl, 50 mM tris-HCl, pH 8.0, 1 mM EGTA and centrifuged at 12,000 rpm. The absorbance value at 278 nm was recorded for each sample, and its concentration determined refractometrically according to Babul and Stellwagen (68).

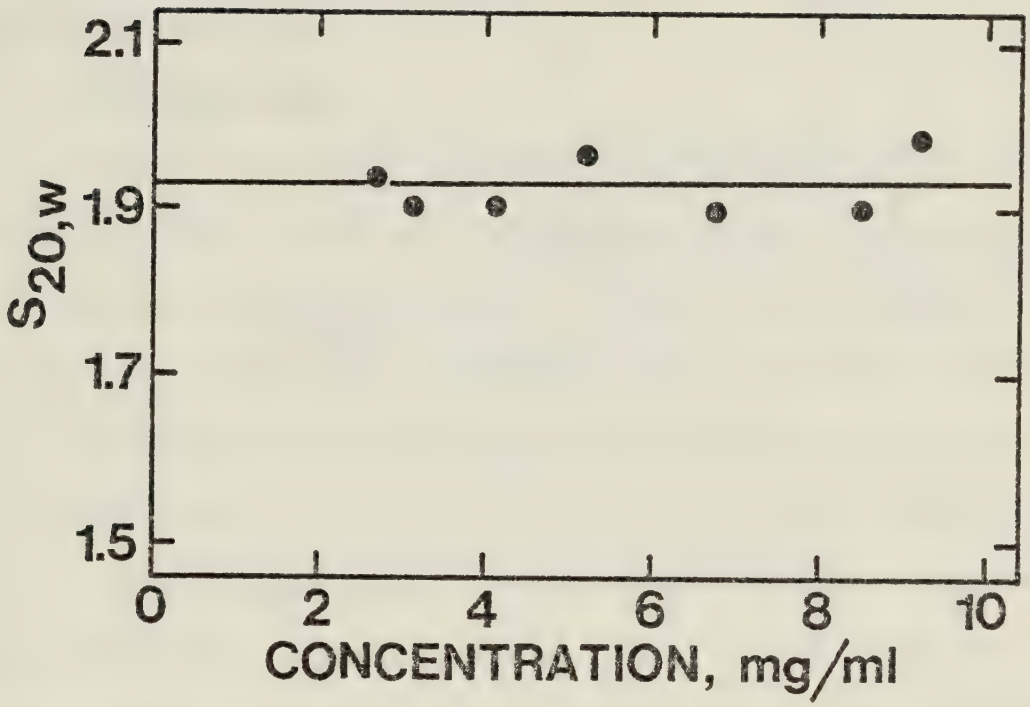

Figure 18. Determination of the intrinsic sedimentation coefficient of TN-C. TN-C samples of various concentrations were prepared in 0.15 M KCl, 50 mM tris-HCl, pH 8.0, 1 mM EGTA and centrifuged at 60,000 rpm to determine corresponding $s_{20,w}$ values.

$CaCl_2$ for EGTA produced a slight, but statistically insignificant, increase in $s^o_{20,w}$. This result is in contrast to that reported for skeletal TN-C (25), in which the binding of Ca^{2+} ions to TN-C produced an increase in $s^o_{20,w}$. This difference is in accord with a similar finding revealed by CD investigations (35), where it was demonstrated that cardiac TN-C undergoes a smaller conformational change upon binding Ca^{2+} than does skeletal TN-C.

4. Molecular Weight

From the amino acid sequence of bovine cardiac TN-C, van Eerd and Takahashi (47) calculated its molecular weight to be 18,459.

On SDS polyacrylamide gels, cardiac TN-C comigrated with rabbit skeletal TN-C, suggesting a molecular weight of 18,000 ± 500 (Figure 19).

Sedimentation equilibrium studies in the analytical ultracentrifuge yielded plots of log c *vs.* r^2 which were linear (Figure 20). The slopes of such lines were used to calculate a weight average molecular weight of 17,700 ± 1,000 for cardiac TN-C. In these calculations, a partial specific volume, $\bar{v}$, for TN-C of 0.73 ml/g, was employed, as estimated from its amino acid composition (70). These runs were performed in 0.15 M KCl, 50 mM tris-HCl, pH 8.0, 1 mM EGTA. Substitution of 1 mM $CaCl_2$ for the EGTA did not affect the calculated molecular weight of cardiac TN-C.

5. UV Absorption Properties

The UV absorption spectrum of cardiac TN-C (Figure 21) reflects its lack of tryptophan by the absence of a shoulder near 290 nm. Tyrosine absorption bands are responsible for the shoulder near 280 nm and the peak near 276 nm. The high phenylalanine to tyrosine ratio is evident in the multiplicity of fine structure in the spectrum between 250

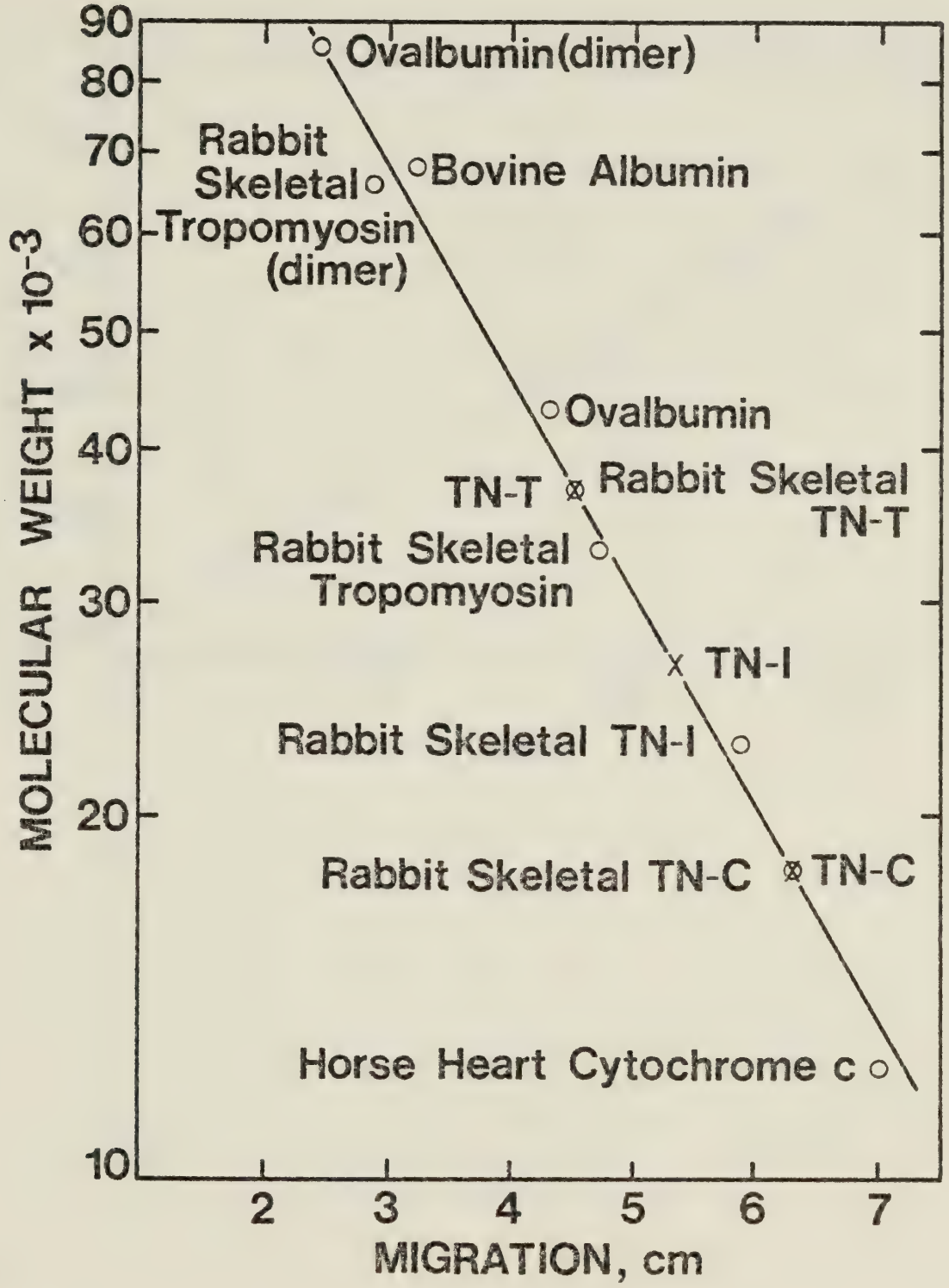

Figure 19. Determination of the molecular weights of the cardiac troponin subunits by SDS polyacrylamide gel electrophoresis. The cardiac components, TN-C, TN-I and TN-T, are designated by — X —, while proteins used to calibrate the gels are designated by — O —.

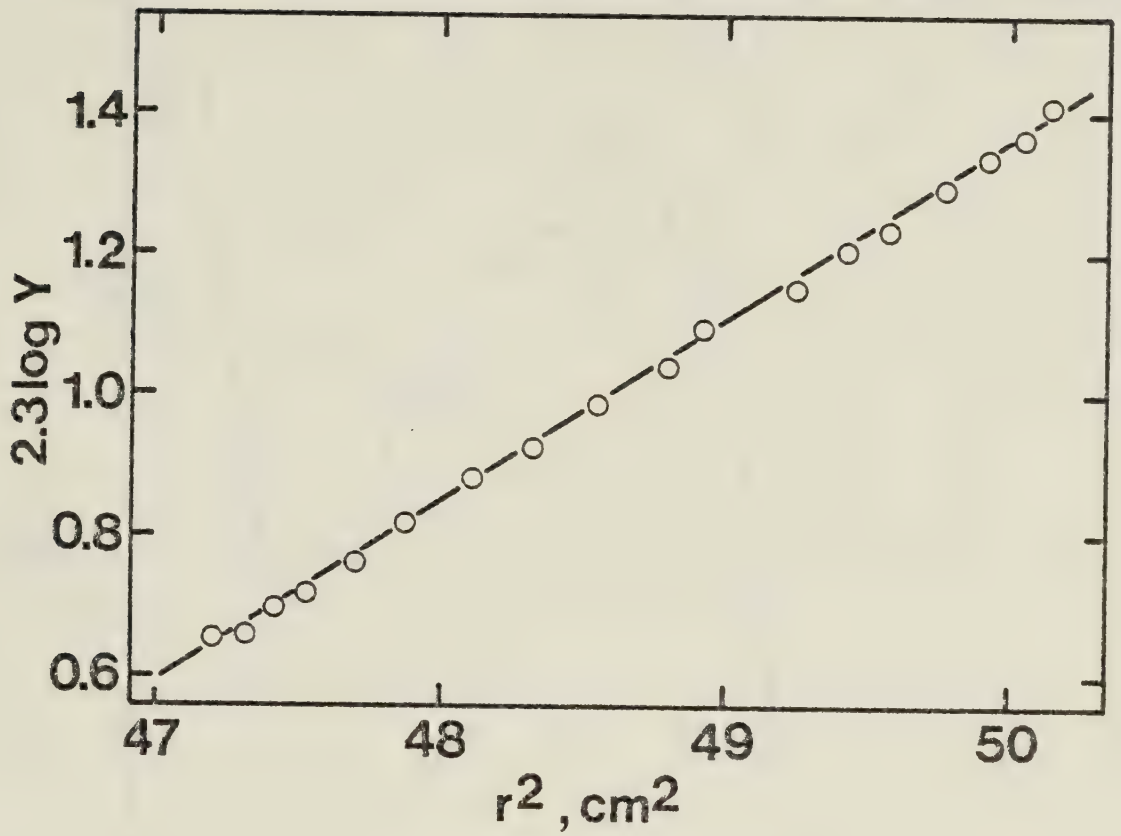

Figure 20. Sedimentation equilibrium log Y versus r^2 plot for TN-C. The protein was dissolved in 0.15 M KCl, 50 mM tris-HCl, pH 8.0, 1 mM EGTA and centrifuged at 16,000 rpm in a centrifuge equipped with Rayleigh interference optics. Y represents protein concentration in terms of fringe displacement units.

Figure 21. UV absorption spectrum of TN-C. The protein was dissolved in 0.15 M KCl, 50 mM tris-HCl, pH 7.5, 1 mM EGTA.

and 270 nm.

The UV difference absorption spectrum of TN-C in the presence and absence of Ca^{2+} ions (Figure 22) reveals that the binding of Ca^{2+} to TN-C alters the conformation of the molecule. A difference spectrum of similar shape was reported by Head and Perry (43) for skeletal TN-C. The maxima near 287 and 277 nm are due to perturbations in the environment of tyrosine. These positive peaks imply that the environments of one or more tyrosine residues have become more nonpolar (88), consistent with a compacting of the TN-C structure upon binding Ca^{2+} such that tyrosine becomes more buried in the core of the protein. The maxima near 269, 265, 259 and 253 nm are attributable to phenylalanine contributions (88). These peaks are more difficult to interpret as they reflect the averaged environmental effects for each of the 9 phenylalanine residues in the molecule.

6. CD Properties

a. Aromatic Absorption Region (250 - 310 nm)

The aromatic CD spectrum of cardiac TN-C (Figure 23, solid line) exhibits bands consistent with the presence of tyrosine (the trough and shoulder at 276 and 280 nm, respectively) and phenylalanine (maxima at 258 and 264 nm, and minima at 261 and 267 nm). Upon addition of $CaCl_2$ to the TN-C solution, a general sharpening of the aromatic CD bands was observed (Figure 23, dashed line). A similar effect was reported for skeletal TN-C (25). These changes further illustrate perturbations in the environments of tyrosine and phenylalanine residues in TN-C upon binding Ca^{2+}.

b. Peptide Absorption Region (190 - 250 nm)

In a "minus Ca^{2+}" solution approximating physiological conditions

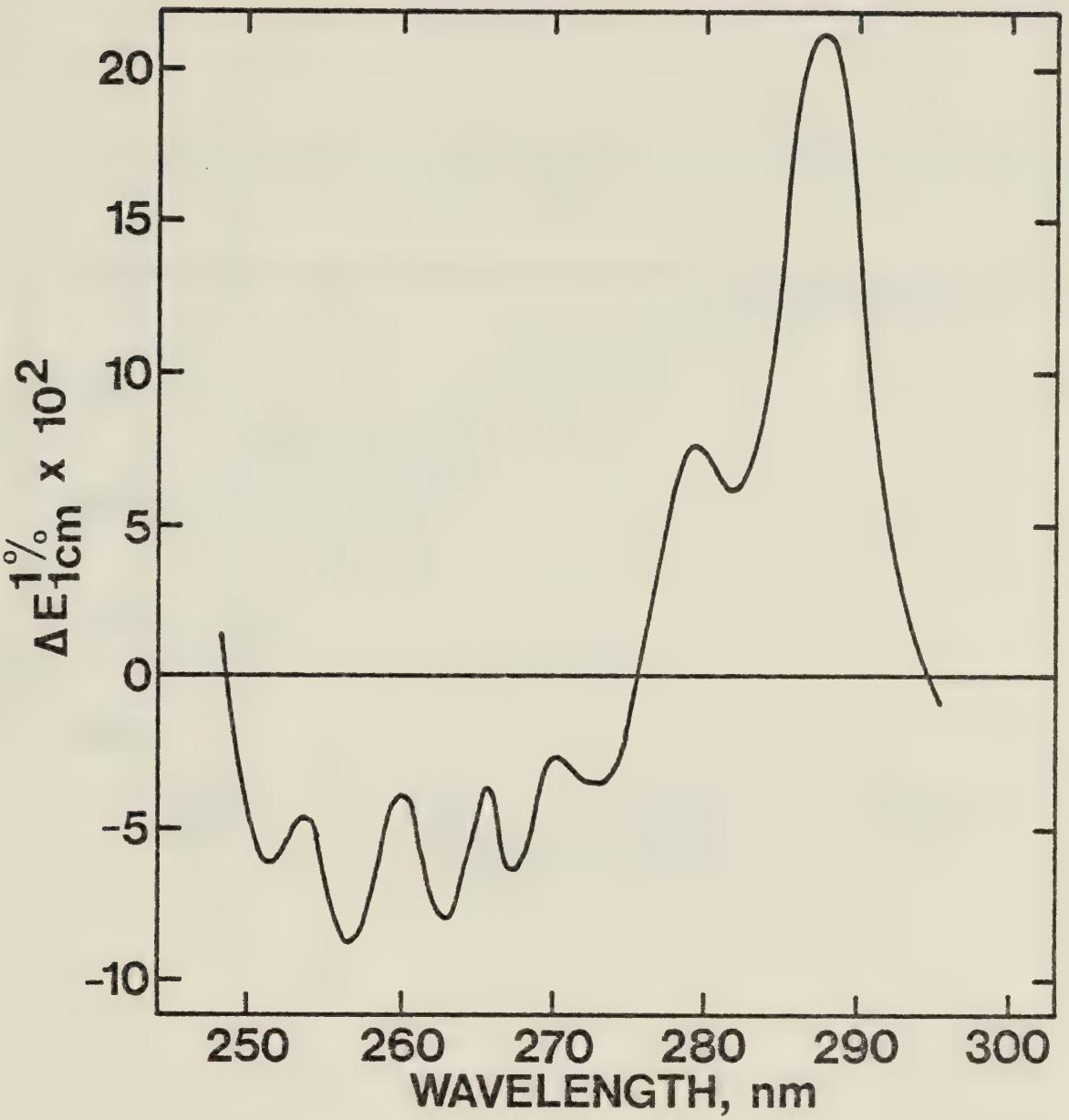

Figure 22. UV difference absorption spectrum of TN-C in the presence and absence of calcium. The protein was dissolved in 0.15 M KCl, 50 mM tris-HCl, pH 7.5, 1 mM EGTA. To the solution in the sample beam, an aliquot of 0.1 M $CaCl_2$ was added such that the free concentration of Ca^{2+} was 2×10^{-4} M. To the solution in the reference beam, an equal volume of distilled water was added.

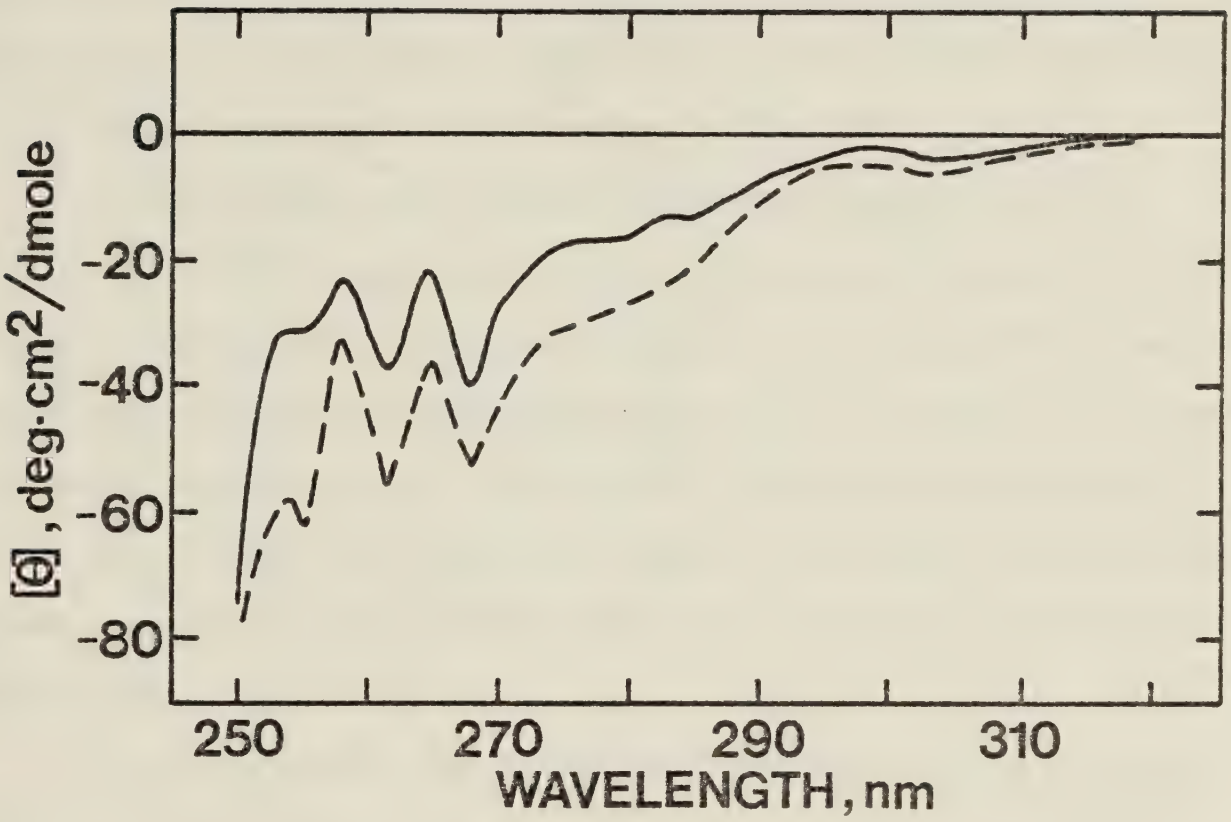

Figure 23. Aromatic CD spectra of TN-C in the presence and absence of calcium. TN-C was dissolved in 0.15 M KCl, 50 mM tris-HCl, pH 7.5, 1 mM EGTA. ———, "minus Ca^{2+}"; — — —, "plus Ca^{2+}".

in resting muscle, 0.15 M KCl, 50 mM tris-HCl, pH 7.5, 1 mM EGTA, cardiac TN-C exhibited a CD spectrum in the peptide absorbance region diagnostic of an α-helix containing protein (Figure 24, solid line). Calculations (66) suggested an apparent α-helical content of 42%. On the addition of $CaCl_2$ to the TN-C solution, such that the Ca^{2+} binding sites on TN-C were saturated, the ellipticity displayed by TN-C increased (Figure 24, dashed line). Calculations of the helix content of TN-C in the "plus Ca^{2+}" medium suggested 54%, an increase of about 29%.

Similar experiments indicated that the binding of Ca^{2+} to skeletal TN-C (25) would increase the helix content by nearly 60%. This value is about double the increase calculated for cardiac TN-C. Such a significant quantitative difference may reflect an important structural difference between the two forms of TN-C. The physiological benefit of each type of TN-C to its respective muscle class is not readily apparent. Again, questions of the relationship between evolutionary pressure and physiological function arise.

In this section describing the far UV CD properties of cardiac TN-C, two other sets of experiments, concerning the effects of different divalent cations and of ionic strength, will be related.

The differential effects of Sr^{2+} on the relaxing systems of cardiac and skeletal muscle were pointed out by Ebashi et al. (28). They claimed the sensitivity of natural cardiac actomyosin to a given concentration of Sr^{2+} was 5 times that of natural skeletal actomyosin, relative to a given concentration of Ca^{2+}. Therefore, the effect of Sr^{2+} on our preparation of TN-C was examined. In fact, the maximum effect caused by the addition of $SrCl_2$ to a TN-C solution was nearly identical to that elicited by $CaCl_2$. Sr^{2+} produced a 28% increase in

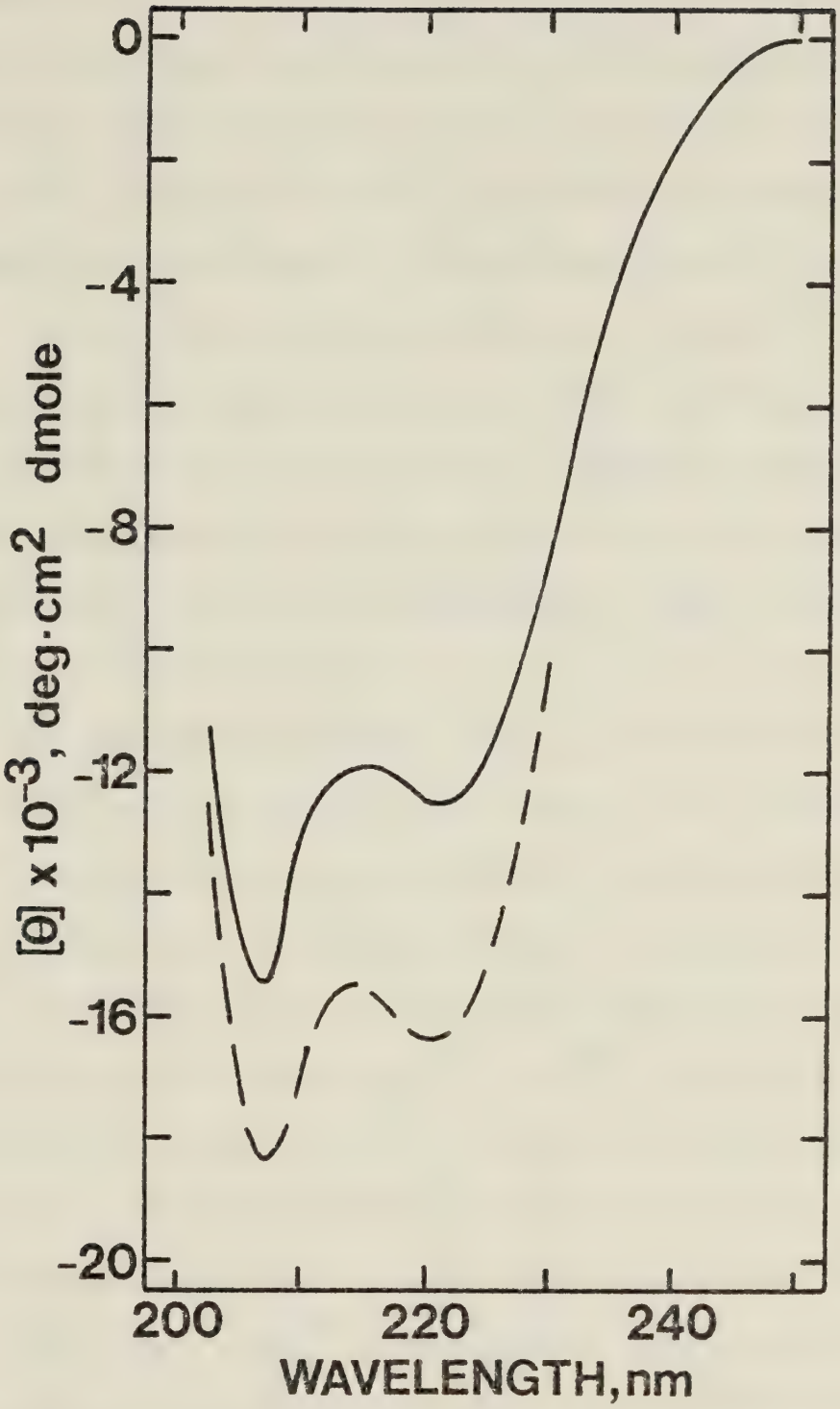

Figure 24. Far UV CD spectra of TN-C in the presence and absence of calcium. TN-C was dissolved in 0.15 M KCl, 50 mM tris-HCl, pH 7.5, 1 mM EGTA. ———, "minus Ca^{2+}"; — — —, "plus Ca^{2+}".

apparent α-helix content, as opposed to 29% for Ca^{2+}, and, therefore, it can substitute for Ca^{2+} as the trigger for the conformational change. However, calculations revealed that the maximal effect of Ca^{2+} occurred prior to the achievement of a free Ca^{2+} concentration of 10^{-5} M, whereas that of Sr^{2+} required a free Sr^{2+} concentration of nearly 10^{-4} M. Cardiac TN-C has a significantly lower affinity for Sr^{2+} than for Ca^{2+} ions.

An ion of more physiological relevance than Sr^{2+} is Mg^{2+}. The exact sarcoplasmic concentration of free Mg^{2+} is in some doubt (89), due to the presence of such natural Mg^{2+} chelating agents as ATP. In calcium binding studies on skeletal TN-C, Potter and Gergely (90) employed 2 mM $MgCl_2$ solutions to approximate a "high" estimate of sarcoplasmic free Mg^{2+} concentration.

The incremental addition of $MgCl_2$ to a TN-C solution up to a concentration of 5 mM was observed to cause a slow increase in the magnitudes of ellipticity values in CD spectra. A maximal change corresponding to a 14% increase in α-helical content was calculated. The presence of Mg^{2+} in a TN-C solution did not affect significantly the final ellipticity values elicited by Ca^{2+} or Sr^{2+}. It seems that Mg^{2+} can substitute only poorly for Ca^{2+} to produce the conformational change in cardiac TN-C. The much higher Mg^{2+} concentrations necessary to induce a significant conformational change indicate a much lower affinity of TN-C for Mg^{2+} than for Ca^{2+}. CD studies on skeletal TN-C (91, 92) yielded similar conclusions about the effect of Mg^{2+} on the interaction between TN-C and Ca^{2+} ions. Estimates for the association constant of Mg^{2+} and cardiac TN-C are similar to those suggested for Mg^{2+} and skeletal TN-C, between 10^3 and 10^4 M^{-1}.

Ionic strength was discovered to play a role in determining the

apparent α helical content of cardiac TN-C. To study interactions between the troponin components using CD techniques, 0.5 M KCl-containing solutions were used to maintain TN-I and TN-T in solution. In the higher ionic strength solvent, TN-C was found, in the "minus Ca^{2+}" state, to contain 47% α helix. In the "plus Ca^{2+}" state this value increased by 21% to 57%. This increase differs from the 29% value, from 42 to 54%, for the protein in a 0.15 M KCl buffer. With respect to the effects of the divalent cations tested, this ionic strength effect is small, but it does suggest that some ionic interactions do occur between TN-C and the salt in the surrounding medium. These salt effects are probably nonspecific due to the rather small net effect, but must be taken into account in certain experiments such as those described in the chapter on interaction studies.

7. Stabilizing Effect of Ca^{2+}

The ellipticity value at 221 nm in a CD spectrum provides a measure of the degree of denaturation of a molecule by reflecting its apparent α helix content. In thermal denaturation studies on TN-C in the "plus" and "minus Ca^{2+}" states, denaturation was followed by plotting $\theta_{T,obs}/\theta_{T,min}$ (the ratio of $[\theta]_{221}$ at a given temperature, T, to $[\theta]_{221}$ at the minimum temperature at which the experiment was conducted, near 10°C in these studies) against the temperature, T (Figure 25). In the "minus Ca^{2+}" state, a melting transition was observed near 50°C. This transition was much less sharp in the presence of Ca^{2+} or Sr^{2+}. The relative magnitudes of the decrease in helix content on thermal denaturation is reduced when Ca^{2+} or Sr^{2+} are bound to TN-C. Ca^{2+} and Sr^{2+} have a stabilizing effect on the molecular structure of TN-C with respect to thermal denaturation.

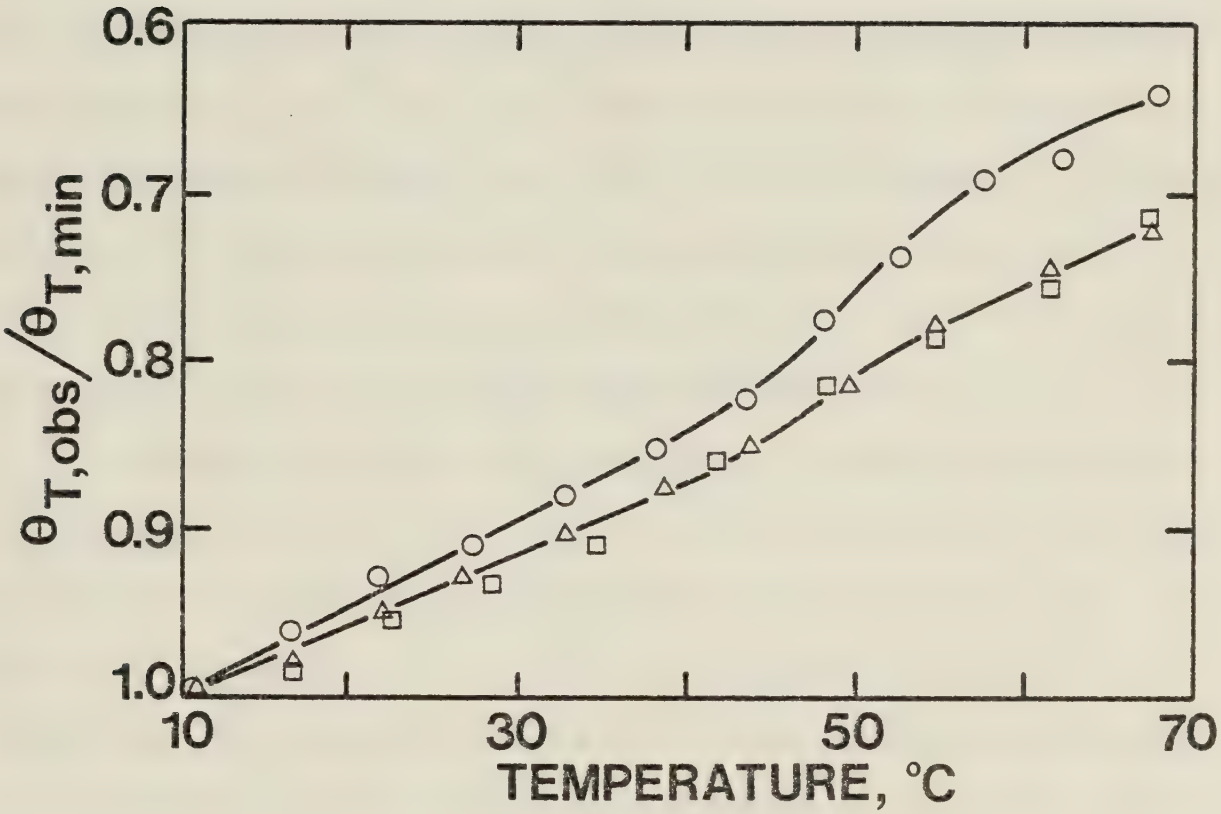

Figure 25. CD thermal denaturation studies of TN-C in the presence or absence of calcium or strontium. TN-C was dissolved in 0.15 M KCl, 50 mM tris-HCl, pH 8.0, 1 mM EGTA. $\theta_{T,obs}/\theta_{T,min}$ is the ratio of $[\theta]_{221}$ at the experimental temperature, T, to $[\theta]_{221}$ at the minimal temperature at which the experiment was performed. —○—○—, "minus Ca^{2+}"; —△—△—, "plus Ca^{2+}"; —□—□—, "plus Sr^{2+}".

8. Ca^{2+} Binding

Troponin in muscle performs its regulatory function by being able to recognize changes in the free Ca^{2+} concentration in the surrounding sarcoplasm. A thorough review and reevaluation of the Ca^{2+} binding parameters of skeletal TN-C and troponin has been performed recently by Potter and Gergely (90). Troponin and TN-C from skeletal muscle each bind, maximally, 4 Ca^{2+} and 4 Mg^{2+} ions per molecule in a possible 6 divalent cation sites. These sites fall into three classes: (1) two high affinity Ca^{2+} binding sites which, in a competitive manner, also bind Mg^{2+}; (2) two sites which have a lower affinity for Ca^{2+}, but which do not bind Mg^{2+}; and (3) two sites which bind Mg^{2+} but not Ca^{2+}.

Collins et al. (18), by an analysis of the skeletal TN-C amino acid sequence, had been able to predict accurately that TN-C could bind 4 Ca^{2+} ions. The basis for this prediction was the presence of 4 stretches of sequence in TN-C which were homologous with the calcium binding regions of carp parvalbumin (49). When van Eerd and Takahashi (47) published the amino acid sequence of bovine cardiac TN-C, they attempted to make a similar prediction. They discovered only 3 regions in the cardiac TN-C sequence homologous to the parvalbumin calcium binding sites. These 3 stretches of sequence corresponded to 3 of the 4 predicted Ca-binding sites of skeletal TN-C. Therefore, it was suggested that each cardiac TN-C molecule bound 3 calcium ions.

In our experiments, the Ca^{2+} binding properties of cardiac TN-C were studied in two ways, one employing CD techniques and a second using gel filtration methods.

a. CD Titration Studies

In these experiments, TN-C was dissolved in 0.15 M KCl, 50 mM

tris-HCl, pH 7.5, and 1 mM EGTA in the presence or absence of 2 mM $MgCl_2$. Increments of $CaCl_2$ were added to the protein solution and the corresponding values of $[\theta]_{221}$ recorded.

The results of additions of $CaCl_2$ to a cardiac TN-C solution in the absence of Mg^{2+} ions are presented in the form of a titration curve in Figure 26. The fraction of completion of the CD spectral change, f, is plotted against the negative logarithm of the free Ca^{2+} concentration in solution, pCa_f. The data were collected from 6 sets of titrations on 3 different preparations of TN-C. The solid curve is a theoretical titration curve calculated assuming TN-C possesses a single calcium binding site and an apparent association constant for Ca^{2+} of 7×10^6 M^{-1}. The mathematical relation describing this curve is (from equation [32]):

$$f = \frac{(7 \times 10^6)[Ca^{2+}]_f}{1 + (7 \times 10^6)[Ca^{2+}]_f} \qquad [34]$$

where:

$$[Ca^{2+}]_f = 10^{-pCa_f} \qquad [35]$$

The close fit of the calculated curve to the experimental data suggests that the binding of only one Ca^{2+} ion to a cardiac TN-C molecule is sufficient to elicit the entire conformational change observed by CD methodology, and the apparent association constant for this interaction is 7×10^6 M^{-1}.

In the absence of added Ca^{2+}, it was shown that 2 mM $MgCl_2$ produced a change in the CD spectrum approximately one half the magnitude of that produced by saturating levels of Ca^{2+}. Therefore, the titration data for additions of $CaCl_2$ to TN-C solutions in the presence of 2 mM $MgCl_2$ are presented on a scale of from 50 to 100% complete (Figure 27).

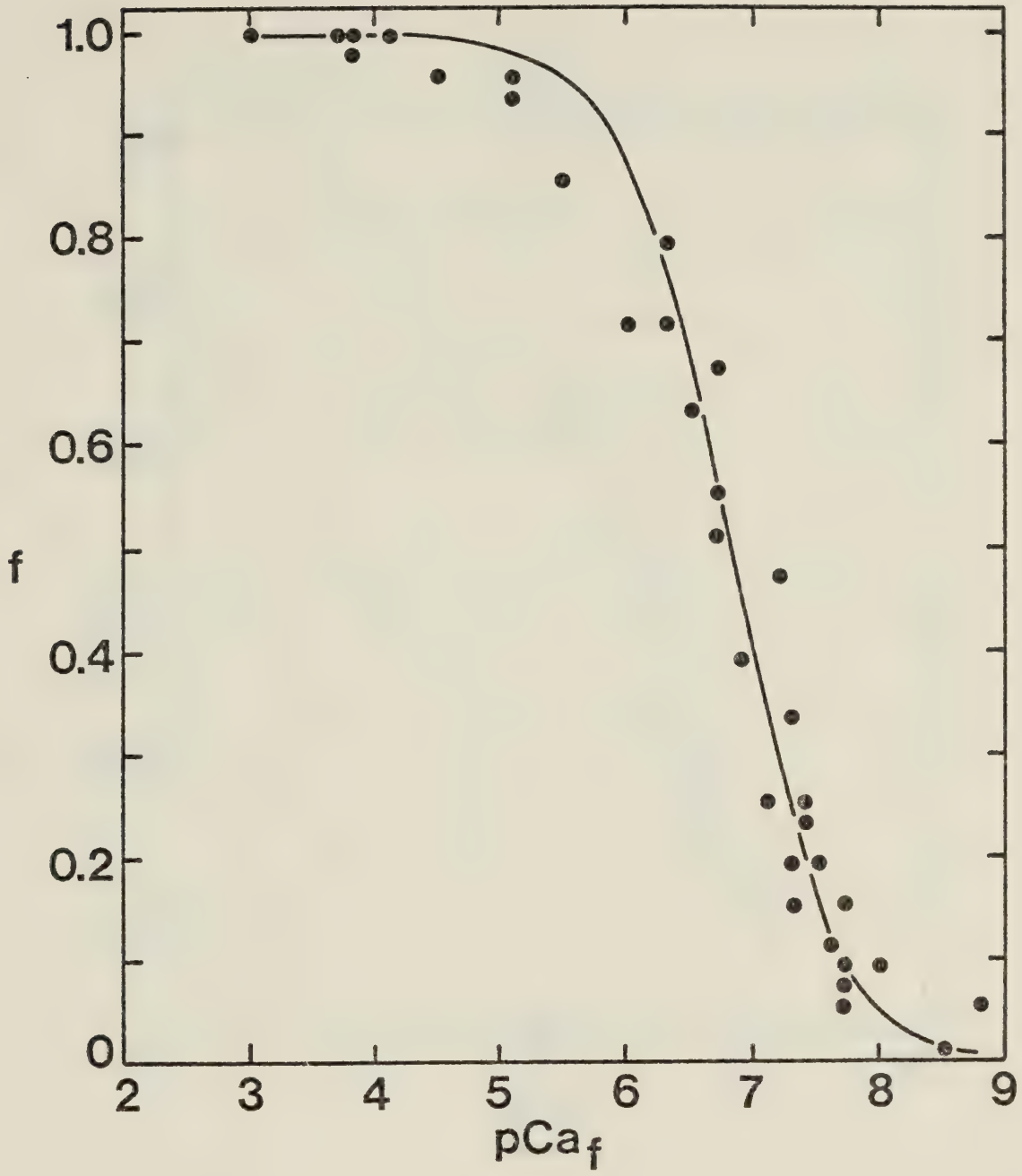

Figure 26. CD calcium titration of the conformational change in TN-C ("minus Mg^{2+}"). The protein was dissolved in 0.15 M KCl, 50 mM tris-HCl, pH 7.5, 1 mM EGTA. $CaCl_2$ was added incrementally and $[\theta]_{221}$ recorded for each addition. f is the fraction of completion of the conformational change and $pCa_f = -\log[Ca^{2+}]_f$. The solid line represents a calculated titration curve assuming that one Ca^{2+} binding site exists on TN-C and the apparent association constant for the interaction is 7×10^6 M^{-1}.

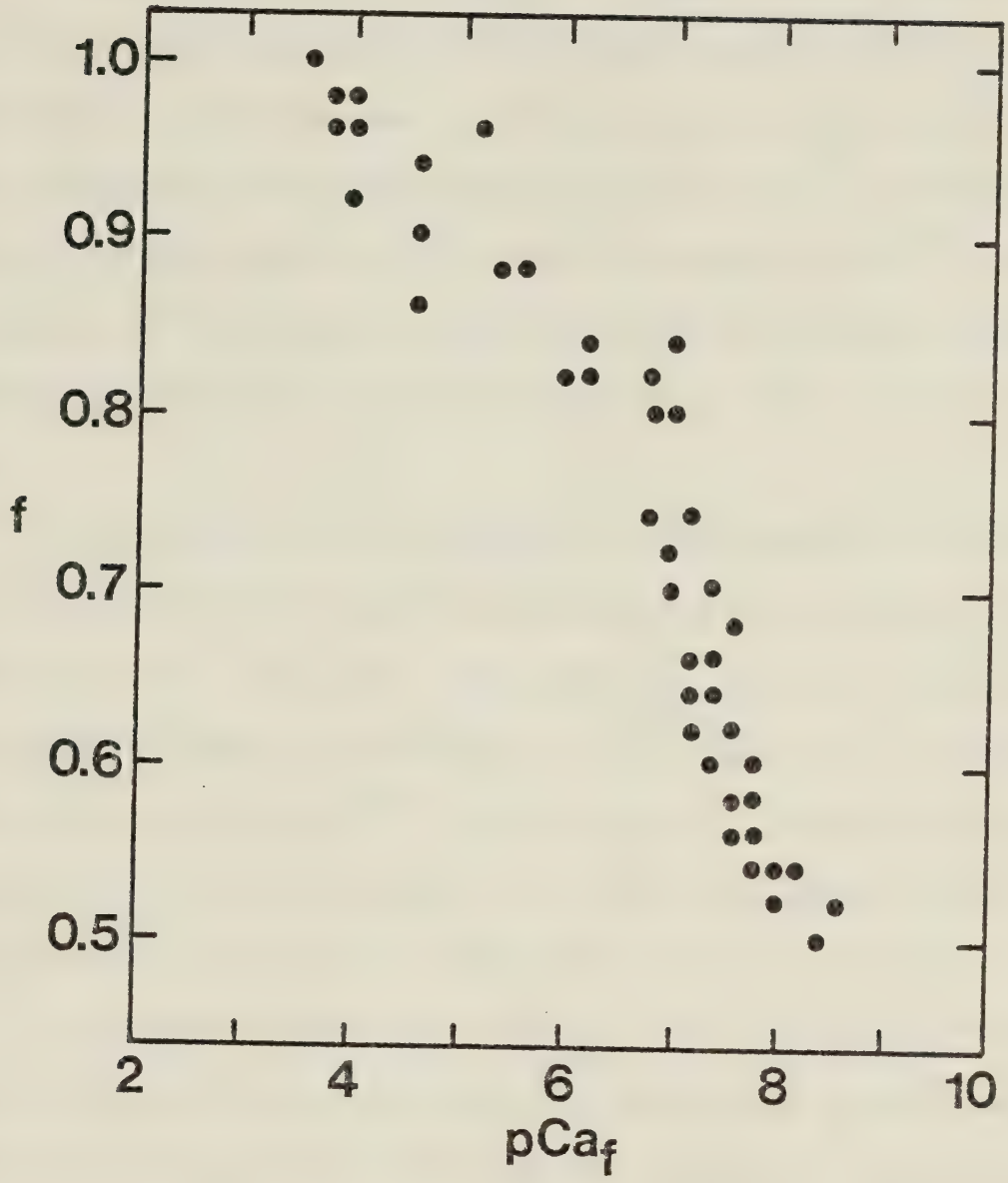

Figure 27. CD calcium titration of the conformational change in TN-C ("plus Mg^{2+}"). The experimental conditions were as described in Figure 26 except that 2 mM $MgCl_2$ was present in all buffers.

The results represent 6 sets of titrations on 3 different preparations of TN-C.

These data were not analysed in terms of the equations presented for the estimation of the binding parameters of Ca^{2+} to TN-C. The situation in the presence of $MgCl_2$ cannot be represented by a two state model considering only plus and minus Ca^{2+} bound forms of TN-C. A certain proportion of the TN-C molecules has Mg^{2+} bound to it and, as Mg^{2+} does affect the CD spectrum of TN-C, this complex represents a third possible state in which the TN-C molecules may exist.

The effect on the CD spectrum of TN-C exerted by Ca^{2+} on top of that produced by Mg^{2+} reaches half maximal in the pCa_f range from 6.5 to 7.0. This is a range similar to that observed for the titration performed in the absence of Mg^{2+} (Figure 27). However, the titration in the "plus Mg^{2+}" situation does not approach completion as rapidly as in the "minus Mg^{2+}" situation, implying that Mg^{2+} may hinder Ca^{2+} binding by competing for the binding site.

Incremental additions of $MgCl_2$ to TN-C solutions in the absence of Ca^{2+} produced increases in observed ellipticity values over a broad concentration range. The data were not suitable for a binding parameter analysis as performed with Ca^{2+}. From the Mg^{2+} concentration required to produce one half of the maximal observed ellipticity change at 221 nm, the apparent association constant for TN-C with Mg^{2+} was estimated to be between 10^3 and 10^4 M^{-1}.

Addition of $MgCl_2$ to TN-C in a "plus Ca^{2+}" solution produced no further change in its CD spectrum. Therefore, Mg^{2+}, if it does bind at a site other than the one responsible for the conformational change

already described, does not induce a further structural change which is detectable in CD spectra.

b. Gel Filtration Studies

Van Eerd and Takahashi (47) had predicted 3 Ca^{2+} could be bound to each cardiac TN-C molecule. Our results demonstrated that the binding of a single Ca^{2+} could elicit the full conformational change observed in CD spectra. The possibility remained that, in total, more than one Ca^{2+} could bind to each TN-C, but that only the one responsible for the altered CD properties had been detected.

To test this hypothesis, the gel filtration technique of Hummel and Dreyer (83), as adapted by Voordouw and Roche (84), was employed to study the binding parameters for the interaction of TN-C with Ca^{2+}. These experiments were performed in the presence and absence of 2 mM $MgCl_2$.

Eluant from the gel filtration column (Figure 28) was monitored for protein content, by measuring its absorbance at 278 nm, and for calcium concentration, using atomic absorption spectrophotometry. One protein peak eluted at the void volume of the column. Two calcium peaks emerged, one coeluting with the protein and one appearing later in the profile. Integration of the amount of calcium eluting in the first peak and division of this value by the total protein in the peak yielded the mole ratio of Ca^{2+} bound to TN-C.

To test the method, the maximal binding of Ca^{2+} to rabbit skeletal TN-C (kindly donated by Dr. W.D. McCubbin) was determined. The column was equilibrated against 0.15 M KCl, 50 mM tris-HCl, pH 7.5, and 1×10^{-4} M $CaCl_2$. Assuming an $E^{1\%}_{1cm,280}$ value for skeletal TN-C of 1.93 (13), it was determined that each mole of skeletal TN-C could bind

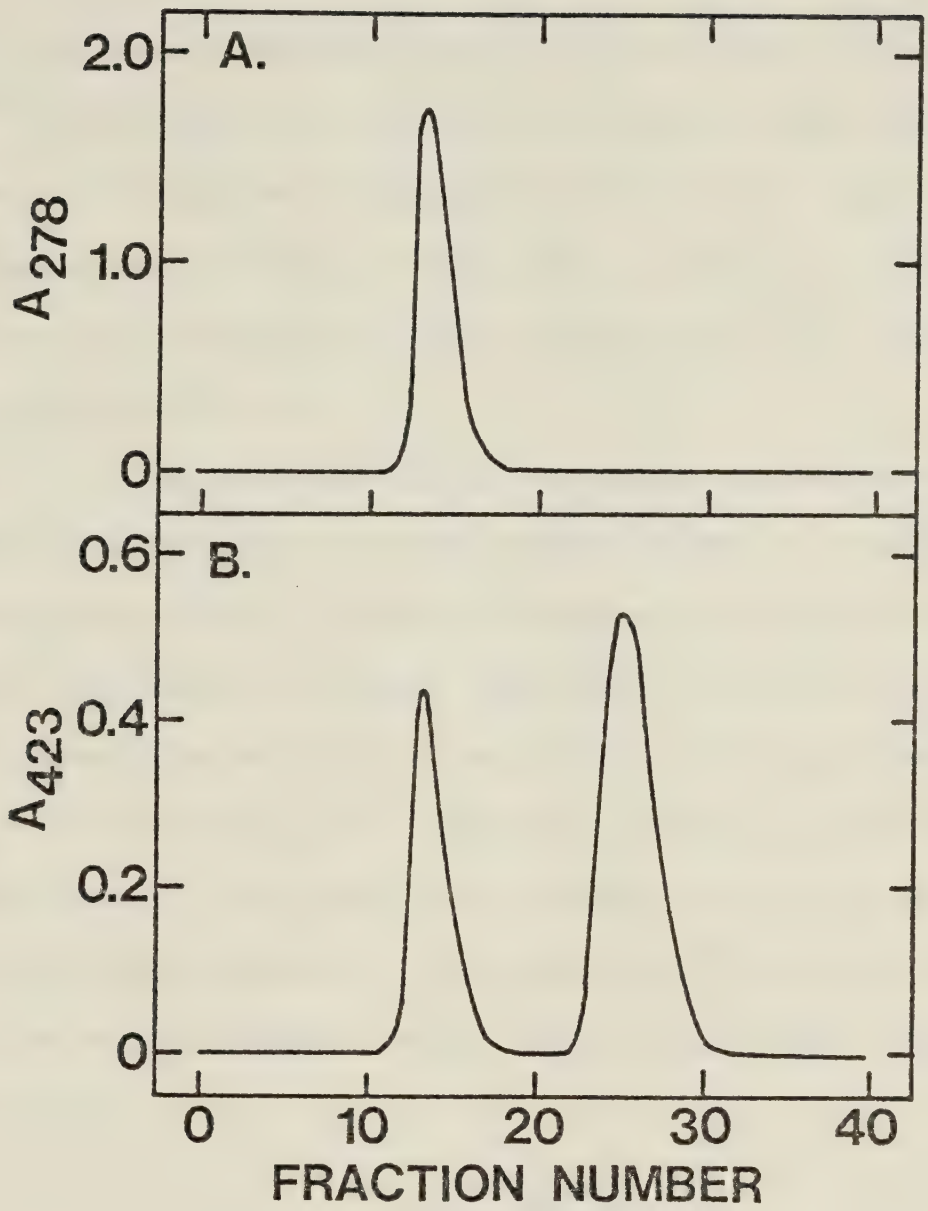

Figure 28. Elution of TN-C and calcium from a Sephadex G-25 column. TN-C (≈1 mg/ml) was applied to a 1.0 x 30 cm column in 0.6 ml of 0.15 M KCl, 50 mM tris-HCl, pH 7.5, 5×10^{-4} M $CaCl_2$ and eluted with the column equilibration buffer, 0.15 M KCl, 50 mM tris-HCl, pH 7.5, 1×10^{-4} M $CaCl_2$. (A) Protein elution profile monitored spectrophotometrically at 278 nm. (B) Calcium elution profile monitored using an atomic absorption spectrophotometer.

3.9 ± 0.2 moles of Ca^{2+}. This was in excellent agreement with the value of four found by Potter and Gergely (90).

Performance of an identical set of experiments using cardiac TN-C suggested that each mole of protein could bind 3.2 ± 0.2 moles of Ca^{2+}. If 2 mM $MgCl_2$ were incorporated into the column equilibration buffer, this value was determined to be 2.9 ± 0.2. Our results provide experimental support for the speculation, based upon amino acid sequence analysis, that bovine cardiac TN-C would bind 3, not 4, Ca^{2+} ions on a mole per mole basis (47).

Incorporation of EGTA into the column equilibration buffer allowed investigation of calcium binding to TN-C as a function of free calcium concentration. Figure 29 presents the results of such experiments. Open squares represent data points collected in the absence of Mg^{2+}; closed squares represent data collected in the presence of 2 mM $MgCl_2$. The solid lines are theoretical titration curves fitted to the observed data. These curves were generated by introducing numerical values for the parameters i, the number of Ca^{2+} bound per TN-C, and K_{app}, the apparent association constant for the interaction, into the equation (90):

$$Ca^{2+}/TN\text{-}C = \frac{i\, K_{app}\, [Ca^{2+}]_f}{1 + K_{app}\, [Ca^{2+}]_f} \qquad [36]$$

The best fit to the data (judged by eye) collected in the absence of Mg^{2+} (Figure 29, open squares) was obtained by setting i = 3.2 and K_{app} = $7 \times 10^6\ M^{-1}$. For data collected in the presence of 2 mM $MgCl_2$ (Figure 29, closed squares), the best fit was generated by setting i = 2.9 and $K_{app} = 1 \times 10^6\ M^{-1}$.

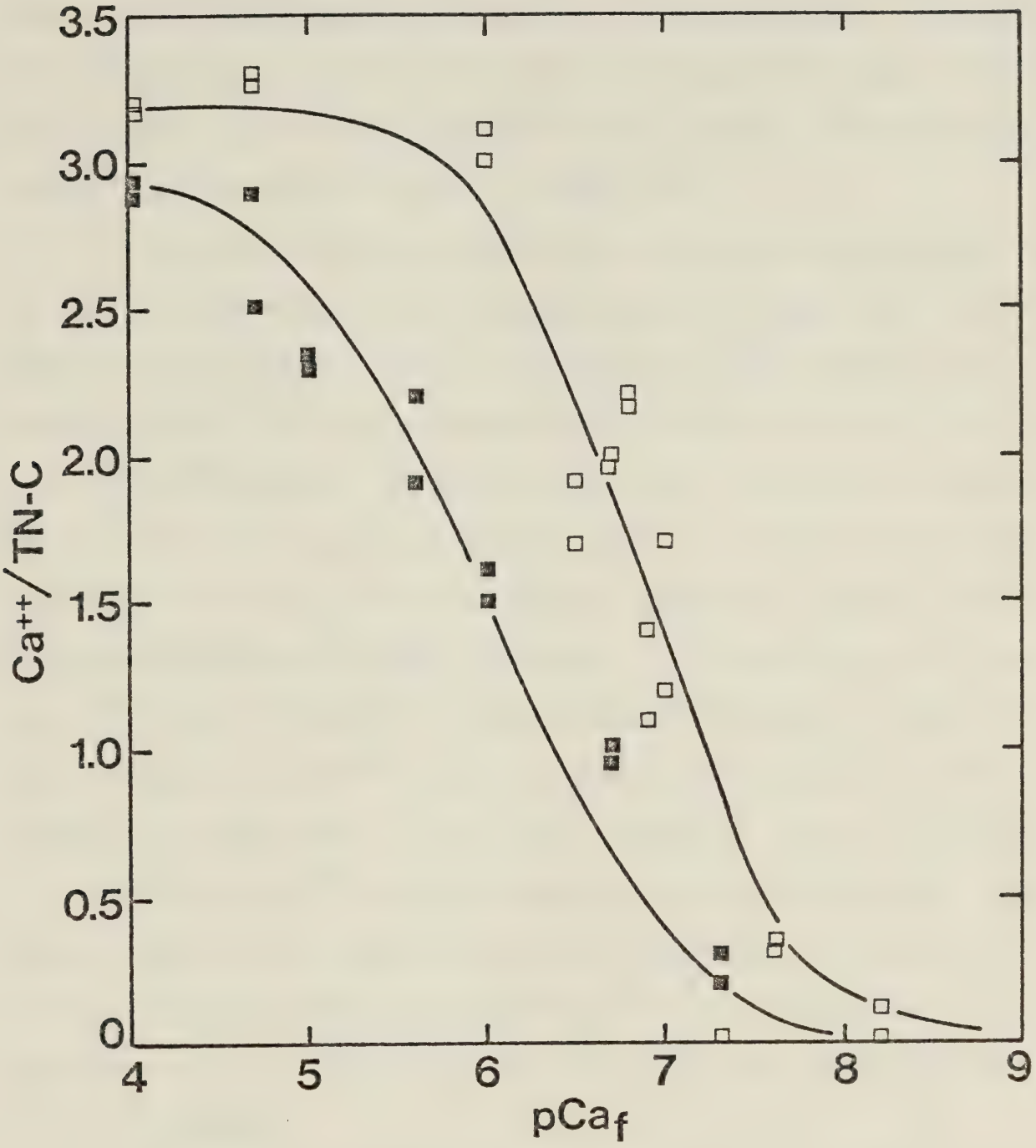

Figure 29. Determination of the moles of calcium bound per mole of TN-C at various concentrations of free calcium ion. Open squares represent data collected in the absence of $MgCl_2$. The solid curve through these data represents a titration curve calculated assuming 3.2 calcium ions bind per TN-C and the association constant for the interaction is 7×10^6 M^{-1}. Closed squares represent data collected in the presence of 2 mM $MgCl_2$. The solid curve through these data was calculated assuming 2.9 Ca^{2+} bind to each TN-C and the association constant for the interaction is 1×10^6 M^{-1}.

The results clearly demonstrate that Mg^{2+} ions in solution compete with Ca^{2+} for binding sites on TN-C. An increased Mg^{2+} concentration increases the level of Ca^{2+} necessary to occupy the sites. Once a sufficiently high Ca^{2+} concentration has been attained, essentially all the Mg^{2+} can be displaced from the binding sites.

Our results differ from those reported by Drabikowski *et al.* (45) and by Brekke and Greaser (46). Drabikowski *et al.* found only 1.64 Ca^{2+} bound per cardiac TN-C. However, the methodology they employed only measured 2.16 Ca^{2+} bound per skeletal TN-C. Brekke and Greaser, similarly, found 2.08 Ca^{2+} bound per cardiac TN-C, but only 2.25 bound per skeletal TN-C. These latter values may be low estimates for the maximal binding capacities of TN-C due to the experimental conditions employed. TN-C was dialysed against 0.5 M KCl, 2 mM $MgCl_2$, 10 mM tris-HCl, pH 7.5, and 1×10^{-6} M $CaCl_2$. Clearly, in the presence of 2 mM $MgCl_2$, a free Ca^{2+} concentration of 1×10^{-6} M would not saturate the binding sites on cardiac TN-C (Figure 29). At $pCa_f = 6$, our results suggest that about 1.5 - 1.7 moles of Ca^{2+} would be bound to a mole of cardiac TN-C. The somewhat higher value found by Brekke and Greaser may reflect that, although working at micromolar levels of Ca^{2+}, they did not use a metal ion buffer system to control precisely free Ca^{2+} concentrations.

c. Summary

Analytical gel filtration studies revealed that cardiac TN-C can bind 3 Ca^{2+} ions per molecule. Only one of these is responsible for the observed alterations of the CD properties of the protein in the presence of Ca^{2+}. The remaining two occupy sites which are "invisible" to circularly polarized light.

The data do not indicate that different classes of sites, with

respect to magnitude of association constant, exist on cardiac TN-C, as reported for skeletal TN-C (90). They do suggest that the sarcoplasmic level of free Mg^{2+} ions does affect the binding parameters for the interaction of TN-C with Ca^{2+}. Although the precise concentration of free Mg^{2+} within cells is unknown (89), a high estimate (2 mM Mg^{2+}) results in a reduction of the association constant from 7×10^6 M^{-1} to about 1×10^6 M^{-1}. The sensitivity of TN-C to a Ca^{2+} induced conformational change would still fall within the range of Ca^{2+} concentrations experienced in the sarcoplasm, 10^{-5} M in actively contracting muscle to 10^{-8} M in resting muscle.

B. TN-I

1. Amino Acid Analysis

The amino acid composition of bovine cardiac TN-I, prepared in our laboratory, is detailed in Table II. The values represent residues per molecule, assuming a molecular weight of 23,500 (52). Also presented are the amino acid compositions of rabbit skeletal TN-I (19) and rabbit cardiac TN-I (52), as calculated from published amino acid sequences.

TN-I, independent of its source, is rich in basic amino acid residues. However, as was found for TN-C, significant differences in the contents of certain residues exist. As the sequences of both rabbit skeletal and rabbit cardiac TN-I are known, there is no question that the observed differences are tissue-related. The small variations observed between bovine and rabbit cardiac TN-I may represent interspecies differences.

2. Solubility

Cardiac TN-I was found to be marginally soluble in non-denaturing

TABLE II

Amino acid composition of bovine cardiac TN-I

Amino Acid	Residues per molecule of protein		
	Rabbit Skeletal TN-I*	Bovine Cardiac TN-I**	Rabbit Cardiac TN-I***
Lys	24	22.8	24
His	4	3.0	3
Arg	16	22.1	23
Asx	15	18.0	17
Thr	3	9.6	10
Ser	10	9.7	8
Glx	33	29.5	31
Pro	5	8.8	5
Gly	8	13.0	11
Ala	14	23.0	23
Val	7	8.9	8
Met	9	3.6	4
Ile	5	6.7	7
Leu	17	21.2	23
Tyr	2	3.0	2
Phe	3	3.9	4
Trp	1	1.2	1
1/2 Cys	3	2.4	2

*Wilkinson and Grand (51).

**Assuming a molecular weight of 23,500.

***Grand et al. (52).

buffers near neutral pH. Solubility in 0.5 M KCl, 50 mM tris-HCl, pH 7.5 could be increased significantly if TN-I were dissolved first in a buffer containing 8 M urea, or simply in 10^{-3} N HCl, and subsequently dialysed against the tris medium. Clarification of protein solutions by centrifugation or millipore filtration was performed routinely prior to conducting analytical studies.

3. Extinction Coefficient

The extinction coefficient of a 1% solution of cardiac TN-I in a 1 cm pathlength cell at 278 nm was determined to be 3.7 (Figure 30).

4. Molecular Weight

Early studies (29, 33) in which SDS gels of crude preparations of whole cardiac troponin were electrophoresed suggested that cardiac TN-I possessed a higher molecular weight than skeletal TN-I. Amino acid sequence studies (52, 19) determined the molecular weights of rabbit cardiac and rabbit skeletal TN-I, respectively, to be 23,550 and 20,897.

In this investigation, cardiac TN-I, on SDS gels, migrated as a protein with a molecular weight of 27,000 ± 1,000 (Figure 19). By comparison, skeletal TN-I possessed a molecular weight of 23,000 using the same technique (17, 93)(Figure 31).

Conventional sedimentation equilibrium runs in 0.5 M KCl, 50 mM tris-HCl, pH 7.5 indicated that cardiac TN-I undergoes aggregation, as plots of log c *vs.* r^2 were not linear but curved upwards (Figure 32). This problem was overcome by centrifuging TN-I in 8 M urea, 50 mM tris-HCl, pH 7.5, 0.2 M NaCl, 1 mM DTT. Log c *vs.* r^2 plots in this medium were linear (Figure 33).

From the amino acid composition, a $\bar{v}$ for TN-I of 0.73 ml/g was calculated (70). In denaturing solvents, such as 8 M urea, Kay (94) has

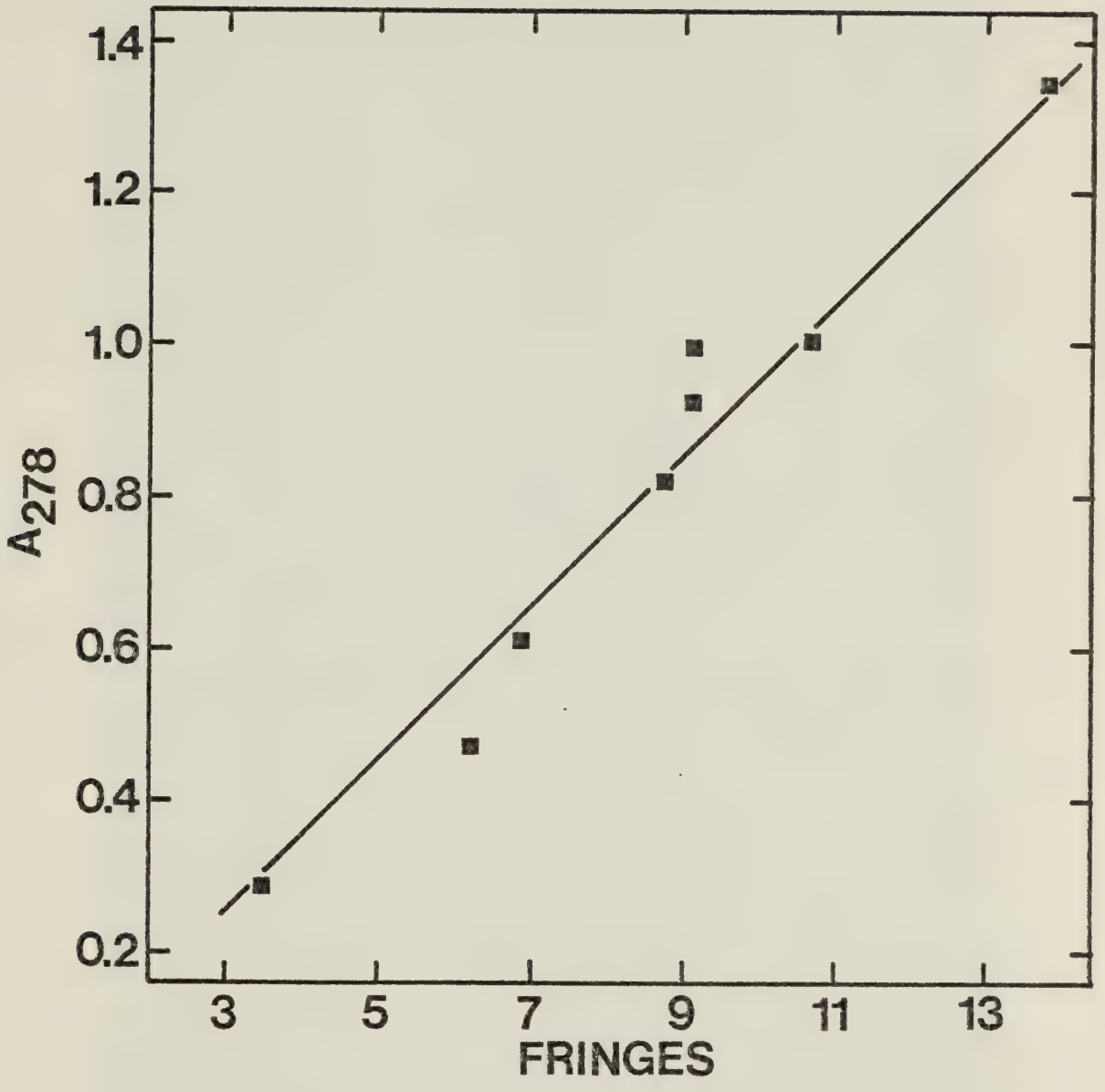

Figure 30. Determination of the extinction coefficient of TN-I. The protein was dissolved in 0.5 M NaCl, 50 mM tris-HCl, pH 7.5 and centrifuged at 12,000 rpm. The absorbance value at 278 nm was recorded for each sample and its concentration determined refractometrically according to Babul and Stellwagen (68).

Figure 31. Comparison of the mobilities of skeletal and cardiac TN-I on SDS polyacrylamide gels. Gel A shows cardiac TN-I. Gel B shows skeletal TN-I. Gel C reveals the different mobilities of the two forms of TN-I. 50 µg of each type of TN-I were applied to gel C.

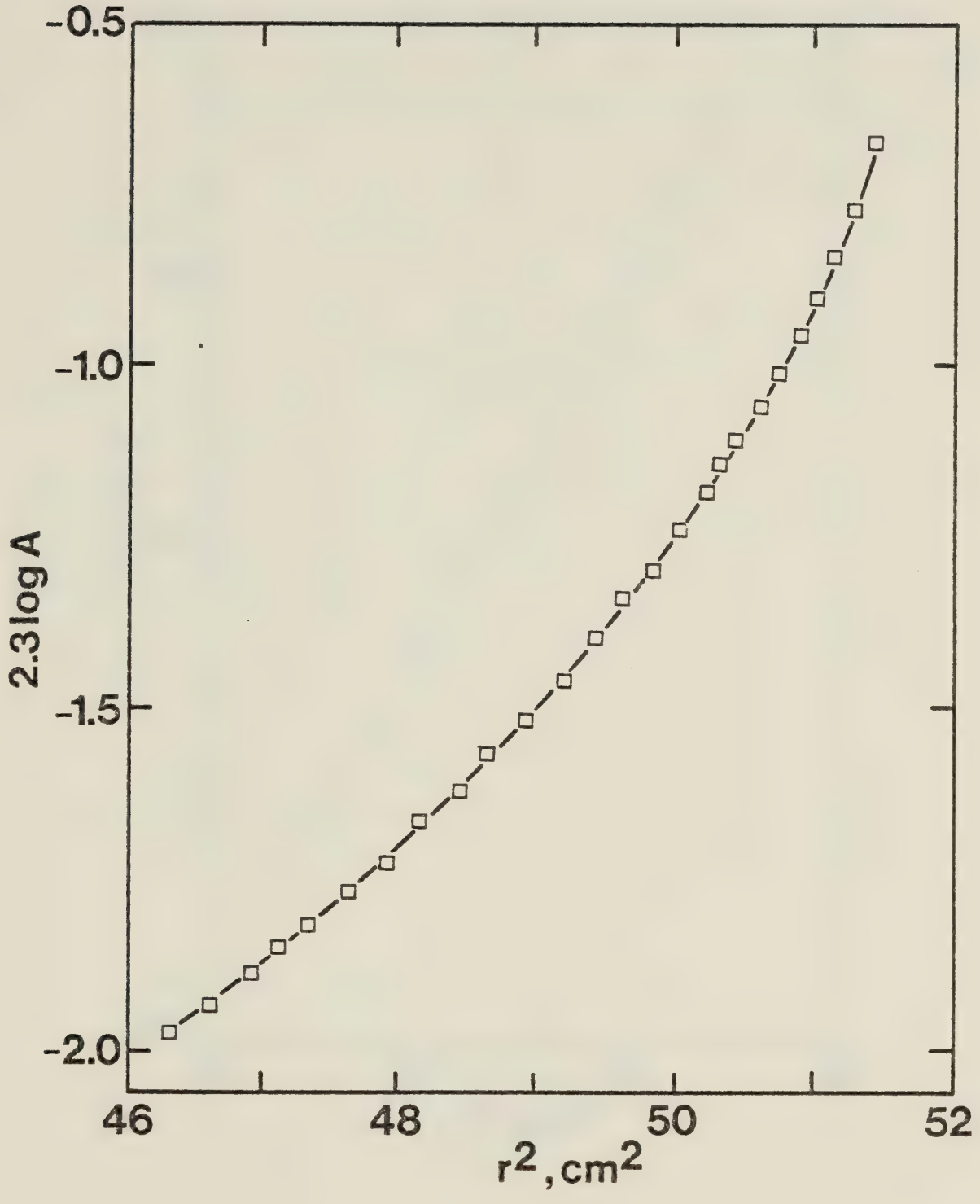

Figure 32. Sedimentation equilibrium log A versus r^2 plot for TN-I in a nondenaturing buffer. TN-I was dissolved in 0.5 M NaCl, 50 mM tris-HCl, pH 7.5, and spun at 9,000 rpm in a centrifuge equipped with a photoelectric scanner. A represents protein concentration in terms of absorption units at 280 nm.

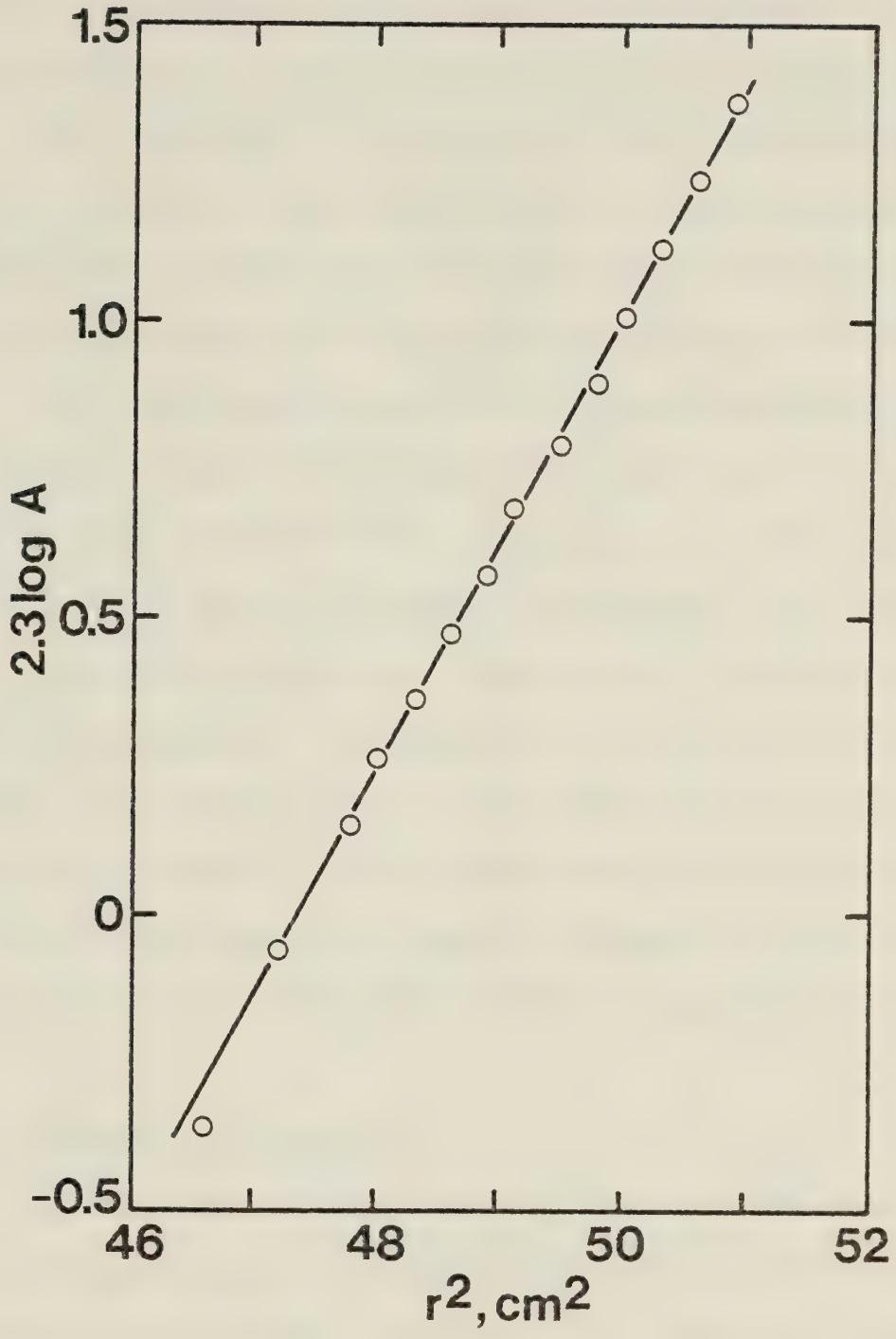

Figure 33. Sedimentation equilibrium log A versus r^2 plot for TN-I in the presence of 8 M urea. TN-I was dissolved in 8 M urea, 0.2 M NaCl, 50 mM tris-HCl, pH 7.5, 1 mM DTT and spun at 20,000 rpm in a centrifuge equipped with a photoelectric scanner. A represents protein concentration in terms of absorption units at 280 nm.

suggested that due to an unfolding of the protein, with the resultant elimination of "excluded volumes" and possible exposure of buried charged groups to the protein surface, $\bar{v}$ could be expected to decrease by 1 - 1.5%. Therefore, in calculations of the weight average molecular weight of TN-I in 8 M urea, $\bar{v}$ was assumed to equal 0.72 ml/g. Such an assumption led to a calculated molecular weight for cardiac TN-I of 22,900 ± 500, a value later supported by sequence studies (52).

As a possible explanation for its anomolous migration on SDS gels, the basic nature of the amino acid composition of TN-I was considered. Weber and Osborn (95) suggested that a protein might migrate abnormally on SDS gels if it possessed an unusually high intrinsic net charge. Histone f1, given as an example, with a molecular weight of 21,000, electrophoresed on SDS gels as though it had a molecular weight of 35,000. The complex between a basic region of a protein and SDS may possess a lower negative charge density than a more random region. This may cause the complex to assume a conformation different than that of a normal protein - SDS complex, leading to anomalous migration on gels.

5. UV Absorption Spectrum

The UV absorption spectrum of cardiac TN-I (Figure 34) is typical of most proteins, displaying a maximum near 278 nm, a minimum near 250 nm, and a shoulder, indicative of a tryptophan contribution at about 290 nm.

6. CD Properties

The CD spectrum in the peptide absorption region of cardiac TN-I (Figure 35) is representative of a protein containing α-helical regions, exhibiting two negatively dichroic bands centred near 207 and 221 nm.

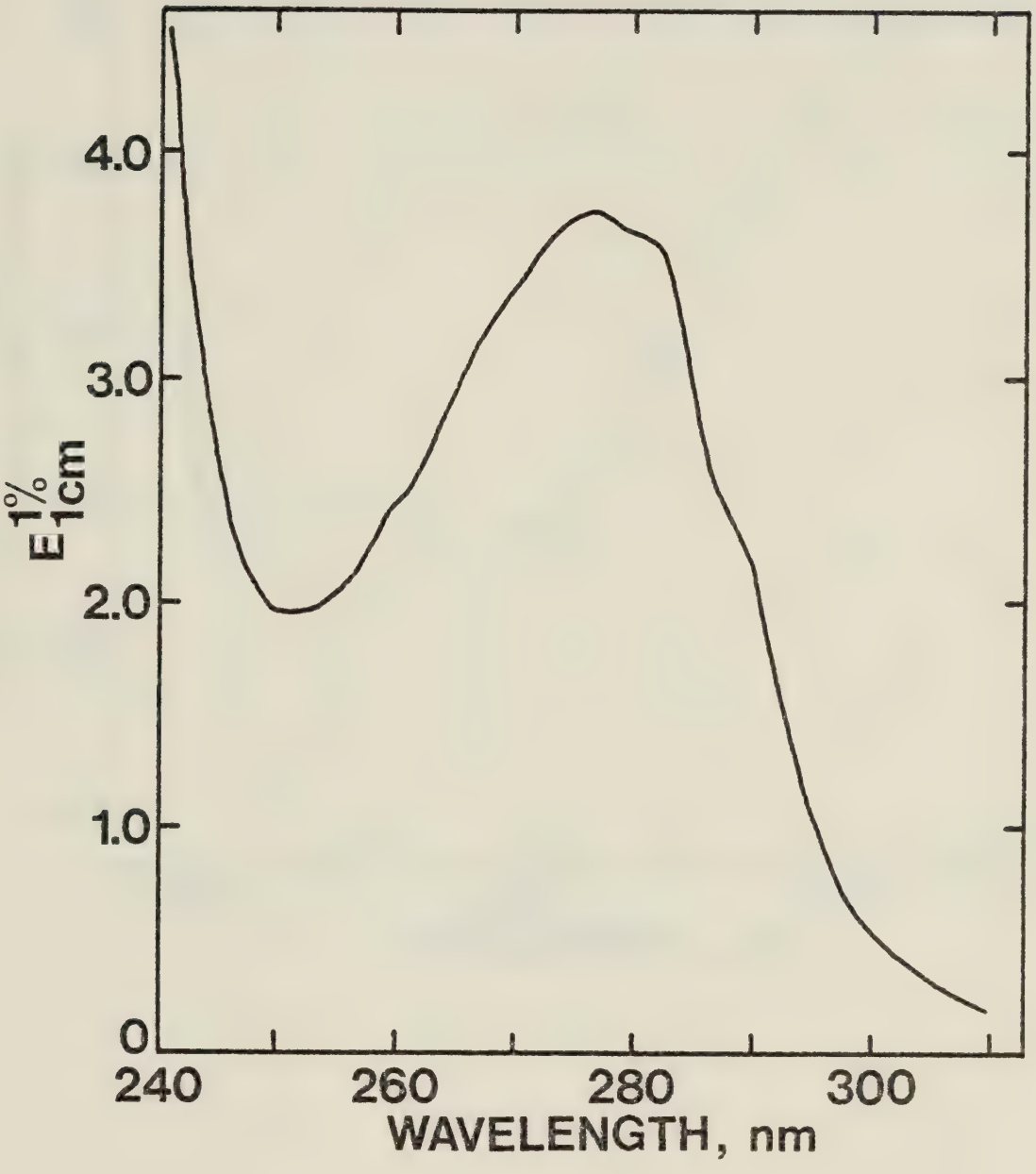

Figure 34. UV absorption spectrum of TN-I. The protein was dissolved in 0.5 M KCl, 50 mM tris-HCl, pH 7.5, 1 mM EGTA.

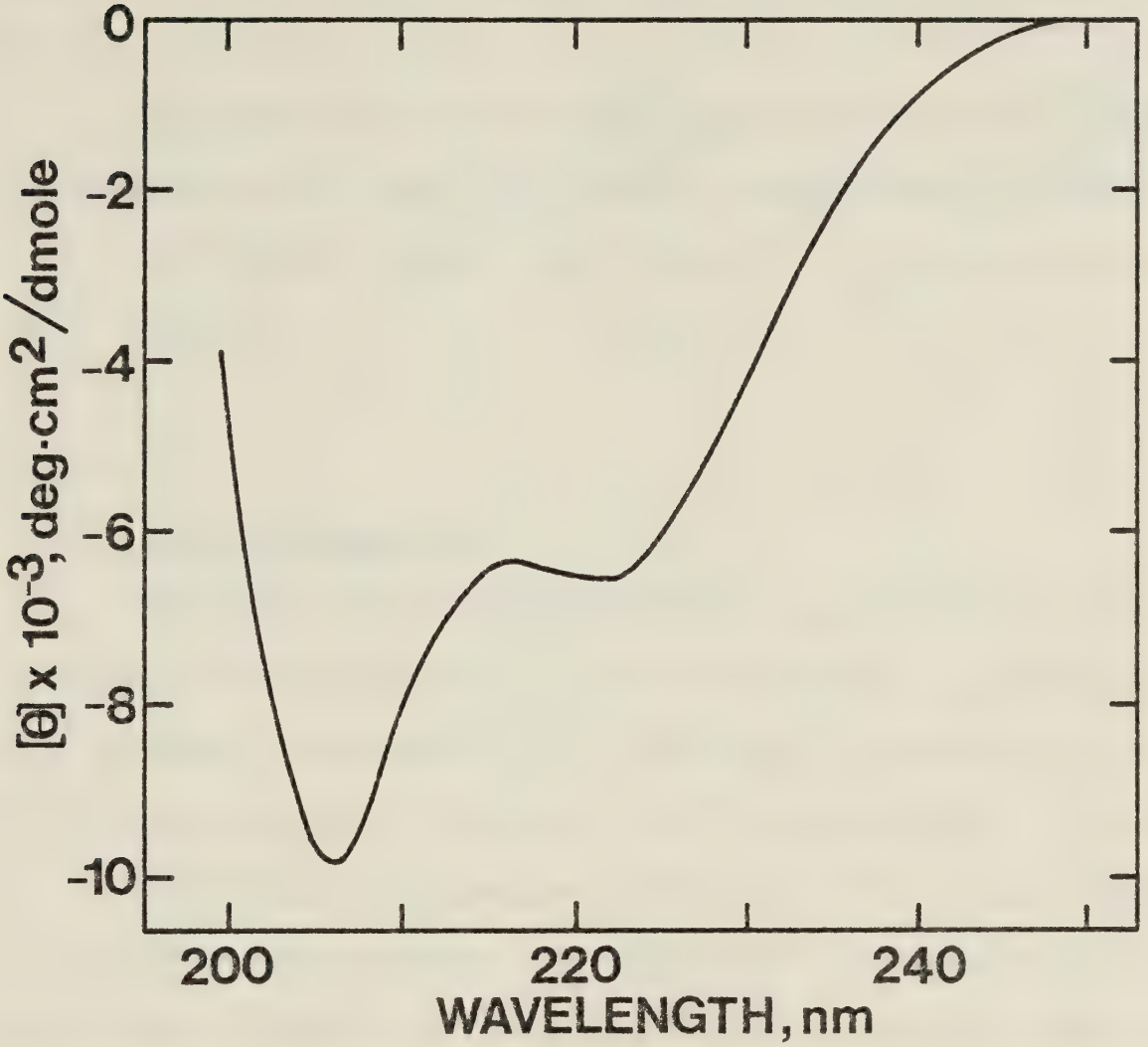

Figure 35. Far UV CD spectrum of TN-I. The protein was dissolved in 0.5 M KCl, 50 mM tris-HCl, pH 7.5, 1 mM EGTA.

Calculations (66) suggest an apparent α helix content of 23%, significantly lower than the 45% value proposed for skeletal TN-I (51). The increased proline content of cardiac TN-I may play a role in this difference.

The shape of the CD spectrum of cardiac TN-I was not affected by the addition of Ca^{2+} and/or Mg^{2+} ions to concentrations as high as 5 mM.

The aromatic region of the cardiac TN-I CD spectrum was essentially featureless.

C. TN-T

1. Amino Acid Analysis

The amino acid composition of bovine cardiac TN-T is presented in Table III, along with that of rabbit skeletal TN-T, as determined from its amino acid sequence (20). The values are presented as residues per molecule, assuming a molecular weight for cardiac TN-T of 36,300.

Completing the pattern set by TN-C and TN-I, the TN-T molecules from different tissue sources show considerable variation in their amino acid content. Cardiac TN-T is richer in acidic residues, contains less proline and methionine, and has approximately one cysteine residue per molecule.

2. Solubility

As with TN-I, cardiac TN-T was marginally soluble in non-denaturing buffers. To increase its solubility in 0.5 M KCl, 50 mM tris-HCl, pH 7.5, it was dissolved in an 8 M urea-containing buffer and dialysed against the tris medium. Prior to any analytical work, TN-T solutions were clarified by centrifugation or filtration through millipore filters.

TABLE III

Amino acid composition of bovine cardiac TN-T

Amino Acid	Residues per molecule of protein	
	Bovine Cardiac TN-T*	Rabbit Skeletal TN-T**
Lys	34.3	39
His	4.4	6
Arg	33.8	25
Asx	27.4	20
Thr	7.6	6
Ser	6.8	9
Glx	88.3	57
Pro	9.1	9
Gly	12.7	8
Ala	26.2	26
Val	12.1	11
Met	3.5	5
Ile	11.5	8
Leu	18.5	19
Tyr	4.5	4
Phe	7.6	5
Trp	2.3	2
1/2 Cys	1.3	0

*Assuming a molecular weight of 36,300.

**Pearlstone *et al.* (20).

3. Extinction Coefficient

The extinction coefficient of a 1% solution of cardiac TN-T in a 1 cm pathlength cell at 278 nm was determined to be 3.9 (Figure 36).

4. Molecular Weight

On SDS polyacrylamide gels, the migration rate of TN-T suggested it had a molecular weight of 37,000 ± 1,000 (Figure 19). This is comparable to the SDS gel molecular weight for skeletal TN-T (96, 97).

Conventional sedimentation equilibrium experiments in 0.5 M NaCl, 50 mM tris-HCl, pH 7.5, gave log c vs. r^2 plots which were not linear, but curved upwards (Figure 37), suggesting aggregation. However, in 8 M urea, 0.2 M NaCl, 50 mM tris-HCl, pH 7.5, 1 mM DTT, the plots were linear (Figure 38). Assuming a $\bar{v}$ for TN-T of 0.72 ml/g, as estimated by calculating a $\bar{v}$ from its amino acid composition (70) and taking into account the effect of 8 M urea (94), a weight average molecular weight for cardiac TN-T of 36,300 ± 2,000 was determined.

The molecular weight of skeletal TN-T found in sequence studies (20) was 30,503, considerably less than the reported gel molecular weight of 37,000. Although ultracentrifugal studies were able to distinguish the true molecular weight of cardiac TN-I, determined by sequence analysis, from its anomolous SDS gel molecular weight, no such distinction could be made for TN-T. Therefore, it was concluded that the molecular weight of cardiac TN-T is in the vicinity of 36,000.

As an interesting aside, Pearlstone et al. (20) found that about 50% of the amino acid residues in rabbit skeletal TN-T would be charged at neutral pH. Also, they noted an almost total lack of clusters of nonpolar residues in the sequence. These facts indicate that skeletal TN-T does not possess a significant hydrophobic core, suggesting

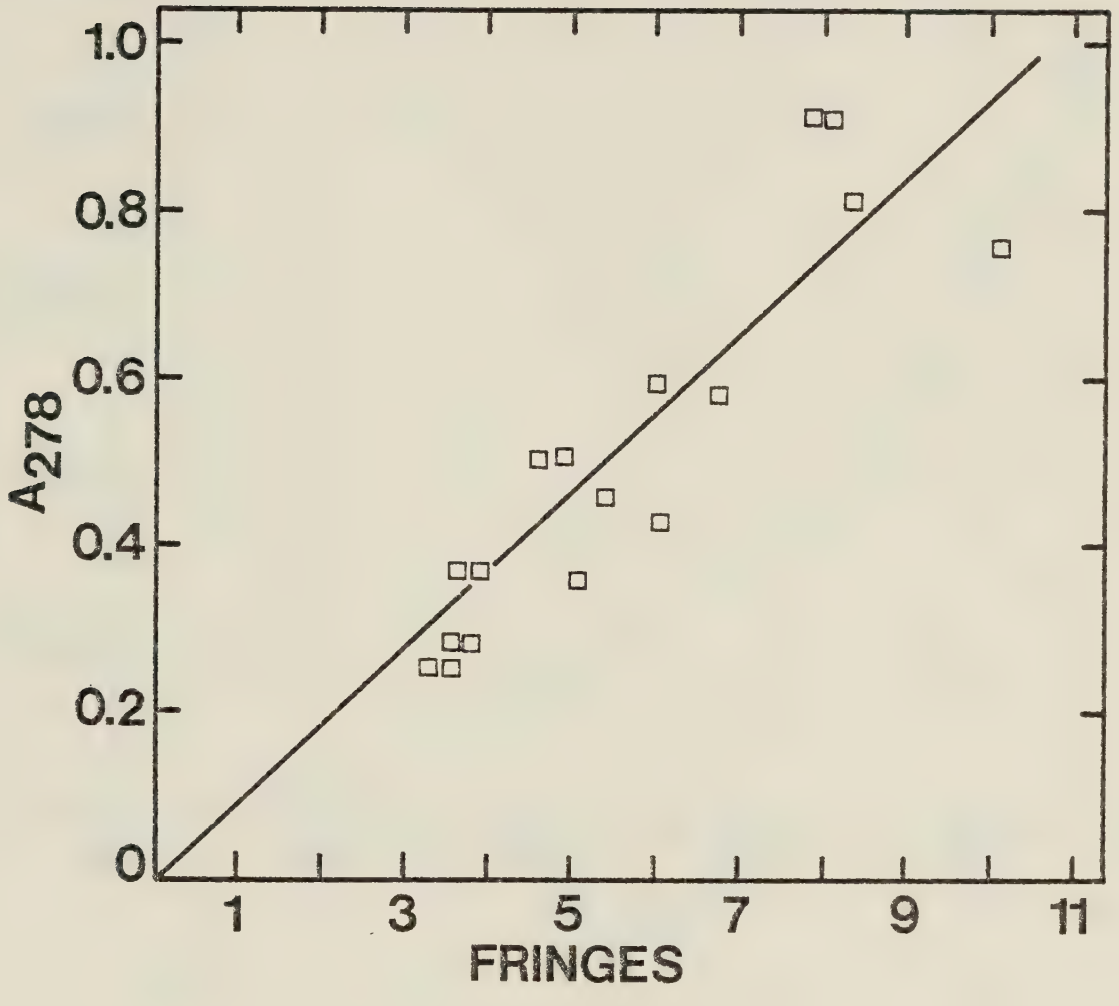

Figure 36. Determination of the extinction coefficient of TN-T. The protein was dissolved in 0.5 M NaCl, 50 mM tris-HCl, pH 7.5 and centrifuged at 12,000 rpm. The absorbance value at 278 nm was recorded for each sample and its concentration determined refractometrically according to Babul and Stellwagen (68).

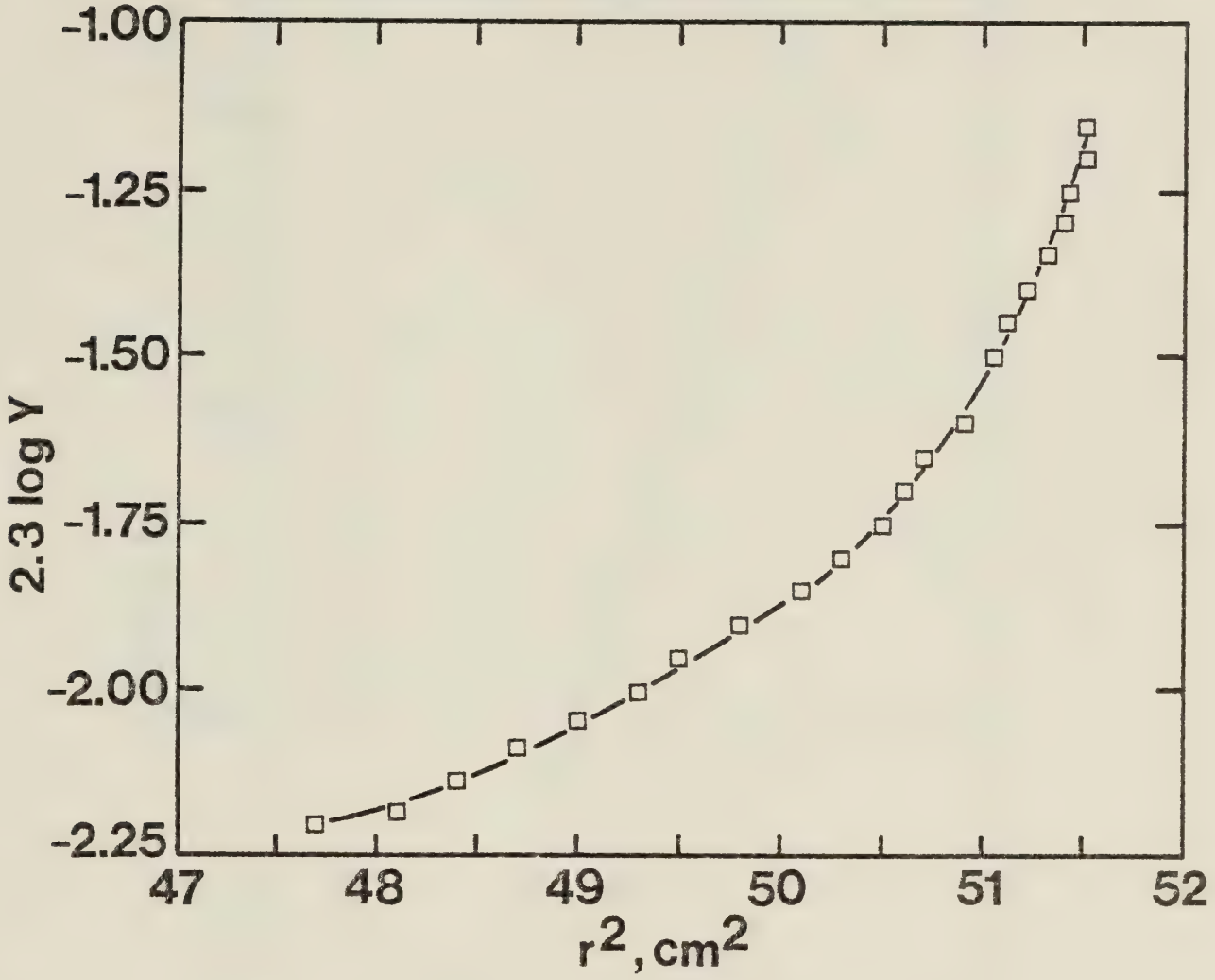

Figure 37. Sedimentation equilibrium log Y versus r^2 plot for TN-T in a nondenaturing buffer. TN-T was dissolved in 0.5 M NaCl, 50 mM tris-HCl, pH 7.5 and spun at 14,000 rpm in a centrifuge equipped with Rayleigh interference optics. Y represents protein concentration in terms of fringe displacement units.

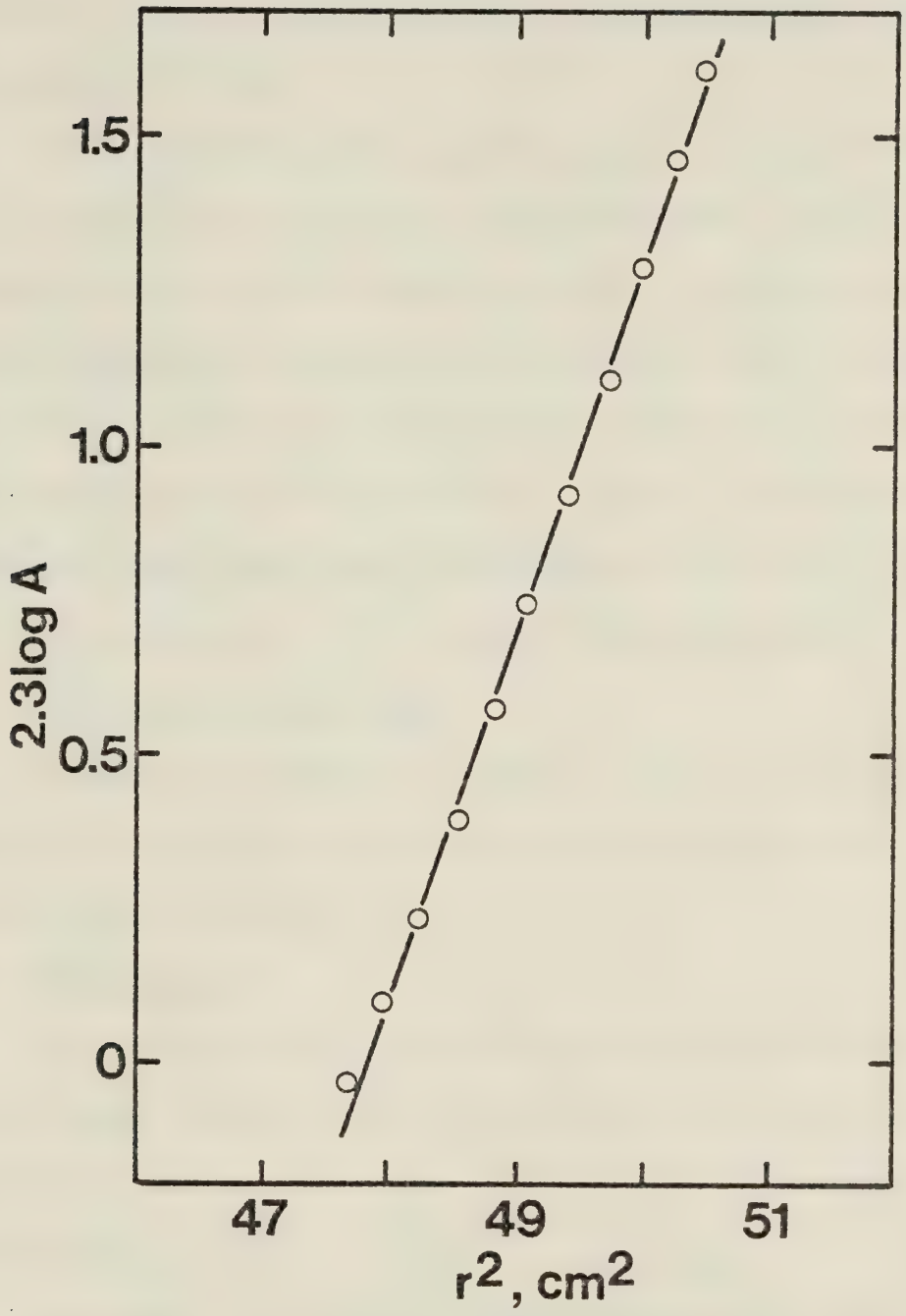

Figure 38. Sedimentation equilibrium log A versus r^2 plot for TN-T in the presence of 8 M urea. TN-T was dissolved in 8 M urea, 0.2 M NaCl, 50 mM tris-HCl, pH 7.5, 1 mM DTT and spun at 20,000 rpm in a centrifuge equipped with a photoelectric scanner. A represents protein concentration in terms of absorption units at 280 nm.

that the molecular structure is readily penetrable by solvent molecules. Considering these conclusions in terms of the $\bar{v}$ of TN-T, it seems that a prediction of $\bar{v}$ from the amino acid composition might lead to an erroneously high value.

It is probably valid to assume a great degree of homology between the structures of skeletal and cardiac TN-T. Since a 1% error in estimating $\bar{v}$ would lead to nearly a 5% error in the calculation of a molecular weight from sedimentation equilibrium data, assuming a $\bar{v}$ for cardiac TN-T of 0.71 ml/g instead of 0.72 ml/g would place its molecular weight significantly less than 36,000. If this were true, the incorrect SDS gel molecular weight could be explained, in a similar fashion to the TN-I case, as being due to the unusual charge properties of the molecule.

5. UV Absorption Properties

Cardiac TN-T possesses a typical protein UV absorption spectrum (Figure 39), exhibiting absorption bands arising from all 3 types of aromatic amino acid residues.

6. CD Properties

The CD spectrum of cardiac TN-T in the far UV wavelength region displays minima near 207 and 221 nm (Figure 40), indicative of α helical regions in its polypeptide chain. Calculations (66) suggest an apparent α helix content of 43%.

The shape of the cardiac TN-T CD spectrum was unaffected by the addition of $CaCl_2$ to 5 mM. However, if 2 mM $MgCl_2$ were present, a 4 - 6% decrease in $[\theta]_{221}$ was observed. The significance of this small change, if any, is not clear at this time.

In the aromatic region of the TN-T CD spectrum, a broad, slightly negative dichroism was observed. This portion of the TN-T CD spectrum

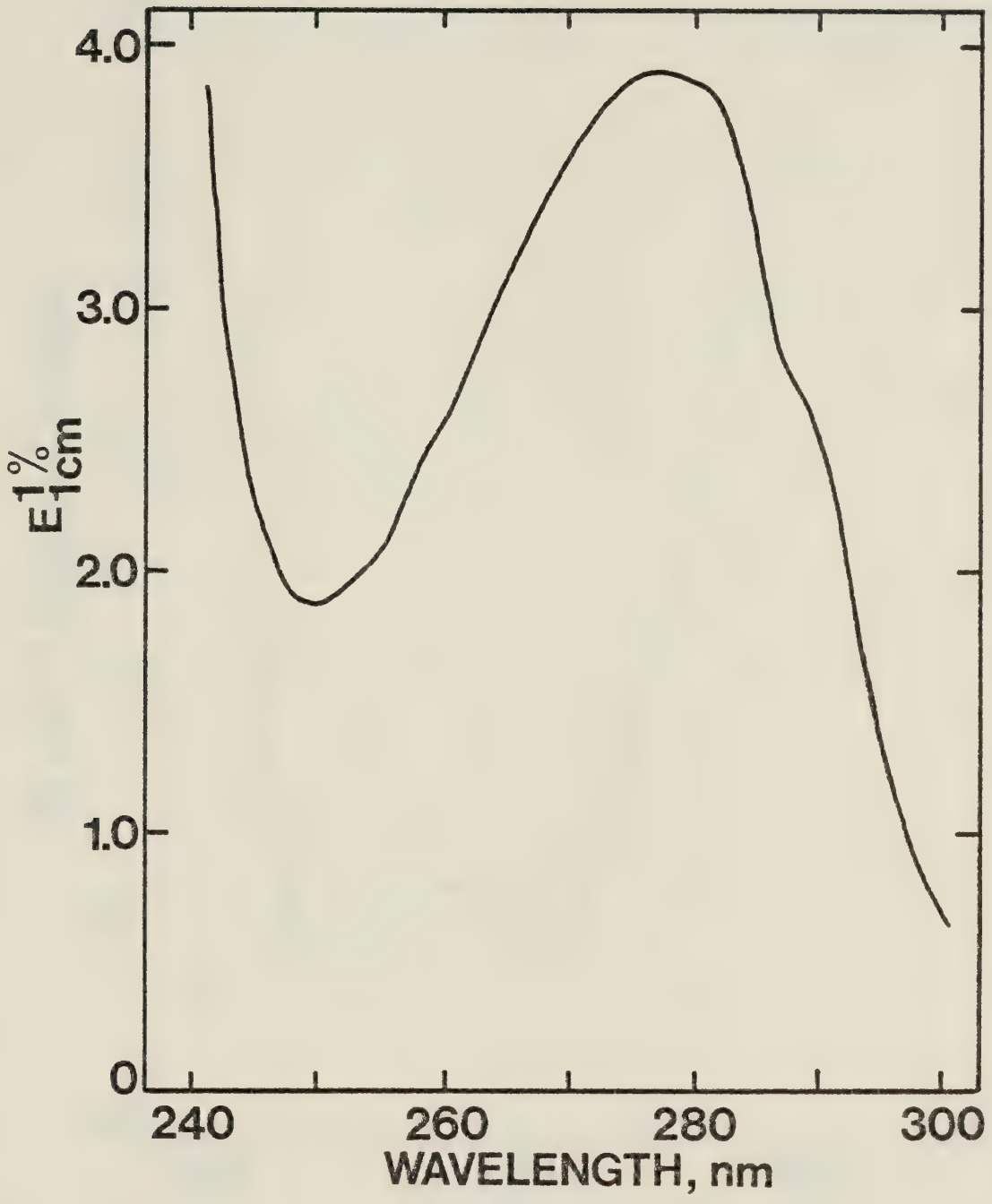

Figure 39. UV absorption spectrum of TN-T. The protein was dissolved in 0.5 M NaCl, 50 mM tris-HCl, pH 7.5, 1 mM EGTA.

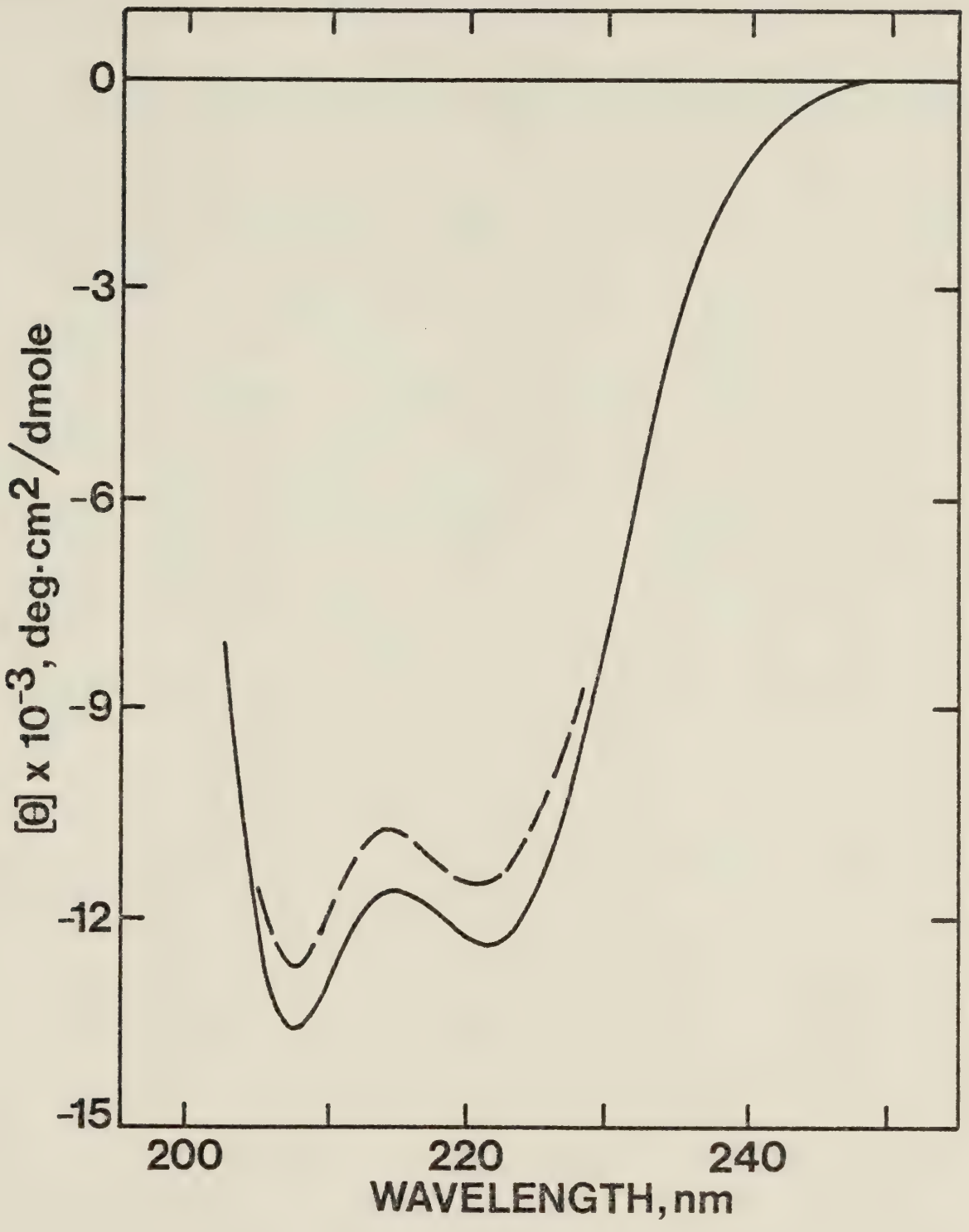

Figure 40. Far UV CD spectra of TN-T in the presence and absence of magnesium. TN-T was dissolved in 0.5 M NaCl, 50 mM tris-HCl, pH 7.5, 1 mM EGTA containing either no added $MgCl_2$ (———), or 2 mM $MgCl_2$ (— — —).

was unaffected by the presence of Ca^{2+} or Mg^{2+} ions in the protein solution.

CHAPTER V

INTERACTION STUDIES

It is clear that the subunits of troponin interact strongly with each other. They adhere to one another while the muscle structure about them is disrupted and subjected to an extensive series of washes which remove most other proteins. They precipitate out of solution together in a narrow range of ammonium sulfate concentration, despite vast differences in net charge and general solubility properties. To separate the components, strongly denaturing conditions (8 M urea) are required. Once isolated, TN-I and TN-T firmly refuse to be returned into solution. But if TN-C is added to the same test tube, these proteins readily dissolve without the necessity of prodding by denaturing conditions.

To fully understand how troponin regulates muscle contraction, the types of intersubunit interactions which occur must be known. Potter (98) recently confirmed, using quantitative SDS gel analysis, that the stoichiometry of the major proteins in the rabbit skeletal muscle myofibril is actin:myosin:tropomyosin:TN-T:TN-I:TN-C equal to 7:1:1:1:1:1. Head and Perry (43) demonstrated that in cardiac muscle the ratio of actin to TN-C is 7:1, so it seems reasonable to assume the protein stoichiometry in cardiac muscle, at least in the thin filament, is similar to that in skeletal muscle. This assumption greatly reduces the number of permutations of possible interactions and, therefore, the amount of material necessary to study the nature of the interactions which occur among the components of the cardiac muscle regulatory system.

Again, the material in this chapter is drawn mainly from published results (37, 38, 41).

A. BIOLOGICAL ACTIVITY

Once each troponin subunit was isolated in pure form, adding it to a synthetic bovine cardiac actomyosin (SAM) system allowed its primary functional role to be assigned. It was, in fact, these studies which justified labelling the subunits TN-I, TN-C and TN-T in the same fashion as the skeletal counterparts.

The addition of cardiac TN-I to a SAM ATPase assay system (Figure 41) led to as much as a 60% inhibition of the Mg^{2+} activated actomyosin ATPase. This inhibitory effect was independent of the presence or absence of free Ca^{2+} ions in the assay mixture. Brekke and Greaser (46) were unable to show a significant inhibitory effect of cardiac TN-I in a similar assay system. All three troponin components were necessary to produce inhibition in the absence of Ca^{2+}. The reason for this discrepancy is not clear at this time.

Upon adding cardiac TN-C to a SAM preparation which had been inhibited partially by the addition of TN-I, the inhibitory effect could be completely reversed (Figure 42). Again, this reversal phenomenon was not dependent upon Ca^{2+} concentration.

To render the assay system sensitive to Ca^{2+} ions, all three cardiac troponin constituents had to be present (Table IV). In the presence of EGTA, TN-I and TN-C, ATP was hydrolysed at the same rate as by a control in which neither troponin component was present. Addition of TN-T caused the ATPase activity to fall to a level equivalent to a situation in which only TN-I was present. However, addition of $CaCl_2$ resulted in the ATPase activity being restored completely.

No cross-functionality was observed among the subunits. Only TN-I could inhibit ATPase activity, and only TN-C could restore the inhibited

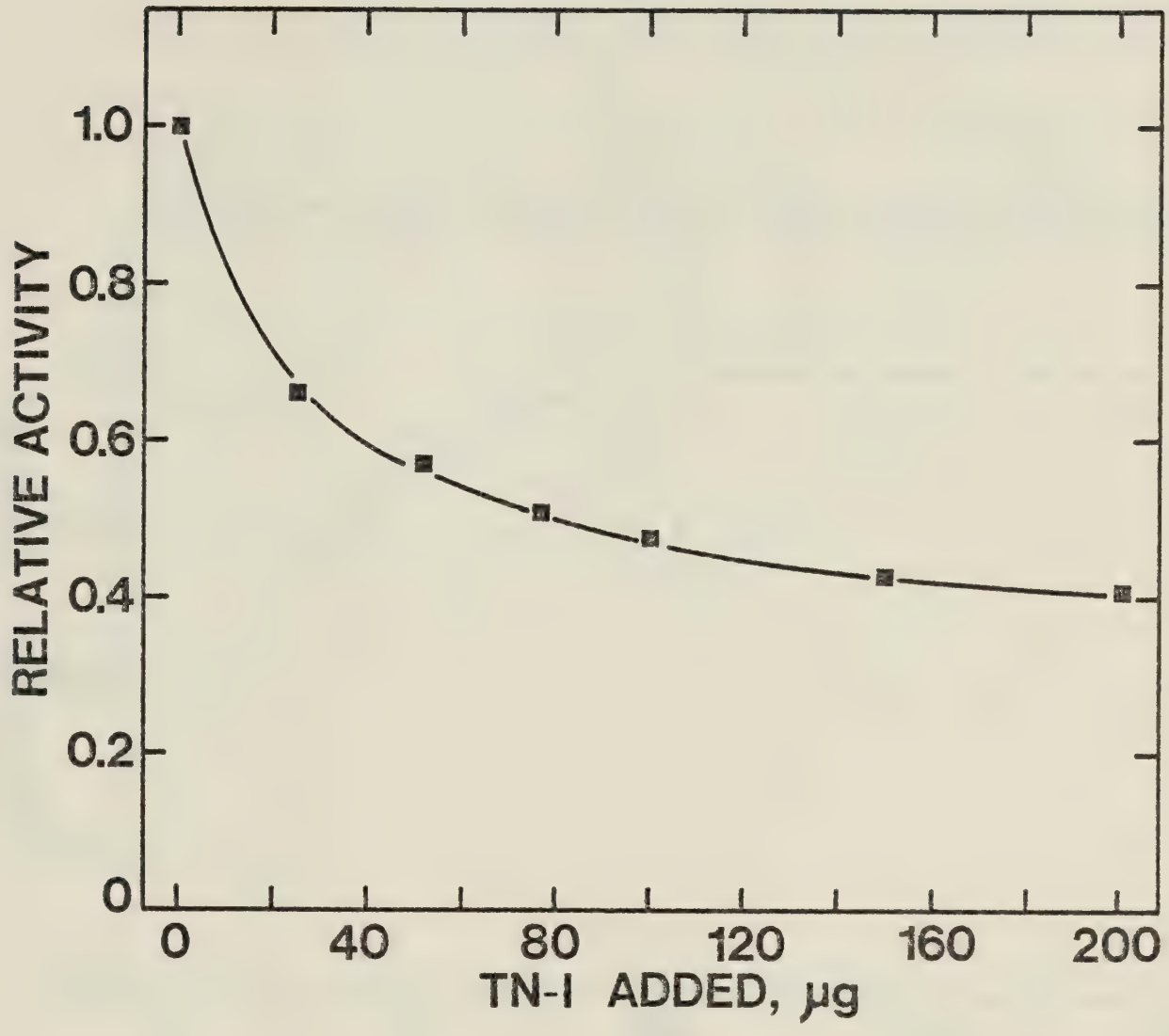

Figure 41. Inhibition of the Mg^{2+} activated ATPase of synthetic cardiac actomyosin by TN-I. The control sample contained 750 µg cardiac SAM and 50 µg cardiac tropomyosin in 10 mM tris-HCl, pH 7.6, 2.5 mM $MgCl_2$, 1 mM EGTA, 2.5 mM ATP at 20°C.

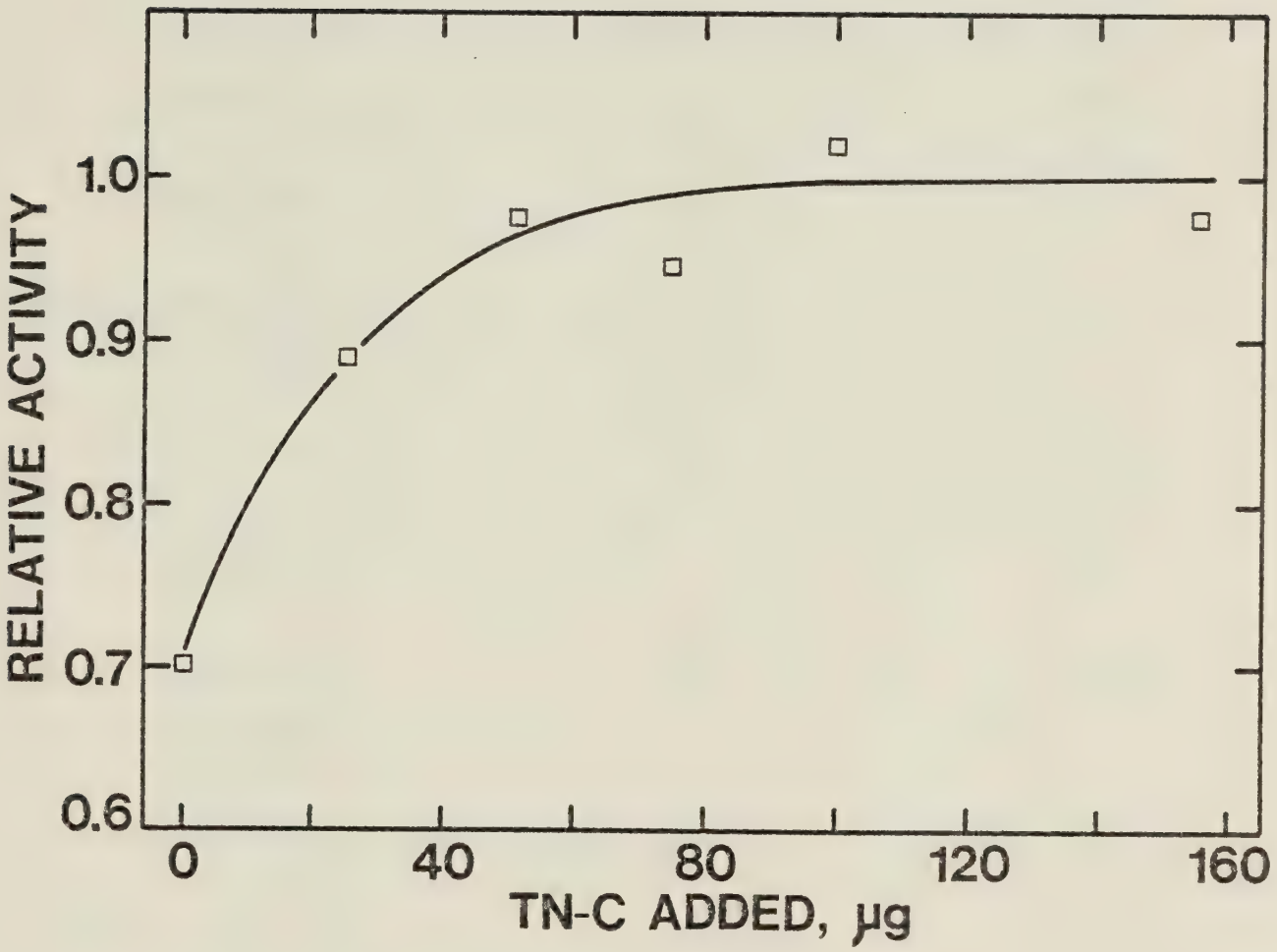

Figure 42. Reversal of the TN-I induced inhibitory effect on synthetic cardiac actomyosin by TN-C. The control sample was as described in Figure 41. The system was then partially inhibited by the addition of 25 µg TN-I, prior to the addition of TN-C.

TABLE IV

Reconstitution of the regulatory system of bovine cardiac muscle

Troponin Components Present	$[Ca^{2+}]_{free}$	Relative Activity
1. Control	0	1.00
2. 50 µg TN-I	0	.61
3. 50 µg TN-I + 50 µg TN-C	0	.97
4. 50 µg TN-I + 50 µg TN-C + 70 µg TN-T	0	.58
5. 50 µg TN-I + 50 µg TN-C + 70 µg TN-T	10^{-3} M	.99

NOTE:

The control contained 750 µg synthetic actomyosin and 50 µg tropomyosin in 10 mM tris-HCl, pH 7.6, 2.5 mM $MgCl_2$, 1 mM EGTA and 2.5 mM ATP at 20°C.

activity. Further, only when TN-T was present did the entire system become Ca^{2+} sensitive.

The regulatory proteins are present in an equimolar ratio in muscle (98), but an equimolar mixture of these proteins does not confer Ca^{2+} sensitivity efficiently upon this assay system. This probably reflects upon the assay system itself, suggesting conditions are not optimal for interprotein interactions. A 1:1 mole ratio of TN-I to tropomyosin inhibits ATPase activity by 30%. A 3:1 ratio is necessary for 50% inhibition. A 1:1 mole ratio of TN-C to TN-I restores the activity to 85%, while a 2:1 ratio is necessary for 95% restoration. TN-T must be added in at least equimolar proportions with TN-I to obtain effective Ca^{2+} sensitization.

This study provided information concerning the functions of the troponin components, but in a multiprotein mixture such as the assay system, it was not possible to determine which proteins interacted with one another directly. More controlled conditions were required.

B. POLYACRYLAMIDE GEL STUDIES

1. TN-IC

Head and Perry (43) had shown that skeletal TN-I and TN-C could form a strong complex, even in the presence of 6 M urea. They ran samples containing a mixture of TN-I and TN-C on polyacrylamide gels in the absence of SDS and discovered a band which migrated at a position between pure TN-I and pure TN-C. This new band represented TN-IC, a complex which formed from TN-I and TN-C.

Using similar methodology, cardiac TN-I and TN-C were observed to form an analogous complex (Figure 43). Cardiac TN-C (gel A), being rich in acidic residues, electrophoresed rapidly at pH 8.5. Conversely,

Figure 43. Polyacrylamide gel electrophoresis of TN-IC. Onto the gels in the photograph were applied (A) 30 µg TN-C, (B) 30 µg TN-I, (C) 30 µg TN-C + 50 µg TN-I, and (D) 30 µg TN-C + 100 µg TN-I.

TN-I (gel B), rich in basic residues, did not move downward from the origin at this pH. When TN-I and TN-C were mixed (gel C), whether the running buffer and sample solutions contained EGTA or $CaCl_2$, a complex with mobility intermediate between that of TN-I and TN-C was formed.

In these experiments, as the mole ratio of TN-I to TN-C was increased beyond roughly 2:1, the residual staining in the TN-C region disappeared (gel D). However, this ratio could not be interpreted as representing a physiological stoichiometry due to the conditions employed (6 M urea).

Cardiac and skeletal TN-IC differ with respect to the effect of Ca^{2+} upon their formation. In the presence of EGTA, no complex between skeletal TN-C and TN-I could be observed (43). Our results demonstrated a strong tendency for cardiac TN-I and TN-C to complex in the presence of EGTA or of free Ca^{2+} ions.

2. TN-CT

When similar gel electrophoresis experiments were performed on solutions containing cardiac TN-C and TN-T in the presence of 6 M urea, no evidence for the existence of the complex, TN-CT, was found. If the gels were run in the absence of urea, evidence for an interaction between TN-C and TN-T could be seen (Figure 44). In gels onto which a mixture of TN-T and TN-C had been applied, two regions of mobility intermediate between those of TN-C and TN-T bound dye faintly (gel C). These bands did not stain in gels onto which only TN-C (gel A) or TN-T (gel B) were applied. The appearance of these dye binding regions did not depend upon the presence or absence of available Ca^{2+} ions in the sample mixtures.

Interpretation of the nature of the interaction between TN-C

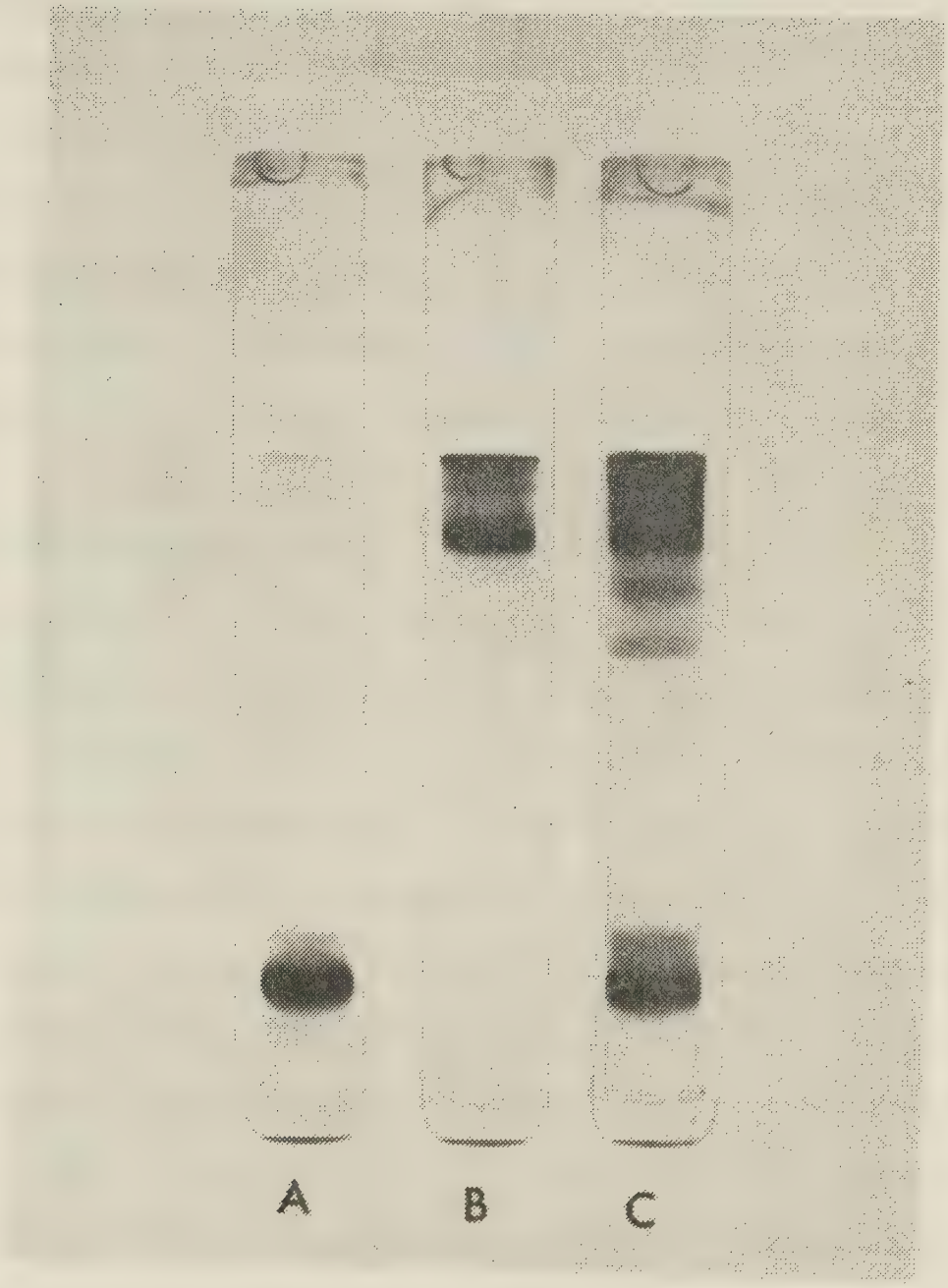

Figure 44. Polyacrylamide gel electrophoresis of TN-CT. Onto the gels in the photograph were applied (A) 40 µg TN-C, (B) 60 µg TN-T, and (C) 40 µg TN-C + 60 µg TN-T.

and TN-T was hindered by the appearance of 2 new bands. The low staining intensity of these regions relative to that of the individual troponin components suggested that, under the experimental conditions used, the interaction was not a strong one.

Using gel electrophoresis, van Eerd and Kawasaki (99) reported the formation of a complex between skeletal TN-C and TN-T. This complex formed in the presence or absence of Ca^{2+}, but possessed a slightly higher mobility in the presence of Ca^{2+}. Gel results, again, reveal differences between the cardiac and skeletal protein analogues.

C. COSEDIMENTATION ANALYSIS

Cosedimentation analysis has been used to demonstrate that if skeletal tropomyosin and TN-T or TN-I are mixed under conditions where all protein components are soluble and subsequently dialysed against a solution in which only tropomyosin is normally soluble, not only TN-I or TN-T precipitate, but tropomyosin does as well (78, 79). Such coprecipitation was interpreted as evidence that tropomyosin could interact with skeletal TN-T or TN-I.

Results of cosedimentation experiments using cardiac tropomyosin and the individual cardiac troponin components clearly demonstrated an interaction between TN-T and tropomyosin but failed to detect an interaction of tropomyosin with either TN-I or TN-C.

As increasing amounts of TN-T were added to solutions containing a constant amount of tropomyosin, a precipitate was obtained (Table V). Tropomyosin to which no TN-T was added did not precipitate under the conditions of the experiment. Analysis of the precipitates by SDS gel electrophoresis (Figure 45) showed them to contain both TN-T and

TABLE V

Cosedimentation analysis of solutions

containing tropomyosin and TN-T

Sample	Mole Ratio (TN-T:tropomyosin)	Degree of Precipitation
1. TN-T	-	1
2. TN-T plus tropomyosin	0.5:1	1
3. TN-T plus tropomyosin	1:1	2
4. TN-T plus tropomyosin	2:1	2
5. tropomyosin	-	0

NOTE:

The degree of precipitation was estimated visually on a scale of 0 to 2, with 0 indicating no visible precipitate.

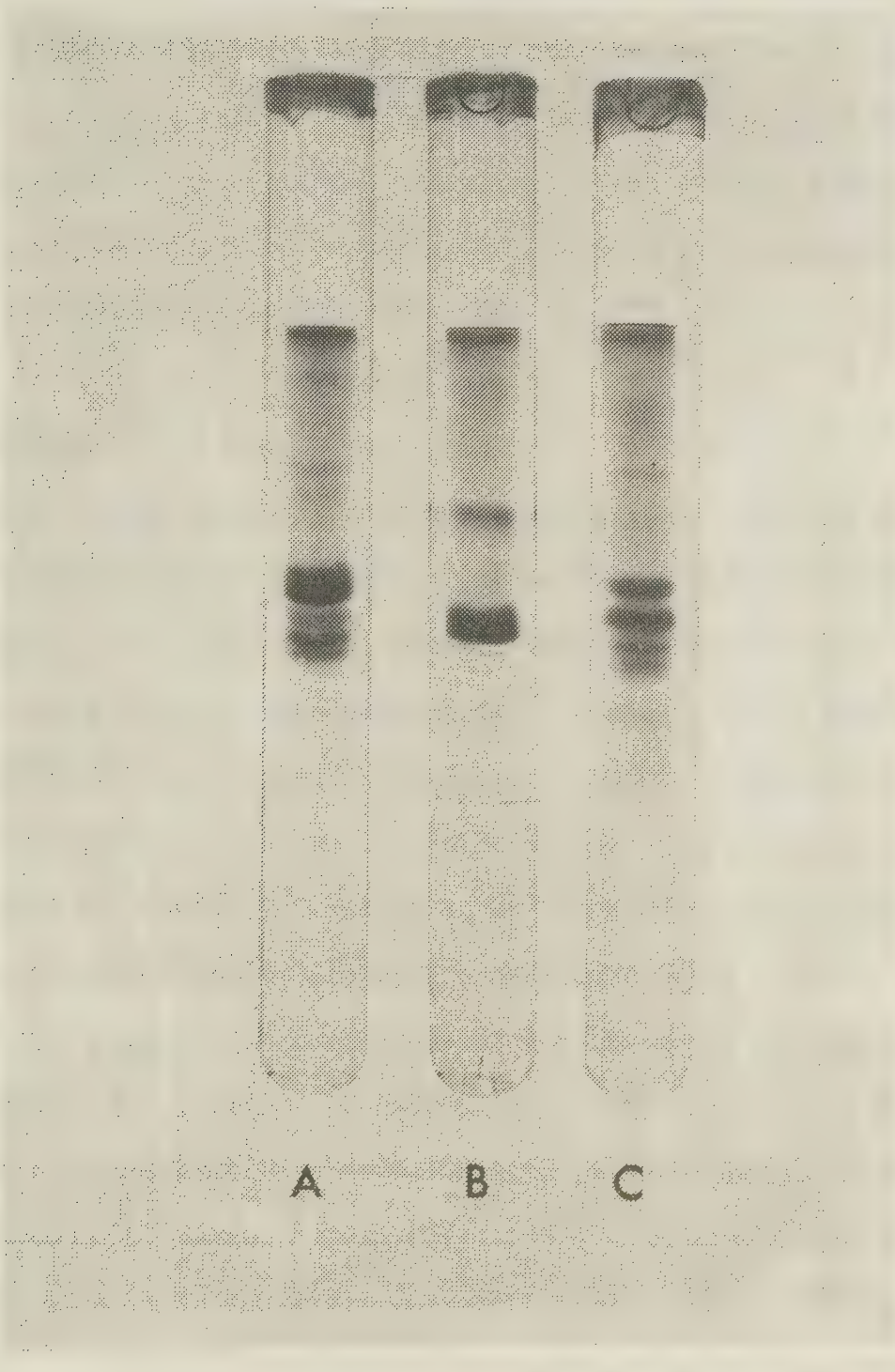

Figure 45. SDS polyacrylmide gel analysis of the precipitates from cosedimentation studies. The gels depict (A) precipitated TN-T, (B) 40 µg of tropomyosin, and (C) precipitate from an equimolar mixture of TN-T and tropomyosin.

tropomyosin. Gel A portrays the precipitate from a sample containing only TN-T; gel B represents cardiac tropomyosin; gel C reveals that both TN-T and tropomyosin are present in the precipitate from an equimolar mixture of the 2 proteins. The bands of lower staining intensity appearing in gels of the precipitates characterize the primary stages of the breakdown of TN-T observed on prolonged dialysis in a nondenaturing buffer, as discussed previously.

D. CD STUDIES

Changes in the CD spectrum of a protein molecule provide information about conformational changes which may occur upon ligand binding. In particular, CD has proved a valuable tool for monitoring the conformational change in TN-C upon binding Ca^{2+} ions (25, 35). Reports from this laboratory involving skeletal muscle troponin components have provided strong evidence for the occurence of interprotein interactions between TN-C and TN-I, TN-C and TN-T, TN-T and tropomyosin and in troponin reconstituted from its isolated constituents (100 - 102).

CD proved, again, in studies on the cardiac troponin subunits, to be a sensitive indicator of interprotein interactions (41). The standard solvent system consisted of 0.5 M KCl, 50 mM tris-HCl, pH 7.5, 1 mM EGTA ("minus Ca^{2+}" solvent).

Far UV CD spectra were recorded, both in the "minus Ca^{2+}" and "plus Ca^{2+}" states, for each component of the cardiac muscle regulatory system, tropomyosin, TN-T, TN-I and TN-C. Of these spectra, only that of TN-C was affected by the addition of Ca^{2+}, displaying an increase in the magnitude of $[\theta]_{221}$ by 24 ± 3% ($\sim$3,400 deg·cm^2/dmole). Using these spectra, a set of calculated spectra were generated, representing each

experimental situation subsequently tested. These calculated spectra simply represented linear combinations of the contributions from each protein present in the test solution. Such a spectrum should match an experimentally measured one in the case where no interprotein interactions occur.

Various test combinations of the components were prepared by mixing the individual proteins in equimolar amounts. Spectra were then recorded for the combinations TN-C plus TN-T, TN-C plus TN-I, TN-I plus TN-T, tropomyosin plus TN-C, tropomyosin plus TN-I, tropomyosin plus TN-T, and reconstituted troponin. Of these combinations, those which produced CD spectra which differed significantly from the calculated ones ($|[\theta]_{221\ \text{calculated}} - [\theta]_{221\ \text{observed}}| > 500$ deg·cm^2/dmole), suggesting the occurence of interprotein interactions, included the complexes TN-T - tropomyosin (Figure 46), TN-CT (Figure 47), TN-IC (Figure 48) and reconstituted troponin, TN-ICT (Figure 49).

The interactions observed appeared to be of two types. For TN-T - tropomyosin and TN-CT, the observed ellipticity values were less negative than the calculated ones, suggesting a net loss in apparent α helix content upon interaction. For the complexes TN-IC and TN-ICT, a net gain in α helix content occurred upon interaction.

Those complexes involving TN-C underwent a conformational change upon binding Ca^{2+} (Figures 47 - 49). For example, with TN-ICT, $[\theta]_{221}$ increased in magnitude by 10% ($\sim$1,200 deg·cm^2/dmole). Therefore, the conformational change observed in isolated TN-C in solution persists in those complexes containing TN-C, including reconstituted troponin. Also, as with isolated TN-C, the addition of $MgCl_2$ to 3 mM prior to the addition of $CaCl_2$ resulted only in a partial (up to 50% of the maximal)

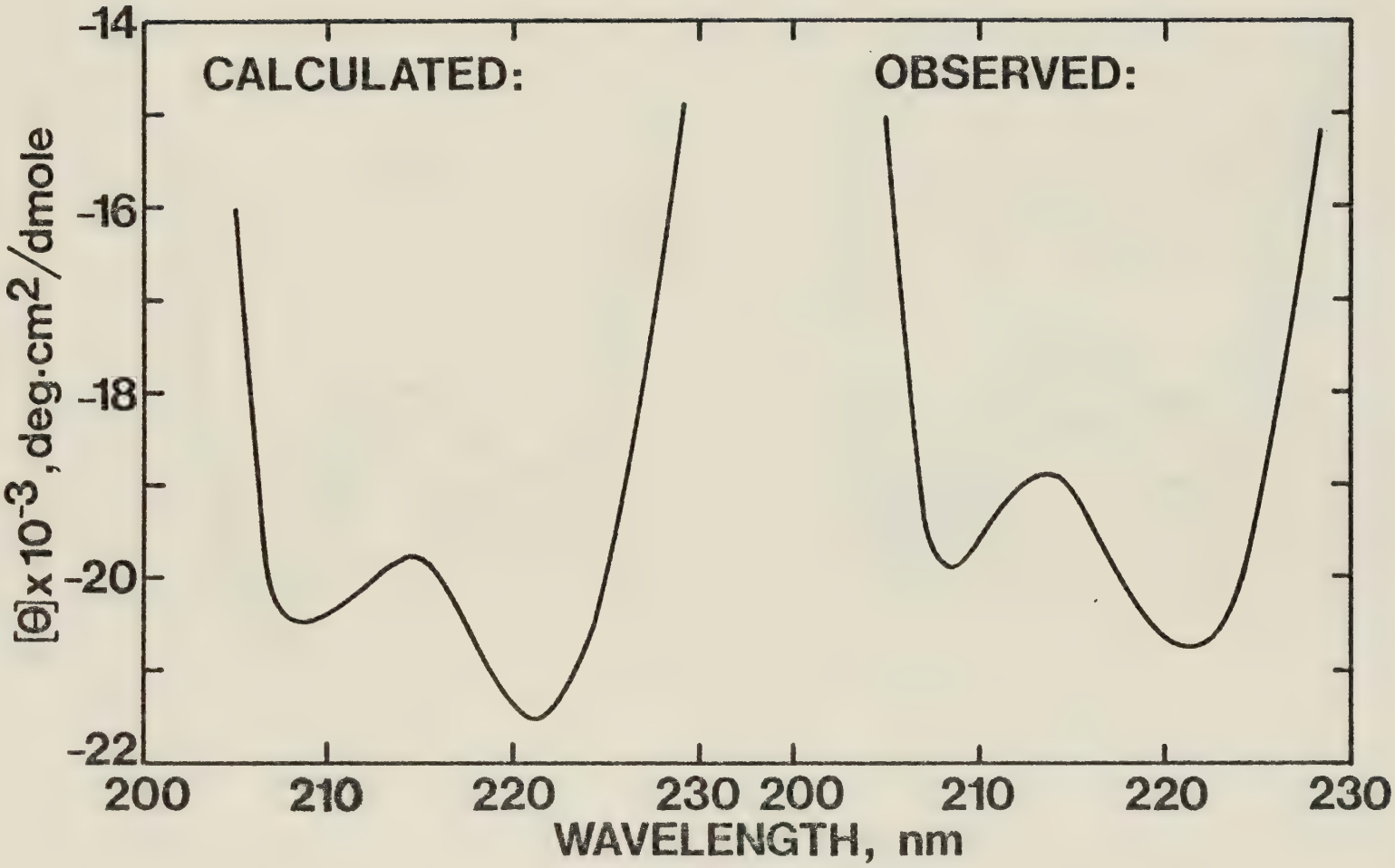

Figure 46. Calculated and observed CD spectra of TN-T - tropomyosin. The proteins were dissolved in 0.5 M KCl, 50 mM tris-HCl, pH 7.5, 1 mM EGTA and mixed in an equimolar ratio.

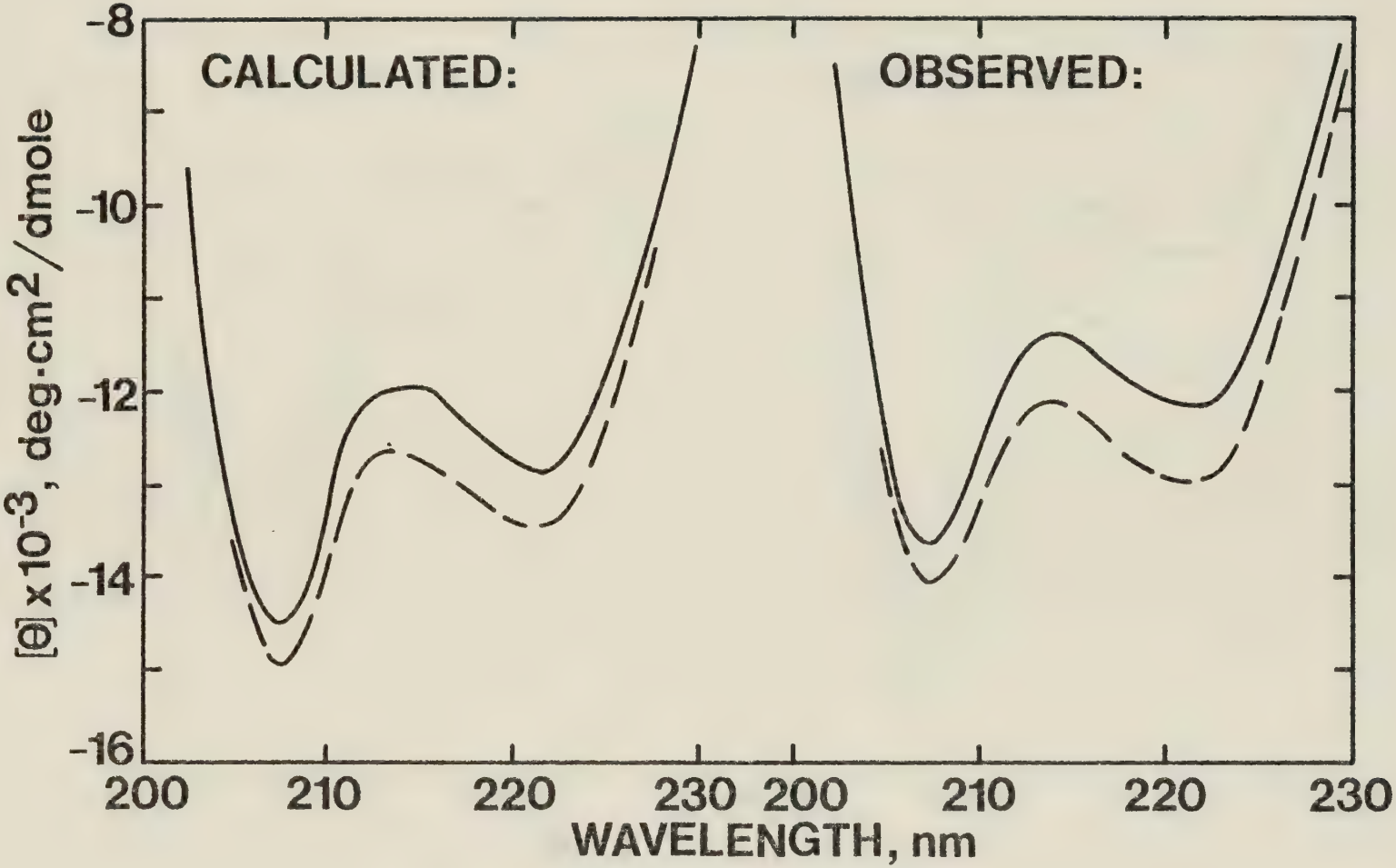

Figure 47. Calculated and observed CD spectra of TN-CT in the presence (— — —) and absence (———) of calcium. The initial solvent composition was as described in Figure 46.

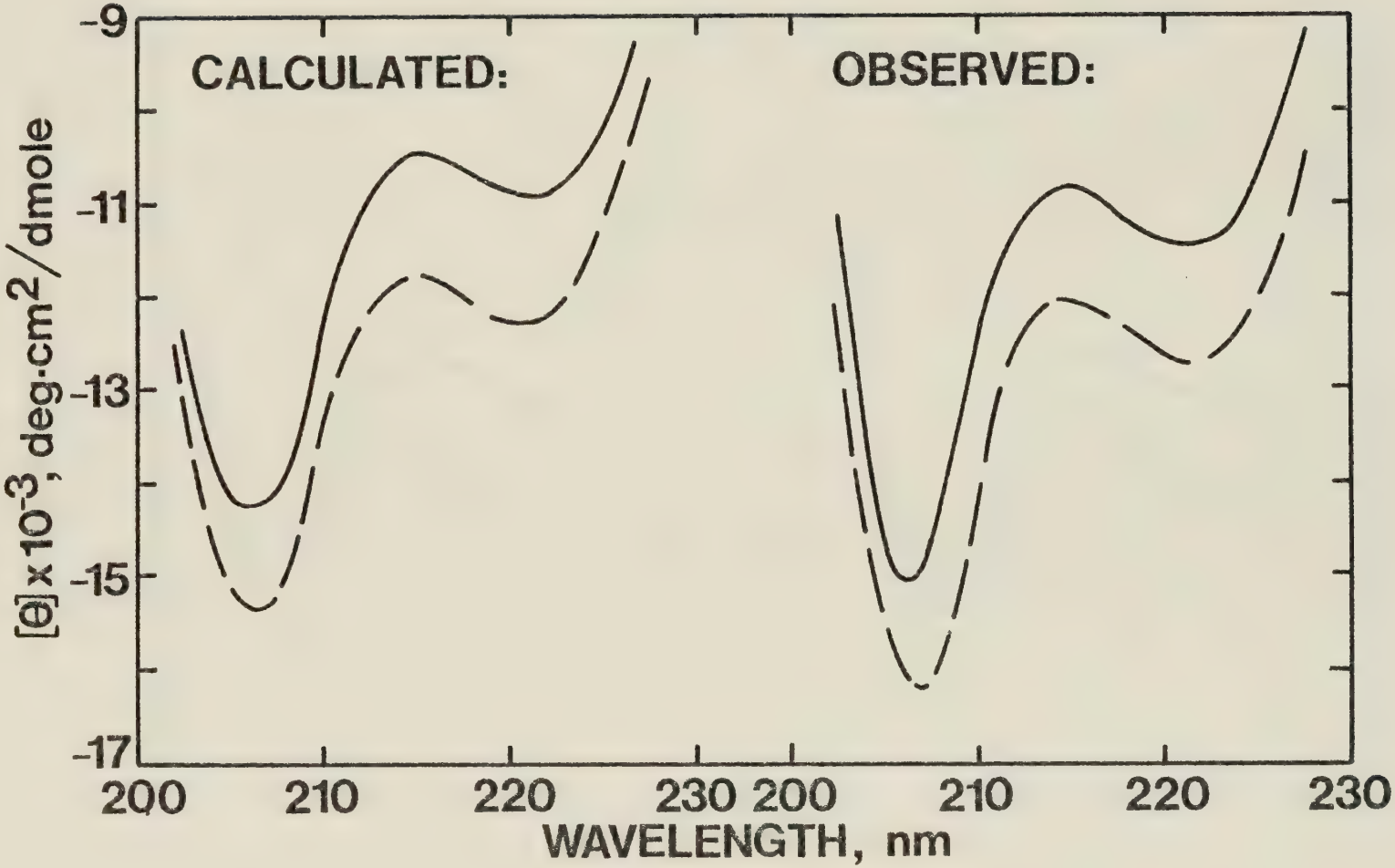

Figure 48. Calculated and observed CD spectra of TN-IC in the presence (— — —) and absence (———) of calcium. The initial solvent composition was as described in Figure 46.

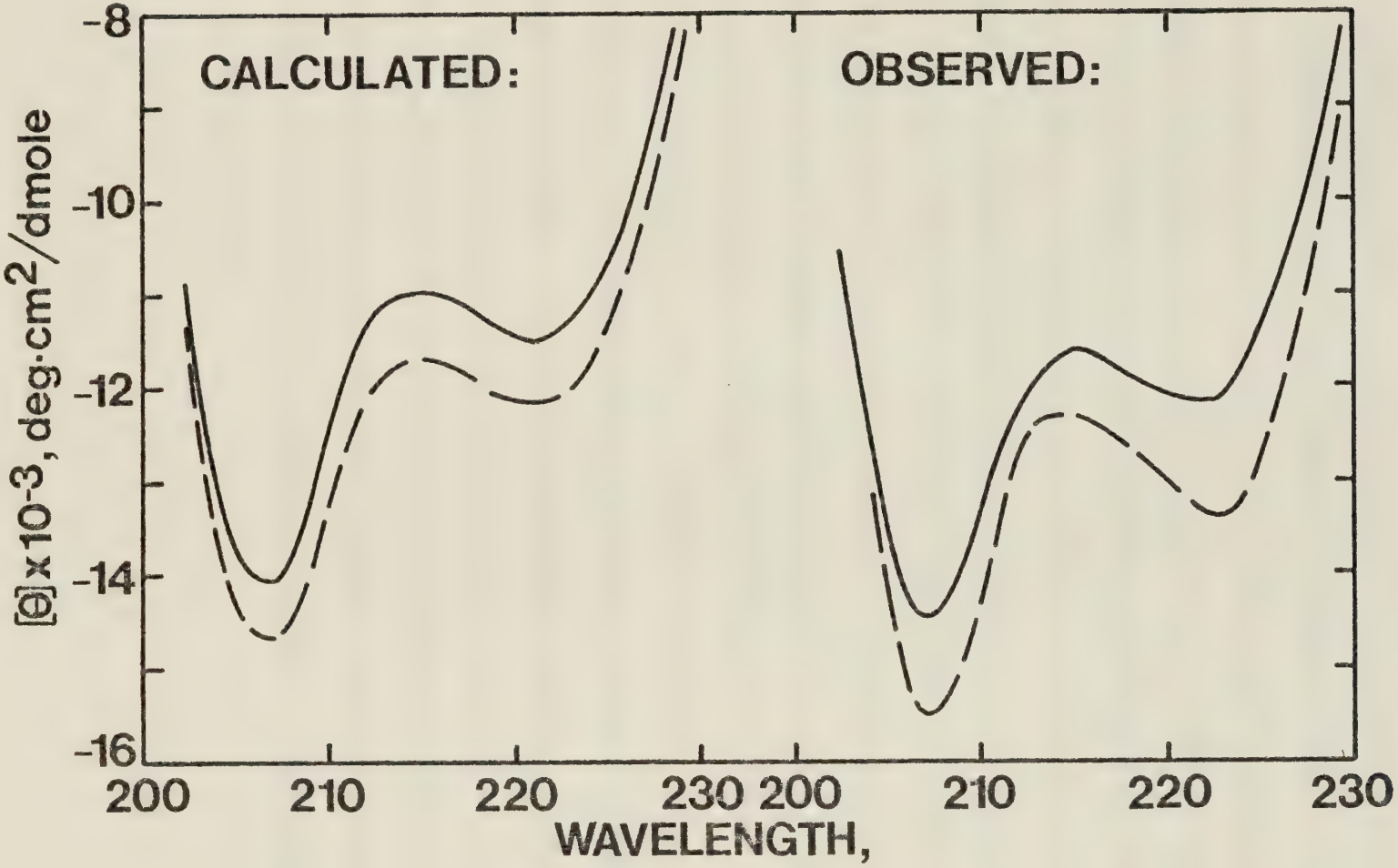

Figure 49. Calculated and observed CD spectra of reconstituted cardiac troponin in the presence (— — —) and absence (————) of calcium. The initial solvent composition was as described in Figure 46.

change in $[\theta]_{221}$ values in the CD spectra of TN-IC, TN-CT and TN-ICT. Subsequent addition of $CaCl_2$ brought about the full change in $[\theta]_{221}$ values.

A detailed comparison of the calculated and observed spectra for TN-ICT in the "minus Ca^{2+}" and "plus Ca^{2+}" states (Figure 49) revealed that the observed change in $[\theta]_{221}$ (10 ± 2%) upon the addition of Ca^{2+} was significantly greater than that predicted (6 ± 1%) by simply taking into account a dilution of the Ca^{2+} effect on TN-C due to the presence of TN-I and TN-T. For the complexes TN-IC and TN-CT, the differences between the calculated and observed changes due to Ca^{2+} binding were not significant. Therefore, a potentiation of the Ca^{2+} effect on isolated TN-C appears to result in the presence of both of the remaining troponin components. Such an amplification may be interpreted as a magnification of the direct effect of Ca^{2+} binding on TN-C. However, it may also represent a situation in which the direct effect on TN-C (i.e., that seen on isolated TN-C in solution) leads to changes in the conformation of one or both of the remaining troponin components due to the nature of the subunit interactions. By extrapolation, such a series of events could result in the shifting of tropomyosin away from a blocking position on the f-actin strands, allowing myosin to interact with the actin. The net result of this process would be an actively contracting muscle system.

CHAPTER VI

GENERAL DISCUSSION

Troponin from cardiac muscle, prepared by the LiCl extraction method, can be separated into three protein subunits by a combination of ion exchange and gel filtration chromatographies. Physico-chemical characterization of these molecules, combined with their assayed biological activities, allows them to be named in accordance with skeletal muscle troponin nomenclature. Troponin I inhibits the Mg^{2+} activated ATPase of cardiac actomyosin. Troponin C binds Ca^{2+} ions and undergoes a concomitant conformational change which is involved in the release of the inhibitory effect of TN-I. Troponin T anchors the troponin complex to tropomyosin. All three components are required to impose Ca^{2+} sensitivity upon the actomyosin ATPase reaction.

Each subunit performs its role via interactions with adjacent members of the regulatory complex. Gel electrophoresis experiments demonstrate a strong interaction between TN-I and TN-C and provide evidence for a TN-C interaction with TN-T. In solutions in which tropomyosin is soluble but TN-T is not, the latter can "pull" tropomyosin out of solution, suggesting a strong interaction of TN-T with tropomyosin. These results are confirmed by CD analysis of mixtures of the troponin components. CD studies also reveal that the effect of Ca^{2+} binding on the conformation of isolated TN-C persists through the complexes TN-IC, TN-CT and TN-ICT (reconstituted troponin).

The results of interaction studies imply that the mode of regulation of cardiac and skeletal muscles by their respective troponin-tropomyosin relaxing systems is essentially the same. However, an examination of

the amino acid compositions and the hydrodynamic, optical and Ca^{2+} binding properties of the cardiac troponin subunits reveals quantitative differences between them and their skeletal muscle counterparts. Analogous subunits of cardiac and skeletal troponins are the products of separate genes. How such differences arose and whether they represent important physiological advantages to an individual muscle type remains to be investigated in more detail. In this regard, studies concerning the phosphorylation of TN-I and its physiological role in cardiac muscle (55, 53) are of particular interest, as a similar role for skeletal TN-I has not been detected.

It is probable that the distinctions which exist between the regulatory proteins of heart muscle and their counterparts in skeletal muscle reflect some aspect of the functional differences between the two tissue types. The beating of the heart, unlike skeletal muscle contraction, is not under direct conscious control. Skeletal muscle must be capable of being switched on and off rapidly and completely. Cardiac muscle beats rhythmically, but never appears to exist in a completely relaxed, or switched off, state. It displays a high resting tension with respect to skeletal muscle. It is likely that differences between the troponin subunit analogues are responsible for this phenomenon. Whereas the Mg^{2+} activated ATPase activity of skeletal actomyosin can nearly be shut down by skeletal TN-I (93), our work, and that of others (33), suggests that cardiac TN-I is a much less potent inhibitor. A direct physiological implication of this discrepancy would be a significant level of ATPase activity in the heart during diastole, resulting in an increased resting tension. A less direct cause could be proposed on the basis of the smaller conformational change undergone by cardiac as opposed to skeletal

TN-C upon binding Ca^{2+}.

This thesis has concentrated upon the role of the troponin-tropomyosin complex in the regulation of the interaction between actin and myosin in vertebrate striated muscle. In addition to this calcium sensitization system, reports in the literature have implicated other factors in the overall control process.

In scallop and smooth muscle actomyosins (11), control of the actin-myosin interaction is exerted at the level of the thick-filament, in the absence of troponin-like molecules altogether. This control complex is also sensitive to Ca^{2+}. Even in vertebrate muscle, Ca^{2+} at physiological levels can induce conformational changes in the thick filaments (103, 104). Also, it has been reported (105) that dinitrophenylation of a cysteine residue on the S1 portion of the cardiac myosin heavy chain could desensitize an actomyosin, into which the modified myosin was incorporated, to Ca^{2+} regulation. Treatment of the modified myosin with mercaptoethanol to remove the blocking group from the cysteine restored its ability to form a Ca^{2+} sensitive actomyosin.

The conformation of actin itself may be important in any complete regulatory model. Cross-linked actin retains its ability to stimulate the Mg^{2+} ATPase of heavy meromyosin subfragment-1 (106). However, incorporation of troponin and tropomyosin into the assay system fails, in the absence of Ca^{2+} ions, to inhibit the Mg^{2+} activated ATPase. Fluorescence energy transfer experiments demonstrate that a Ca^{2+} sensitive movement of tropomyosin occurs both when the troponin-tropomyosin complex is bound to native or cross-linked actin filaments. Therefore, cross-linking actin apparently "freezes" its conformation in an "on" position, and the movement of tropomyosin cannot override this switch.

Although much is now understood about thin filament regulation in vertebrate skeletal and cardiac muscle, the fine details of the control mechanism must be brought into clearer focus. Probing the structures of the regulatory proteins by chemical and X-ray crystallographic methods undoubtedly will lead to modifications of existing models. Further alterations may have to be incorporated with an increased perception of the roles of actin and myosin in governing their own interaction.

BIBLIOGRAPHY

1. Huxley, H.E. (1972) in The Structure and Function of Muscle (ed. G.H. Bourne), Vol. 1, 2nd edition, pp. 301-387, Academic Press, Inc., New York.

2. Squire, J.M. (1975) Ann. Rev. Biophys. Bioeng. 4, 137-163.

3. Mannherz, H.G. and Goody, R.S. (1976) Ann. Rev. Biochem. 45, 427-465.

4. Katz, A.M. (1970) Physiological Reviews 50, 63-158.

5. Ebashi, S., Masaki, T. and Tsukui, R. (1974) Adv. Cardiol. 12, 59-69.

6. Léger, J.J., Berson, G., Delcayre, C., Klotz, C., Schwartz, K., Léger, J., Stephens, M. and Swynghedauw, B. (1975) Biochimie 57, 1249-1273.

7. Ebashi, S. and Endo, M. (1968) Progr. Biophys. Mol. Biol. 18, 123-183.

8. Perry, S.V. (1973) PAABS Revista 2, 651-720.

9. Weber, A. and Murray, J.M. (1973) Physiological Reviews 53, 612-673.

10. Ebashi, S. (1974) Essays in Biochemistry 10, 1-36.

11. Szent-Györgi, A.G. (1975) Biophys. J. 15, 707-723.

12. Ebashi, S., Wakabayashi, T. and Ebashi, F. (1971) J. Biochem. 69, 441-445.

13. Greaser, M.L. and Gergely, J. (1971) J. Biol. Chem. 246, 4226-4233.

14. Murray, A.C. and Kay, C.M. (1971) Biochem. Biophys. Res. Commun. 44, 237-244.

15. Wilkinson, J.M., Perry, S.V., Cole, H.A. and Trayer, I.P. (1972) Biochem. J. 127, 215-228.

16. Hartshorne, D.J. and Dreizen, P. (1972) Cold Spring Harbor Symp. Quant. Biol. 37, 225-234.

17. Drabikowski, W., Dabrowska, R. and Barylko, B. (1973) Acta Biochim. Polon. 20, 181-199.

18. Collins, J.H., Potter, J.D., Horn, M.J., Wilshire, G. and Jackman, N. (1973) FEBS Lett. 36, 268-272.

19. Wilkinson, J.M. and Grand, R.J.A. (1975) Biochem. J. 149, 493-496.

20. Pearlstone, J.R., Carpenter, M.R., Johnson, P. and Smillie, L.B. (1976) Proc. Nat. Acad. Sci. (U.S.A.) 73, 1902-1906.

21. Hitchcock, S.E., Huxley, H.E. and Szent-Györgi, A.G. (1973) J. Mol. Biol. 80, 825-836.

22. Margossian, S.S. and Cohen, C. (1973) J. Mol. Biol. 81, 409-413.

23. Potter, J.D. and Gergely, J. (1974) Biochemistry 13, 2697-2703.

24. Ebashi, S., Endo, M. and Ohtsuki, I. (1969) Quart. Rev. Biophys. 2, 351-384.

25. Murray, A.C. and Kay, C.M. (1972) Biochemistry 11, 2622-2627.

26. Van Eerd, J.-P. and Kawasaki, Y. (1972) Biochem. Biophys. Res. Commun. 47, 859-865.

27. Wakabayashi, T., Huxley, H.E., Amos, L.A. and Klug, A. (1975) J. Mol. Biol. 93, 477-497.

28. Ebashi, S., Ebashi, F. and Kodama, A. (1967) J. Biochem. 62, 137-138.

29. Greaser, M.L., Yamaguchi, M., Brekke, C., Potter, J. and Gergely, J. (1972) Cold Spring Harbor Symp. Quant. Biol. 37, 235-244.

30. Staprans, I., Takahashi, H., Russell, M.P. and Watanabe, S. (1972) J. Biochem. 72, 723-735.

31. Reddy, Y.S. and Honig, C.R. (1972) Biochim. Biophys. Acta 275, 453-463.

32. Dabrowska, R., Dydynska, M., Szpacenko, A. and Drabikowski, W. (1973) Int. J. Biochem. 4, 189-194.

33. Tsukui, R. and Ebashi, S. (1973) J. Biochem. 73, 1119-1121.

34. Burtnick, L.D., McCubbin, W.D. and Kay, C.M. (1974) Proc. Can. Fed. Biol. Soc. 17, 24.

35. Burtnick, L.D., McCubbin, W.D. and Kay, C.M. (1975) Can. J. Biochem. 53, 15-20.

36. Burtnick, L.D., McCubbin, W.D. and Kay, C.M. (1975) Proc. Can. Fed. Biol. Soc. 18, 72.

37. Burtnick, L.D., McCubbin, W.D. and Kay, C.M. (1975) Can. J. Biochem. 53, 1207-1213.

38. Burtnick, L.D., McCubbin, W.D. and Kay, C.M. (1976) Can. J. Biochem. 54, 546-552.

39. Burtnick, L.D., McCubbin, W.D. and Kay, C.M. (1976) Biophys. J. 16, 199a.

40. Burtnick, L.D., McCubbin, W.D. and Kay, C.M. (1975) Proc. X Int. Congr. Biochem., 202.

41. Burtnick, L.D. and Kay, C.M. (1976) FEBS Lett. 65, 234-237.

42. Brittain, H.G., Richardson, F.S., Martin, R.B., Burtnick, L.D. and Kay, C.M. (1976) Biochem. Biophys. Res. Commun. 68, 1013-1019.

43. Head, J.F. and Perry, S.V. (1974) Biochem. J. 137, 145-154.

44. Hirabayashi, T. and Perry, S.V. (1974) Biochim. Biophys. Acta 351, 273-289.

45. Drabikowski, W., Dabrowska, R. and Barylko, B. (1975) in Recent Advances in Studies on Cardiac Structure and Metabolism (ed. A. Fleckenstein and N.S. Dhalla), Vol. 5, pp. 245-252.

46. Brekke, C.J. and Greaser, M.L. (1976) J. Biol. Chem. 251, 866-871.

47. Van Eerd, J.-P. and Takahashi, K. (1975) Biochem. Biophys. Res. Commun. 64, 122-127.

48. Collins, J.H. (1974) Biochem. Biophys. Res. Commun. 58, 301-308.

49. Kretsinger, R.H. and Nockolds, C.E. (1973) J. Biol. Chem. 248, 3313-3326.

50. Syska, H., Perry, S.V. and Trayer, I.P. (1974) FEBS Lett. 40, 253-257.

51. Wilkinson, J.M. and Grand, R.J.A. (1975) in Proc. of the 9th FEBS Meeting, Proteins of Contractile Systems (ed. E.N.A. Biro), Vol. 31, pp. 137-144, North-Holland Publishing Co., Amsterdam-London, with Akademiai Kiado, Budapest.

52. Grand, R.J.A., Wilkinson, J.M. and Mole, L.E. (1976) Biochem. J. 159, 633-641.

53. Solaro, R.J., Moir, A.J.G. and Perry, S.V. (1976) Nature 262, 615-617.

54. Cole, H.A. and Perry, S.V. (1975) Biochem. J. 149, 525-533.

55. England, P.J. (1975) FEBS Lett. 50, 57-60.

56. Ray, K.P. and England, P.J. (1976) FEBS Lett. 70, 11-16.

57. Yamaguchi, M., Greaser, M.L. and Cassens, R.G. (1974) J. Ultrastruct. Res. 48, 33-58.

58. Schaub, M.C. and Perry, S.V. (1969) Biochem. J. 115, 993-1004.

59. Shapiro, A.L., Vinuela, E. and Maizel, J.V. (1967) Biochem. Biophys. Res. Commun. 28, 815-820.

60. Weber, K. and Osborn, M. (1969) J. Biol. Chem. 244, 4406-4412.

61. Moore, S. and Stein, W.H. (1963) in Methods in Enzymology (ed. C.H.W. Hirs), Vol. 6, pp. 819-831, Academic Press, Inc., New York.

62. Moore, S. (1963) J. Biol. Chem. 238, 235-237.

63. Goodwin, T.W. and Morton, R.A. (1946) Biochem. J. 40, 628-632.

64. Bencze, W.L. and Schmid, K. (1957) Anal. Chem. 29, 1193-1196.

65. Oikawa, K., Kay, C.M. and McCubbin, W.D. (1968) Biochim. Biophys. Acta 168, 164-167.

66. Chen. Y.-H., Yang, J.T. and Chau, K.H. (1974) Biochemistry 13, 3350-3359.

67. Chervenka, C.H. (1969) A Manual of Methods for the Analytical Ultracentrifuge, Spinco Division of Beckman Instruments, Inc., Palo Alto, California.

68. Babul, J. and Stellwagen, E. (1969) Anal. Biochem. 28, 216-221.

69. Schachman, H.K. (1959) Ultracentrifugation in Biochemistry, Academic Press, Inc., New York.

70. Cohn, E.J. and Edsall, J.T. (1965) Proteins, Amino Acids and Peptides as Ions and Dipolarions, Hafner Publishing Co., Inc., New York.

71. Richards, E.G., Teller, D.C. and Schachman, H.K. (1968) Biochemistry 7, 1054-1076.

72. Wolodko, W.T. (1974) in a Ph.D. thesis submitted to the University of Alberta, Edmonton, Canada, Physical and Chemical Studies of Rabbit Cardiac Myosin and Subfragments Produced by Limited Papain Digestion.

73. Tonomura, Y., Appel, P. and Morales, M.F. (1966) Biochemistry 5, 515-521.

74. Spudich, J.A. and Watt, S. (1971) J. Biol. Chem. 246, 4866-4871.

75. Eisenberg, E. and Kielley, W.W. (1974) J. Biol. Chem. 249, 4742-4748.

76. Shigekawa, M. and Tonomura, Y. (1972) J. Biochem. 72, 957-971

77. Fiske, C.H. and SubbaRow, Y. (1925) J. Biol. Chem. 66, 375-400.

78. Drabikowski, W. and Dabrowska, R. (1975) in Proc. of the 9th FEBS Meeting, Proteins of Contractile Systems (ed. E.N.A. Biro), Vol. 31, pp. 85-104, North-Holland Publishing Co., Amsterdam-London, with Akademiai Kiado, Budapest.

79. Dabrowska, R., Podlubnaya, Z., Nowak, E. and Drabikowski, W. (1976) J. Biochem. 80, 89-99.

80. Perrin, D.D. and Dempsey, B. (1974) Buffers for pH and Metal Ion Control, Chapman and Hall, Ltd., London.

81. Schwarzenbach, G., Senn, H. and Anderegg, G. (1957) Helv. Chim. Acta 40, 1886-1900.

82. Willick, G.E. and Kay, C.M. (1971) Biochemistry 10, 2216-2222.

83. Hummel, J.P. and Dreyer, W.J. (1962) Biochim. Biophys. Acta 63, 530-532.

84. Voordouw, G. and Roche, R.S. (1974) Biochemistry 13, 5017-5021.

85. Unicam Methods Sheets (1966) Method Ca-2, Pye-Unicam Ltd., Cambridge, England.

86. Dabrowska, R., Barylko, B., Nowak, E. and Drabikowski, W. (1973) FEBS Lett. 29, 239-242.

87. Wilkinson, J.M. (1976) FEBS Lett. 70, 254-256.

88. Donovan, J.W. (1969) in Physical Principles and Techniques of Protein Chemistry (ed. S.J. Leach), Part A, pp. 101-170, Academic Press, Inc., New York.

89. Polimeni, P.I. and Page, E. (1973) Circulation Research 33, 367-374.

90. Potter, J.D. and Gergely, J. (1975) J. Biol. Chem. 250, 4628-4633.

91. Kawasaki, Y. and van Eerd, J.-P. (1972) Biochem. Biophys. Res. Commun. 49, 898-905.

92. McCubbin, W.D. and Kay, C.M. (1973) Biochemistry 12, 4228-4232.

93. Mani, R.S., McCubbin, W.D. and Kay, C.M. (1973) FEBS Lett. 29, 243-247.

94. Kay, C.M. (1960) Biochim. Biophys. Acta 38, 420-427.

95. Weber, K. and Osborn, M. (1975) in The Proteins (eds. H. Neurath and R.L. Hill), 3rd edition, Vol. 1, pp. 179-229, Academic Press, Inc., New York.

96. Mani, R.S., McCubbin, W.D. and Kay, C.M. (1974) FEBS Lett. 38, 357-360.

97. Wilkinson, J.M. (1974), Biochim. Biophys. Acta 359, 379-388.

98. Potter, J.D. (1974) Arch. Biochem. Biophys. 162, 436-441.

99. Van Eerd, J.-P. and Kawasaki, Y. (1973) Biochemistry 12, 4972-4980.

100. McCubbin, W.D., Mani, R.S. and Kay, C.M. (1974) Biochemistry 13, 2689-2694.

101. Mani, R.S., McCubbin, W.D. and Kay, C.M. (1974) Biochemistry 13, 5003-5007.

102. Mani, R.S., McCubbin, W.D. and Kay, C.M. (1975) FEBS Lett. 52, 127-131.

103. Morimoto, K. and Harrington, W.F. (1974) J. Mol. Biol. 88, 693-709.

104. Haselgrove, J.C. (1975) J. Mol. Biol. 92, 113-143.

105. Bailin, G. (1975) Arch. Biochem. Biophys. 171, 206-213.

106. Poo, W.-J. and Hartshorne, D.J. (1976) Biochem. Biophys. Res. Commun. 70, 406-412.

107. Demaille, J., Dutruge, E., Eisenberg, E. Capony, J.-P. and Pechère, J.-F. (1974) FEBS Lett. 42, 173-178.

108. Weeds, A.G. and McLachlan, A.D. (1974) Nature 252, 646-649.

109. Tufty, R.M. and Kretsinger, R.H. (1975) Science 187, 167-169.

110. Collins, J.H. (1976) Nature 259, 699-700.

111. Kretsinger, R.H. and Barry, C.D. (1975) Biochim. Biophys. Acta 405, 40-52.

112. Frank, G. and Weeds, A.G. (1974) Eur. J. Biochem. 44, 317-334.

113. Donato, H. and Martin, R.B. (1974) Biochemistry 13, 4575-4579.

114. Miller, T.L., Nelson, D.J., Brittain, H.G., Richardson, F.S., Martin, R.B. and Kay, C.M. (1975) FEBS Lett. 58, 262-264.

115. Moews, P.C. and Kretsinger, R.H. (1975) J. Mol. Biol. 91, 229-232.

116. Lehninger, A.L. (1970) Biochemistry, Worth Publishers, Inc., New York.

APPENDIX

STRUCTURAL HOMOLOGIES AMONG MUSCLE PROTEINS

Muscle cells contain a set of structurally related proteins which apparently perform different functions (48, 107 - 110). Interest in this topic began to mushroom with the resolution of the 3-dimensional structure of a soluble carp muscle calcium binding protein, belonging to a class generally known as parvalbumins, and the characterization of its calcium binding sites (49). Each of the 2 sites, related by an approximate two-fold axis of symmetry, lies in a corner between two helical regions. A structural analogy was made to a right hand with the outstretched thumb and forefinger representing the two helices and the approximate right angle between them representing the locus of calcium binding. The basic unit became known as an "EF hand", being typified by the E and F helices of the parvalbumin structure, and can be symbolized by E-Ca-F. Kretsinger proposed that parvalbumin arose by duplication of a primordial gene coding for E-Ca-F. This may be depicted as $(E_1\text{-}Ca\text{-}F_1)\text{-}L\text{-}(E_2\text{-}Ca\text{-}F_2)$ (108), where L is a linking sequence of amino acid residues.

The amino acid sequence of rabbit skeletal TN-C (48) was shown to contain four EF hands and was proposed to have evolved by 2 duplications of the precursor gene to give $[(E_1\text{-}Ca\text{-}F_1)\text{-}L_1\text{-}(E_2\text{-}Ca\text{-}F_2)]\text{-}J\text{-}[(E_3\text{-}Ca\text{-}F_3)\text{-}L_2\text{-}(E_4\text{-}Ca\text{-}F_4)]$. On the basis of the sequence homologies, a model of the 3-dimensional structure of TN-C also was proposed (111). When the sequences of the 2 alkali (112) and one DTNB (110) light chains of rabbit skeletal muscle myosin became available, each appeared to be related to TN-C and parvalbumin and to consist of 4 repeated sections of closely

homologous sequences. As might be expected, the sequence of bovine cardiac TN-C (47) showed extensive homology with that of skeletal TN-C, and another member was added to the group of parvalbumin-like proteins.

The validity of proposals concerning the intricate structure of proteins based solely upon amino acid sequence homologies might understandably cause scepticism. However, evidence is available from physical studies to demonstrate, at least, that the calcium binding sites of carp parvalbumin (113), rabbit skeletal TN-C (114) and bovine cardiac TN-C (42) are similar. By substituting terbium for calcium in these 3 proteins, Dr. Bruce Martin and his coworkers have examined the total emission (TE) and circularly polarized emission (CPE) spectra of terbium bound to these molecules.

For parvalbumin, terbium emission at 545 nm was maximal at an excitation wavelength of 259 nm, implicating energy transfer from a phenylalanine residue to a nearby terbium. Maximum emission at 545 nm in skeletal and cardiac TN-C was elicited by excitation at 280 nm, implicating a nearby tyrosine in the energy transfer process.

Of the 3 tyrosines in cardiac and 2 in skeletal TN-C, only tyrosine 109 in cardiac and tyrosine 111 in skeletal TN-C occur in homologous regions of sequence. In each TN-C, this tyrosine has been suggested to be part of a calcium binding site (18, 47). Furthermore, phenylalanine 57 of parvalbumin is found to be in a homologous position with these TN-C tyrosine residues (18), and in the crystal structure of carp parvalbumin, the aromatic side chain of this phenylalanine overlaps the terbium in one of the calcium binding sites (115).

More subtle conformational information may be obtained by studying the CPE of terbium bound to the 3 proteins. CPE, like CD, provides a

measure of the optical asymmetry of the microenvironment of the chromophore of interest. CPE at a given wavelength is quantitated by the dissymmetry factor g:

$$g = \frac{\Delta I}{I} = \frac{I_L - I_R}{I_L + I_R} \qquad [37]$$

where I_L and I_R are, respectively the left and right circularly polarized emission intensities, I is the total emission intensity and ΔI is the CPE intensity. Table VI (from (42)) summarizes the CPE properties of the 3 proteins and emphasized their essential identity.

In our collaborative study with Dr. Martin and his colleagues (42), further additions of cardiac TN-I and TN-T were made to TN-C solutions. In the presence of either TN-I or TN-T, the CPE of TN-C was quenched completely and the TE was reduced significantly, suggesting that TN-C can interact with both TN-I and TN-T. In reconstituted cardiac troponin, the TE was reduced by about 60% and the CPE quenched entirely. This may be compared with a similar result employing native skeletal troponin (114) (Table VI).

In conclusion, these studies provided direct information concerning the structural homology and the geometry of the calcium binding sites of parvalbumin and skeletal and cardiac TN-C, as well as the nature of the changes in the microenvironments of the binding sites on TN-C when it interacts with the remaining troponin subunits.

TABLE VI*

Emission dissymmetry factors for Tb(III) emission** in muscle proteins

	g	nm
Bovine cardiac TN-C	-0.030	544.5
	+0.024	549.8
TN-C + TN-I	0.000	544.7***
TN-C + TN-T	0.000	544.6***
TN-C + TN-I + TN-T	0.000	544.6***
Rabbit skeletal TN-C	-0.029	544.3
	+0.027	549.7
Rabbit skeletal troponin	0.000	544.8***
Carp parvalbumin	-0.025	544.9
	+0.029	549.9

*From Brittain et al. (42).

**In region of Tb(III) $^5D_4 \longrightarrow {}^7F_5$ transition.

***Maximum wavelength in total emission spectrum.